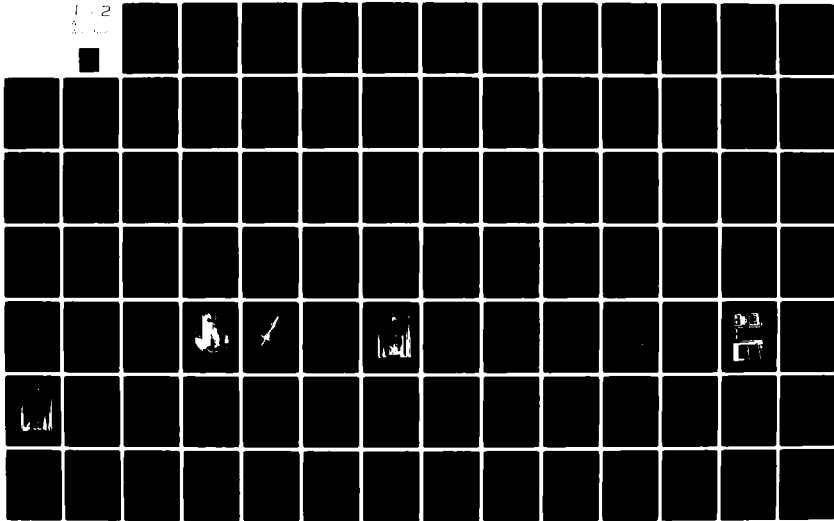


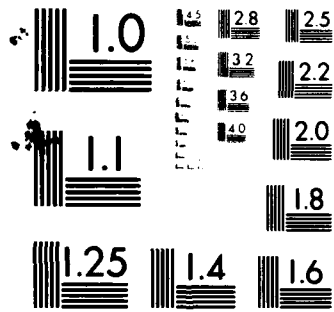
AD-A108 518

ARMY ENGINEER WATERWAYS EXPERIMENT STATION VICKSBURG--ETC F/G 8/13  
INVESTIGATION OF COMPACTION CRITERIA FOR AIRPORT PAVEMENT SUBGR--ETC(U)  
OCT 81 W N BRABSTON DOT-FA78WAI-876  
WES/TR/6L-81-11 FAA/RD-81/48 NL

UNCLASSIFIED

1-2  
1-1





MICROCOPY RESOLUTION TEST CHART  
NATIONAL BUREAU OF STANDARDS 1963-A

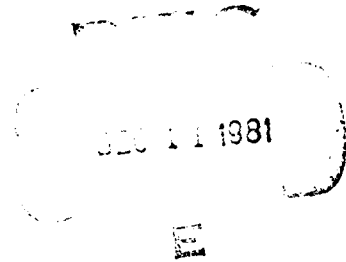
**LEVEL II**

12

Report No. DOT/FAA/RD-81/48  
WES/TR/81-11  
Systems Research &  
Development Service  
Washington, D.C. 20590

# Investigation of Compaction Criteria for Airport Pavement Subgrade Soils

AD A108518



William N. Brabston

U.S. Army Engineer Waterways Experiment Station  
Geotechnical Laboratory  
P.O. Box 631, Vicksburg, Miss. 39180

October 1981  
Final Report

This document is available to the U.S. public  
through the National Technical Information  
Service, Springfield, Virginia 22161.



U.S. Department of Transportation  
Federal Aviation Administration

DTIC FILE COPY

8112 11 086

#### NOTICES

This document is disseminated under the sponsorship of the Department of Transportation in the interest of information exchange. The United States Government assumes no liability for its contents or use thereof.

The United States Government does not endorse products or manufacturers. Trade of manufacturers' names appear herein solely because they are considered essential to the object of this report.

Technical Report Documentation Page

1. Report No. DOT/FAA/RD-81/48		2. Government Accession No. 4D-1108518		3. Recipient's Catalog No.	
4. Title and Subtitle INVESTIGATION OF COMPACTION CRITERIA FOR AIRPORT PAVEMENT SUBGRADE SOILS				5. Report Date October 1981	
				6. Performing Organization Code	
7. Author(s) William N. Brabston				8. Performing Organization Report No. TR-GL-81-11	
9. Performing Organization Name and Address U. S. Army Engineer Waterways Experiment Station Geotechnical Laboratory P. O. Box 631, Vicksburg, Miss. 39180				10. Work Unit No. (TRAIS)	
				11. Contract or Grant No. DOT FA78WAI-876	
12. Sponsoring Agency Name and Address U. S. Department of Transportation Federal Aviation Administration Systems Research & Development Service Washington, D. C. 20591				13. Type of Report and Period Covered Final Report March 1978 to April 1981	
				14. Sponsoring Agency Code	
15. Supplementary Notes					
16. Abstract A study was conducted to determine the effect of lowering soil density requirements for subgrades under airport pavements. The investigation was primarily a laboratory effort in which molded specimens of three different soil types, compacted to densities at and below those currently specified by FAA criteria, were subjected to repeated axial loadings in a triaxial compression chamber. The primary response parameters of interest were permanent and resilient axial strain. Test results were formulated into a statistical model to predict permanent soil strain based on soil characteristics such as density, clay content, compaction characteristics, and shear strength. The strain model was used to calculate values of permanent soil deformation at the surface of the subgrade for various combinations of soil density. Results of the test indicated that the wide variation in soil response among the three materials tested precluded any general alteration in current FAA compaction criteria.					
17. Key Words Flexible pavements Rigid pavements Soil density requirements Repetitive triaxial techniques Subgrade compaction			18. Distribution Statement Distribution is available to the public through the National Technical Information Service, Springfield, Va. 22151.		
19. Security Classif. (of this report) Unclassified		20. Security Classif. (of this page) Unclassified		21. No. of Pages 174	22. Price



TABLE OF CONTENTS

	<u>Page</u>
INTRODUCTION . . . . .	1
BACKGROUND . . . . .	1
OBJECTIVES OF THE STUDY . . . . .	4
SCOPE OF WORK . . . . .	4
REVIEW OF PREVIOUS STUDIES . . . . .	7
SELECTION OF TEST PARAMETERS . . . . .	23
SOIL TYPES . . . . .	23
SOIL DENSITY AND MOISTURE CONTENT . . . . .	25
MOISTURE-DENSITY RELATIONS . . . . .	26
REVISED TARGET DENSITIES . . . . .	31
STRESS STATES . . . . .	32
PREPARATION OF SOIL SPECIMENS, REPETITIVE LOAD EQUIPMENT, AND TEST PROCEDURES . . . . .	46
PREPARATION OF SOIL SPECIMENS . . . . .	46
REPETITIVE LOAD EQUIPMENT . . . . .	53
TEST PROCEDURES . . . . .	56
TEST RESULTS AND DISCUSSION . . . . .	63
TEST RESULTS . . . . .	63
DISCUSSION . . . . .	92
STRAIN MODEL AND EFFECT ON PAVEMENT PERFORMANCE . . . . .	105
STRAIN MODEL . . . . .	105
EFFECT ON PAVEMENT PERFORMANCE . . . . .	120
CONCLUSIONS AND RECOMMENDATIONS . . . . .	131
CONCLUSIONS . . . . .	131
RECOMMENDATIONS . . . . .	131
REFERENCES . . . . .	133
APPENDIX A: OUTPUT DATA FROM REPETITIVE LOAD TESTS . . . . .	A-1

## LIST OF ILLUSTRATIONS

<u>Figure No.</u>		<u>Page</u>
1	Axial strain after 10,000 stress applications and interval of time between compacting and testing . . . . .	13
2	General shapes of hypothetical curves . . . . .	14
3	Deformation versus number of load applications, limestone residual soil . . . . .	16
4	Permanent axial strain versus number of load cycles (OCR = 10) . . . . .	17
5	Effect of number of cycles on plastic axial strain for CBR = 7.5, Phase II tests . . . . .	19
6	Axial permanent strain versus number of load applications experimental data, and statistical relationship . . . . .	20
7	Comparison of test data for Keuper Marl clay and curves generated from Equation 4 . . . . .	22
8	Gradation and classification data for silty clay, buckshot clay, and silty sand soils . . . . .	24
9	Moisture-density relations for silty clay . . . . .	27
10	Moisture-density relations for buckshot clay . . . . .	29
11	Moisture-density relations for silty sand . . . . .	30
12	Flexible pavement design . . . . .	34
13	Rigid pavement design . . . . .	34
14	Loading configuration . . . . .	37
15	Elastic constants for flexible and rigid pavements . . . . .	40
16	Vertical stress-depth relation for flexible and rigid pavements . . . . .	41
17	Stress wave forms used in repetitive load tests . . . . .	44
18	Axial stress conditions for typical repeated load test . . . . .	45
19	Pneumatic tamper . . . . .	48

<u>Figure No.</u>		<u>Page</u>
20	Manual tamper . . . . .	49
21	General view of repetitive load chamber . . . . .	51
22	Method of preparation on base of triaxial chamber specimen . . . . .	52
23	Schematic drawing of closed-loop electrohydraulic repetitive load system . . . . .	54
24	WES triaxial compression chamber . . . . .	55
25	General view of controller-recorder-display console . . .	57
26	Specimen mounted on base . . . . .	59
27	Resilient axial strain versus repeated deviator stress for silty clay . . . . .	68
28	Resilient axial strain versus repeated deviator stress for buckshot clay . . . . .	69
29	Resilient axial strain versus repeated deviator stress for silty sand . . . . .	70
30	Permanent axial strain versus number of load repetitions (semilogarithmic), tests 2, 3, and 5 . . . . .	72
31	Permanent axial strain versus number of load repetitions (semilogarithmic), tests 6, 7, and 8 . . . . .	73
32	Permanent axial strain versus number of load repetitions (semilogarithmic), tests 25, 26, and 27 . . . . .	74
33	Permanent axial strain versus number of load repetitions (semilogarithmic), tests 12, 13, and 15 . . . . .	75
34	Permanent axial strain versus number of load repetitions (semilogarithmic), tests 16, 17, and 22 . . . . .	76
35	Permanent axial strain versus number of load repetitions (semilogarithmic), tests 19 and 21 and average data from tests 23 and 24 . . . . .	77
36	Permanent axial strain versus number of load repetitions (semilogarithmic), tests 29, 30, and 31 . . . . .	78

<u>Figure No.</u>		<u>Page</u>
37	Permanent axial strain versus number of load repetitions (semilogarithmic), tests 35, 36, and 39 . . . . .	79
38	Permanent axial strain versus number of load repetitions (semilogarithmic), tests 33, 34, and 40 . . . . .	80
39	Permanent axial strain versus number of load repetitions (arithmetic), tests 2, 3, and 5 . . . . .	81
40	Permanent axial strain versus number of load repetitions (arithmetic), tests 6, 7, and 8 . . . . .	82
41	Permanent axial strain versus number of load repetitions (arithmetic), tests 25, 26, and 27 . . . . .	83
42	Permanent axial strain versus number of load repetitions (arithmetic), tests 12, 13, and 15 . . . . .	84
43	Permanent axial strain versus number of load repetitions (arithmetic), tests 16, 17, and 22 . . . . .	85
44	Permanent axial strain versus number of load repetitions (arithmetic), tests 19 and 21 and average data from tests 23 and 24 . . . . .	86
45	Permanent axial strain versus number of load repetitions (arithmetic), tests 29, 30, and 31 . . . . .	87
46	Permanent axial strain versus number of load repetitions (arithmetic), tests 35, 36, and 39 . . . . .	88
47	Permanent axial strain versus number of load repetitions (arithmetic), tests 33, 34, and 40 . . . . .	89
48	Repeated deviator stress versus permanent axial strain at 75,000 repetitions for silty clay . . . . .	97
49	Repeated deviator stress versus permanent axial strain at 75,000 repetitions for buckshot clay . . . . .	98
50	Repeated deviator stress versus permanent axial strain at 75,000 repetitions for silty sand . . . . .	99
51	Stress ratio versus permanent axial strain at 75,000 load repetitions . . . . .	101
52	Maximum dry density versus compaction effort for silty clay (CL), buckshot clay (CH), and silty sand (SM) . . . . .	107

<u>Figure No.</u>		<u>Page</u>
53	Log-log plot of strain versus repetitions, tests 2, 3, 5, and 5 adjusted . . . . .	110
54	Log-log plot of strain versus repetitions, tests 6, 7, 7 adjusted, and 8 . . . . .	111
55	Log-log plot of strain versus repetitions, tests 25, 26, and 27 . . . . .	112
56	Log-log plot of strain versus repetitions, tests 12, 13, and 15 . . . . .	113
57	Log-log plot of strain versus repetitions, tests 16, 17, and 22 . . . . .	114
58	Log-log plot of strain versus repetitions, tests 19, 21, 21 adjusted, and average data from tests 23 and 24 . . . . .	115
59	Log-log plot of strain versus repetitions, tests 29, 30, 30 adjusted, and 31 . . . . .	116
60	Log-log plot of strain versus repetitions, tests 35, 36, 36 adjusted, and 39 . . . . .	117
61	Log-log plot of strain versus repetitions, tests 33, 34, 34 adjusted, and 40 . . . . .	118
62	Subgrade layers for computation of permanent deformation . . . . .	123

LIST OF TABLES

<u>Table No.</u>		<u>Page</u>
1	FAA Compaction Criteria, Fill Section . . . . .	3
2	Target Density and Moisture Content - Silty Clay . . . .	28
3	Target Density and Moisture Content - Buckshot Clay . . .	28
4	Target Density and Moisture Content - Silty Sand . . . .	31
5	Revised Target Density and Moisture Content . . . . .	32

<u>Table No.</u>		<u>Page</u>
6	Design Traffic . . . . .	33
7	Summary of Estimated In Situ and Target Stress Conditions . . . . .	42
8	Summary of Test Conditions for Repetitive Load Tests . .	64
9	Summary of Test Data for Static Load Triaxial Tests . . .	65
10	Summary of Resilient Axial Strain and Resilient Modulus . . . . .	67
11	Summary of Repeated Axial Stress and Resilient Axial Strain Data - WES and University of Illinois Tests . . .	93
12	Summary of Stress Ratio and Permanent Axial Strain at 75,000 Repetitions . . . . .	95
13	Effect of Changes in Density on Failure Deviator Stress - Silty Clay . . . . .	100
14	Effect of Changes in Density on Failure Deviator Stress - Buckshot Clay . . . . .	102
15	Effect of Changes in Density on Failure Deviator Stress - Silty Sand . . . . .	103
16	Summary of Variables Used in Statistical Analysis . . . .	119
17	Actual and Estimated Values of A and B Parameters, and Permanent Axial Strain at 75,000 Load Repetitions . . .	121
18	Layer Thickness and Midlayer Stress Values Used in Stress Calculations . . . . .	123
19	Layer and Total Deformations - Rigid Pavement Subgrade . . . . .	124
20	Layer and Total Deformations - Flexible Pavement Subgrade . . . . .	125
21	Comparison of Compressive Strength Values from Static Load Tests . . . . .	129

## INTRODUCTION

### BACKGROUND

In the design of airport pavements, one of the first considerations must be an evaluation of the foundation material, or subgrade, on which the pavement is to be built. If the natural or in situ soil is sufficient to serve as a foundation material for the pavement and to withstand repeated loadings of aircraft traffic without shearing or undergoing excessive deformation, the subgrade may simply be graded or cut to the desired elevation and the pavement structure constructed directly thereon. If, however, the in situ soil is not suitable, or because of elevation considerations, a fill embankment is needed to provide a suitable subgrade for the overlying pavement, then the determination of design density values for compaction of the fill material becomes an important step in the overall design process.

The importance of adequate density cannot be overemphasized, and since densification of a soil may be achieved through compaction, the significance of proper compaction procedures is apparent. Some of the major reasons for compacting or densifying subgrade soils are to reduce compressibility, increase strength, control volume change characteristics, decrease permeability, control resilience properties, and reduce frost susceptibility.<sup>1</sup> Thus, a wide range of soil properties may be influenced by the compaction process. The mechanics of compaction and means of evaluating various characteristics of compacted soils have been discussed in great length in the literature.<sup>1-3</sup>

In the pavement design procedures used by the Federal Aviation Administration (FAA),<sup>4</sup> the engineering properties of the subgrade soil that are of primary concern are the compressibility and strength characteristics. The first consideration, compressibility, is satisfied in design by means of compaction criteria that specify minimum density values to which a soil must be compacted in the field to provide a satisfactory foundation material. Inherent in the density specifications is the requirement that the material also be compacted near the

optimum water content for the compaction effort used in order to prevent the development of excessive pore pressures and subsequent shear failure that might result from further densification. Densification may also occur without the development of shear, however, resulting in failure through loss of soil volume.

Density criteria, often termed compaction requirements, are essentially empirical and were developed based almost entirely on field observation and performance data. For example, compaction criteria developed by the U. S. Army Corps of Engineers (CE) for flexible pavements<sup>5</sup> were the result of an extensive study of existing airfields. The density criteria that were developed from this study were basically evolved by separating density values found in the subgrades of pavements that were performing satisfactorily from those found in pavements that did not perform adequately. Thus, the density values now found in the criteria are designed to ensure that if a subgrade soil is compacted as required, the compressibility potential of the material is minimized and the subgrade will sustain repetitive traffic loadings without excessive permanent deformation. Very large cumulative subgrade deformation can result in the development of premature pavement deterioration evidenced by surface rutting in flexible pavements and slab cracking in rigid pavements.

The soil strength parameter on which the design thickness of a pavement is based, whether it be California Bearing Ratio (CBR) or modulus of soil reaction (k), is not a directly controlled property of the soil but a resultant property dictated by the soil density and water content. In other words, if a particular soil is compacted at or near the optimum water content, the soil strength may be said to be primarily a function of the density obtained as a result of compaction. The density criteria with which this study will be involved are those specified by the FAA for subgrades in fill sections.<sup>4</sup> Table 1 presents these criteria.

Table 1 shows the density criteria specified in terms of a percentage of the maximum laboratory dry density obtained with ASTM Designation: D 1557.<sup>6</sup> The procedure is practically identical with the

Table 1. FAA Compaction Criteria, Fill Section

Pavement Type	Required Dry Density (Percent ASTM D 1557 Maximum Dry Density)	
	Cohesive Soil	Noncohesive Soil
Rigid	90	Top 6 in. 100 Below 6 in. 95
Flexible	Top 9 in. 95 Below 9 in. 90	Top 9 in. 100 Below 9 in. 95

Note: 1 in. = 2.54 cm.

CE compaction effort termed CE 55\*.<sup>7</sup> For these criteria, a noncohesive soil is one having a plasticity index (PI) of less than 6 percent. All other soils are considered to be cohesive materials. For a rigid pavement, the criteria specify that a cohesive soil be compacted to a minimum density of 90 percent for the full depth of the soil, the top 6 in. (15.24 cm) in noncohesive soil be compacted to 100 percent, and the remainder of the fill to 95 percent for the full depth. For a flexible pavement, the criteria require a minimum dry density of 95 percent for the top 9 in. (22.86 cm) in a cohesive soil and 90 percent for the remainder of the fill. For noncohesive soils, the top 9 in. (22.86 cm) of subgrade must be compacted to 100 percent while the remainder of the fill requires a minimum density of 95 percent.

The stringent density values required and their imposition for the full depth of a fill have at times been questioned. First, a review of the density criteria for cut sections will reveal that in subgrades of this type the criteria specify decreasing density values with increasing depth. The rationale applied for cut section soils appears to be that since stresses applied at the surface of a pavement tend to attenuate with depth, then an accompanying decrease in required density is also appropriate. The question then arises as to the applicability of a similar pattern of gradually decreasing densities with

\* The term CE 55 refers to a Corps of Engineers laboratory compaction procedure in which the compaction used in molding the soil specimens requires 55,000 ft-lb/ft<sup>3</sup> (2660 kJ/m<sup>3</sup>) of compaction energy.

depth for compacted soils. Second, the criteria as they now stand distinguish between soil types solely on the basis of cohesive or non-cohesive materials. Obviously different soils have different compactibility characteristics, and one soil compacted to 90 percent density will not necessarily exhibit compressibility similar to that of another type of soil compacted to 90 percent density. Compaction criteria based on soil type have, in fact, been proposed recently by other researchers.<sup>8</sup> A third factor that demands a review of current compaction criteria is one of economy of resources. Lower densities require less compaction effort and, therefore, the expenditure of less energy, construction time, and manpower.

#### OBJECTIVES OF THE STUDY

The overall objective of the study was to determine the potential impact on pavement performance of reducing density requirements now generally specified by the FAA for compacted subgrade soils in airports. To accomplish this overall objective, the following associated objectives were pursued:

- a. Investigate the deformation characteristics under repetitive axial loading of certain subgrade soils compacted to density levels below those generally specified for airport pavements.
- b. Determine the significant parameters that contribute to observed deformation patterns.
- c. Relate the deformation characteristics of these soils to pavement deterioration potential.
- d. Determine therefrom whether a basis exists for modification of current density criteria for compacted subgrade soils.

#### SCOPE OF WORK

This investigation was primarily a laboratory study based on the concept of observing the deformation response of three different soils tested in a triaxial compression chamber and subjected to repetitive axial loadings. From the observed behavior, a predictive framework was formulated and used to estimate the field response of similar soils in a subgrade environment. The principal steps involved in conducting this study were as follows.

#### SOIL TYPES

The original concept in this study was to evaluate five soil types of significantly different geological origins. However, due to equipment difficulties and specimen loss, circumstances dictated that only three soils could be tested.

#### SOIL DENSITY AND MOISTURE CONTENT

Since the concept of the study was to investigate the estimated impact of relaxing current density criteria, it was determined that for each soil type the study should include one group of specimens prepared at the lower end of the current density criteria spectrum and two groups molded at densities below current density specifications. Since field specifications generally require that soils be compacted at moisture contents centering around some optimum value, it was decided that the desired test moisture content would be near the optimum moisture content for the particular density value selected.

#### TEST STRESSES

It was desired that the stress values for the repetitive load tests should be representative of the stresses found in the subgrade of a pavement at a typical present-day airport having a high volume of traffic and including heavy wide-bodied aircraft. For each group of soils, three stress states were used. Thus, for each soil type, nine tests were required.

#### STRESS WAVE FORM

In much of the previous work conducted involving repetitive load triaxial testing on pavement materials, various types of wave forms have been used including full sine, approximate sinusoidal, triangular, and square wave.<sup>9-11</sup> For this program, it was felt that to be more representative, the wave form used should duplicate as closely as possible that generated at a particular point in the subgrade by an aircraft approaching, passing directly over, and moving away from the point. Therefore, special wave forms were developed based on stress analysis of subgrades under rigid and flexible pavement structures.

#### LABORATORY TEST PROCEDURES

The primary method of testing was the repetitive load triaxial procedure similar to that used by Seed, Chan, and Monismith.<sup>12</sup> Static load triaxial tests were also conducted to determine the ratio of the repetitive stress to the deviator stress at failure.

#### DATA ANALYSIS

The primary responses of concern were the permanent and resilient axial strain of the soil specimens. These data along with information concerning specimen properties, engineering characteristics of the soil, and other parameters were analyzed by statistical methods. It was anticipated that based on the statistical analysis, a strain model or a group of submodels from which subgrade deformation could be estimated could be developed.

#### PAVEMENT DETERIORATION

Deterioration potential of each type of pavement was evaluated based on the assumption that subgrade deformation would result in flexure under a rigid pavement slab and in rutting in a flexible pavement structure. Rigid pavement deterioration would be a result of fatigue, and flexible pavement deterioration would be manifested by surface depression.

## REVIEW OF PREVIOUS STUDIES

The first extensive work involving the application of repetitive axial loading to soil specimens in a triaxial chamber is described in References 12-16.

Seed, Chan, and Monismith<sup>12</sup> conducted repeated load tests on Vicksburg, Mississippi, silty clay to determine the effects of repetitive loading on the strength and deformation characteristics. The specimens were compacted using kneading compaction procedures to density values in the range of 95 to 105 percent of the maximum modified American Association of State Highway and Transportation Officials (AASHTO) density and at saturation states ranging from 92 to 97 percent. The specimens were tested unconfined in a triaxial cell that was mounted on a frame having mechanical load levers. The desired load was obtained by means of weights placed in hangers suspended from the levers. The load levers were moved up and down to effect repeated loading by means of a double-action hydraulic piston activated by an electrically driven pump. Some significant conclusions from the investigations were: (1) up to 100,000 applications of a constant stress, the specimen deformation depends only on the number of stress applications and is independent of the frequency of stress applications within the frequency range of 3 to 20 applications per minute; (2) for the particular specimens tested, the soil may withstand a considerable number of stress applications without any apparent sign of significant deformation and then fail relatively suddenly after application of only a small number of additional applications; and (3) for identical specimens subjected to different test stress levels, it is possible to establish a relationship between the magnitude of stress and the number of stress applications causing the same deformation.

Seed and Chan,<sup>13</sup> later using the same procedures and similar soil, studied the effect of stress history and frequency of stress applications on the deformation characteristics of the soil. One of their conclusions concerning the effect of frequency on stress applications seemed to contradict somewhat earlier findings of Seed, Chan,

and Monismith.<sup>12</sup> They found that for specimens that had a high degree of saturation and showed some thixotropic strength gain, the effect of frequency of stress applications was significant, particularly for specimens at 95 percent saturation. The frequency effect was insignificant at water contents below optimum, which was apparently the condition of the specimens on which the earlier conclusion was drawn. They also found that the effect of stress history was significant. For example, two identical specimens of the silty clay at 91 percent saturation and under 14.2-psi (97.89-kPa) confining pressure were each subjected to 100 stress applications of a 5.6-psi (38.61-kPa) deviator stress after which each had indicated about 1.0 percent permanent axial deformation. For one specimen, the deviator stress was then increased to 7.1 psi (48.95 kPa). However, on the other specimen the deviator stress was continued at 5.6 psi (38.61 kPa) to 10,000 repetitions after which it was increased to 7.1 psi (48.95 kPa). Both specimens received a total of 100,000 load applications. Test results indicated that the specimen with only 100 applications of the 5.6-psi (38.61-kPa) stress deformed continually under the 7.1-psi (48.95-kPa) stress and after 100,000 applications indicated a total axial strain of 2.8 percent. The specimen receiving 10,000 applications of the 5.6-psi (38.61-kPa) deviator stress showed very little increase in axial deformation after 1,000 applications of the 7.1-psi (48.95-kPa) deviator stress and after 100,000 stress applications indicated a total deformation of 2.15 percent.

Another important observation reported from the study was the stiffening effect in the clay as a result of repeated load applications. They reported that, in general, a specimen of the clay would exhibit some amount of increased resistance to deformation after about 1,000 cycles of load repetitions but that a marked increase in deformation characteristics can be produced by numbers of applications in the range of 10,000 to 100,000.

They indicated that the explanation for this increase in stiffness may be attributed to a rearrangement of the structural arrangement of the clay particles rather than the densification of the specimen, particularly if the saturation level is rather high. They felt that

adsorbed water was possibly being extracted from between the clay particles, bringing them closer together at points of contact resulting in a strength increase. They support this concept by the fact that no similar stiffening effects are observed in sands.

Seed, McNeill, and de Guenin<sup>14</sup> further studied the stiffening effect of repeated loading on the strength characteristics of Vicksburg silty clay. Tests were conducted on specimens cut from 6-in.- (15.24-cm-) diam by 4-1/2-in.- (11.43-cm-) high samples that were molded using a kneading compactor. Each specimen was 1.4 in. (3.56 cm) in diameter and 4 in. (10.16 cm) in height and was maintained in a triaxial chamber for 10 days before tests were initiated.

Each specimen was placed under a confining pressure of 1 kg/cm<sup>2</sup> (14.22 psi) and then subjected to 80,000 to 180,000 applications of a constant deviator stress sufficient to produce between 1 and 2 percent of permanent axial strain during a four-day period. Each specimen was then removed, placed in another cell under similar confining pressure, and tested to failure using standard static load triaxial testing techniques. Duplicate specimens of the silty clay that had not been subjected to repeated loading were then tested to failure under similar static loading conditions. Test results indicated several significant differences between the two sets of specimens.

First, the specimens that were initially subjected to repeated loading showed significantly higher strengths than those not receiving repeated load applications. Second, the form of the static load stress-strain curve for the two sets of specimens differed significantly. For the specimens subjected to repeated loading, the stress-strain curve increased to a peak value and then decreased to some residual strength level, whereas the stress-strain curve for the specimens not subjected to repeated loading simply increased until the specimens failed at a strength level generally equal to the residual strength level of the repetitively stressed specimens. In addition, the initial slopes of the curves for the specimens receiving repetitive loading were generally higher, indicating greater stiffness.

To study the effect of density increase, one specimen was

subjected to 90,000 load applications and a hypothetical final density was calculated based on the assumption that all deformation of the specimen was vertical with no lateral expansion. The specimen was then tested to failure under static triaxial conditions. This curve was then compared with a similar stress-strain curve that was developed for a soil that was initially compacted to identical conditions of moisture content and density. The conclusion reached was that the specimen densified by repetitive loading would in all cases have a higher strength even though both had the same density and water content.

Seed and McNeill<sup>15</sup> conducted tests on two soils of low plasticity to study their deformation characteristics under static and repetitive triaxial loading. One soil was the Vicksburg silty clay previously studied,<sup>12-14</sup> and the other material was a clayey silt soil taken from the subgrade of the Idaho road tests. Liquid and plastic limit values for both materials were practically the same. Compacted specimens of both materials at 35 to 90 percent saturation were tested to failure in a static triaxial device under a confining pressure of  $1 \text{ kg/cm}^2$  (14.22 psi). Duplicate specimens were subjected to 1000 applications of repetitive load testing under a  $1.25\text{-kg/cm}^2$  (17.78 psi) deviator stress and  $1\text{-kg/cm}^2$  (14.22-psi) confining pressure. By interpolating test results, it was possible to compare hypothetical test results for the two materials for similar stress or strain conditions. For example, an examination of the stress-strain curves for the static load triaxial tests indicated that specimens of the Vicksburg silty clay at a water content of 14.6 percent exhibited almost the same characteristics as specimens of the Idaho clayey silt at a water content of 21.3 percent. Similar comparisons of the static load curves were also found at higher values of moisture content. Extending the comparison of the repeated load tests, the investigators found that the plots of permanent axial deformation versus number of stress applications for the Vicksburg silty clay at 14.6 percent water content and the Idaho clayey silt at 21.3 percent water content in general were similar but did not compare as well as the stress-strain curves from the static load triaxial tests. For both soils at higher water content values, the curves did

not compare favorably and the correlation that had been observed for the static load tests generally was not found. For example, a specimen of Vicksburg silty clay at a water content of 17.1 percent indicated a static load stress-strain relationship similar to that of a specimen of the Idaho clayey silt at a water content of 22.8 percent. In the repeated load tests, both specimens indicated similar behavior for the first few cycles of loading, but after 1000 applications the Idaho soil had deformed about 50 percent more than the Vicksburg silty clay. In addition to the variance of response in permanent axial strain, the investigators reported that the resilient deformation of the two soils was considerably different.

Another important observation made by the researchers was the influence of the degree of compaction. They reported that

For both soils the higher the degree of compaction the smaller is the resilient deformation during repeated loading. However, for the Vicksburg silty clay the resilient strain changes only slightly for degrees of compaction ranging from 90 to 95 percent, while for a similar range of degrees of compaction the Idaho clayey silt shows an appreciable change in resilient deformation. Furthermore, for the range of degrees of compaction of practical interest the Idaho soil exhibits much higher resilient deformations than the silty clay.

At equal degrees of compaction the two soils require approximately equal stresses to cause 5 percent strain in the normal compression tests. In the repeated load tests, however, a specimen of the Idaho soil deforms about 50 percent more than a specimen of silty clay having an equal degree of compaction. This fact again indicates that deformation characteristics determined under normal loading conditions will not necessarily indicate the behavior of soil under repeated loading conditions.

Seed and Chan<sup>16</sup> conducted tests on a silty clay to determine the effect of thixotropy on the strain response under repeated loading. Specimens molded to a saturation state of about 95 percent were tested in a repetitive load device having a confining pressure of  $1 \text{ kg/cm}^2$  (14.22 psi) and a repetitive deviator stress of  $0.8 \text{ kg/cm}^2$  (11.38 psi) for 10,000 applications of stress. Various specimens were tested

20 min, 1 day, and 3 days after compaction. In each case, there was a decrease in permanent axial deformation with time elapsed since preparation of the specimen. Permanent axial strains for specimens tested 20 min, 1 day, and 3 days after compaction were about 5.0, 3.8, and 3.1 percent, respectively. Thus, it appears that the rate of strength increase would begin to decrease after 1 day. In the same study, the investigators examined the effect on thixotropy of molding water content using standard triaxial tests to measure changes in soil stiffness.

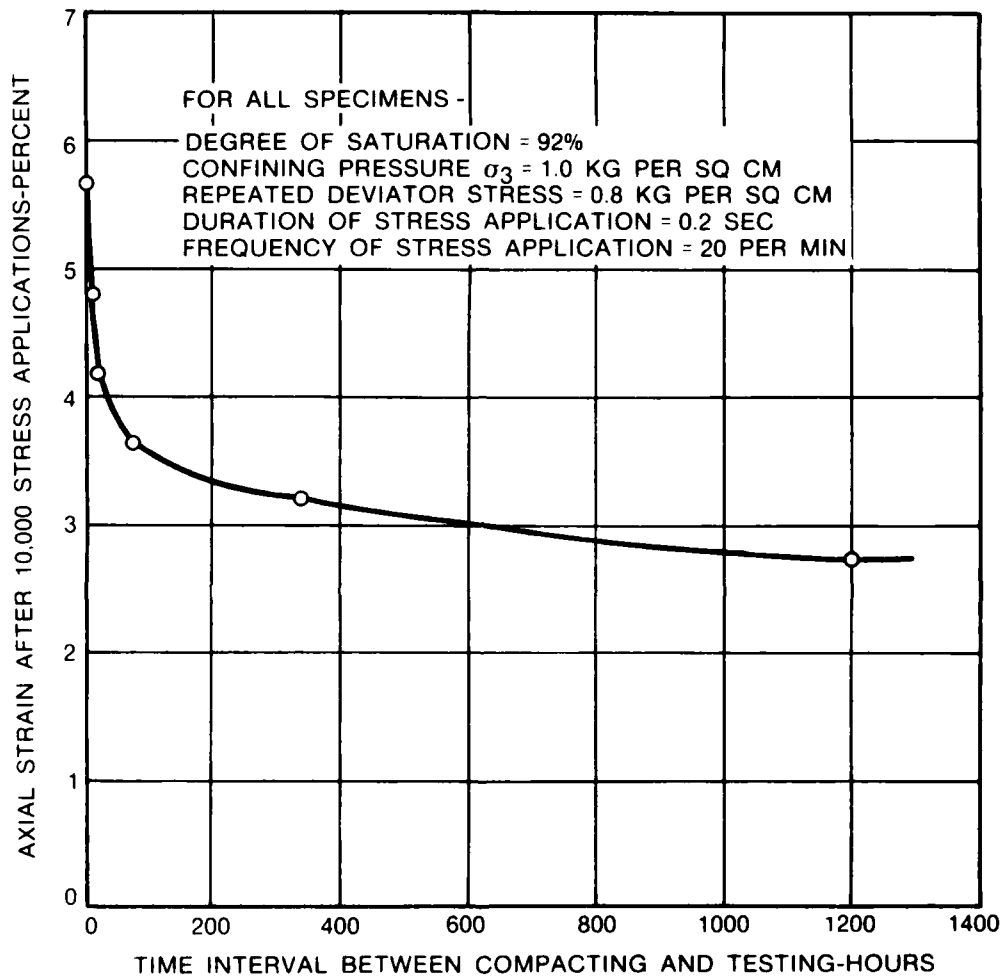
Their conclusions were:

1. that thixotropic effects became increasingly significant at smaller strains
2. that thixotropic effects are relatively small for samples compacted on the dry side of optimum for the compactive effort being used, and
3. thixotropic effects even after 1 week may be quite appreciable for samples compacted on the wet side of optimum.

In their study, they also investigated the response of specimens tested at longer time intervals after molding; i.e., 0, 1, 3, 7, 14, and 28 days. All specimens were tested at  $1 \text{ kg/cm}^2$  (14.22 psi) confining pressure and  $0.8 \text{ kg/cm}^2$  (11.38 psi) repetitive deviator stress. A significant conclusion was that a 3-day storage period prior to testing caused a reduction of almost 50 percent in the axial deformation of the specimen, and further reduction resulted from longer periods of storage.

A plot of axial strain after 10,000 stress applications versus time intervals between compacting and testing is shown in Figure 1. Although the investigators do not generally address the strength gain experienced in the 1- to 3-day period (24 to 72 hr) after molding, it would appear from Figure 1 that a significant part of thixotropic strength increase occurred during this period.

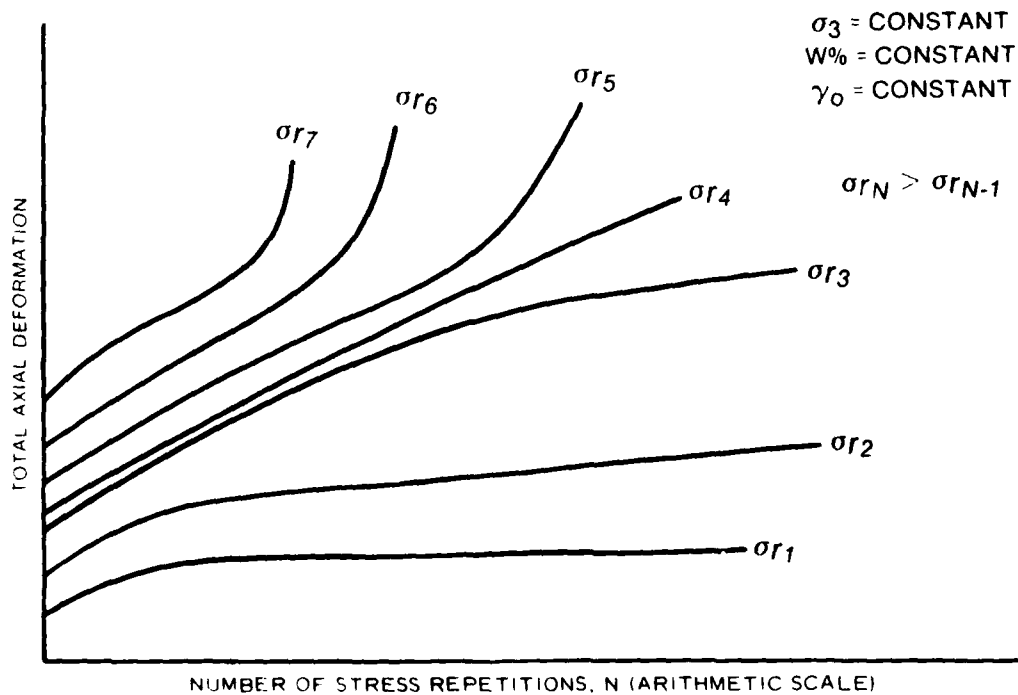
Kashmeeri<sup>17</sup> studied the effect of thixotropic strength gain under static loading of Vicksburg silty clay and Vicksburg buckshot clay. He found that for specimens compacted within a certain range of water contents on the wet side of optimum, a significant increase in shear strength was observed even after 1 day of storage.



(Reprinted with permission from the paper entitled "Thixotropic Characteristics of Compacted Clay" by H. B. Seed and C. K. Chan, *Journal of the Soil Mechanics and Foundations Division, Proceedings of the American Society of Civil Engineers*, Vol 83, No. SM4, November 1957)

Figure 1. Axial strain after 10,000 stress applications and interval of time between compacting and testing  
 (1 kg/cm<sup>2</sup> = 14.22 psi)

Larew,<sup>18</sup> and Larew and Leonards<sup>19</sup> conducted studies to investigate means of formulating strength criteria to define failure limits for soils subjected to repetitive axial loading. They postulated that the shape of the plot of total axial strain versus number of load repetitions depended largely on the ratio of the applied repetitive stress ( $\sigma_r$ ) to the stress at failure of the identical soil subjected to static axial loading ( $\sigma_f$ ). It was noted that other investigators had observed that for a given set of stress conditions, a soil specimen might withstand a considerable number of load repetitions without any appreciable deformation and then fail rather suddenly, often after only a small number of additional load repetitions, but that under a different set of stress conditions no distinct failure level may be observed. The general shapes of the hypothetical curves of total axial deformation versus number of load repetitions are shown in Figure 2.



*Reprinted from a paper entitled "A Strength Criterion for Repeated Loads" by H. G. Larew and G. A. Leonards with permission granted by the Transportation Research Board)*

Figure 2. General shapes of hypothetical curves

Three soils were tested: a micaceous silt, a limestone residual soil, and a sand-clay material. All specimens were partially saturated. Water contents centered around optimum and density values were between standard and modified Proctor maximum density. For most of the tests, the repeated deviator stress ranged from about 15 to 70 psi (103.41 to 482.58 kPa) with some tests having deviator stress levels as high as 200 psi (1378.8 kPa). Confining pressures were 5, 10, and 20 psi (34.47, 68.94, and 137.88 kPa). Most tests were carried to 60,000 to 80,000 cycles with some tests being carried to 400,000 cycles. Typical curves of permanent axial strain versus number of load repetitions obtained for the limestone residual soil are shown in Figure 3.

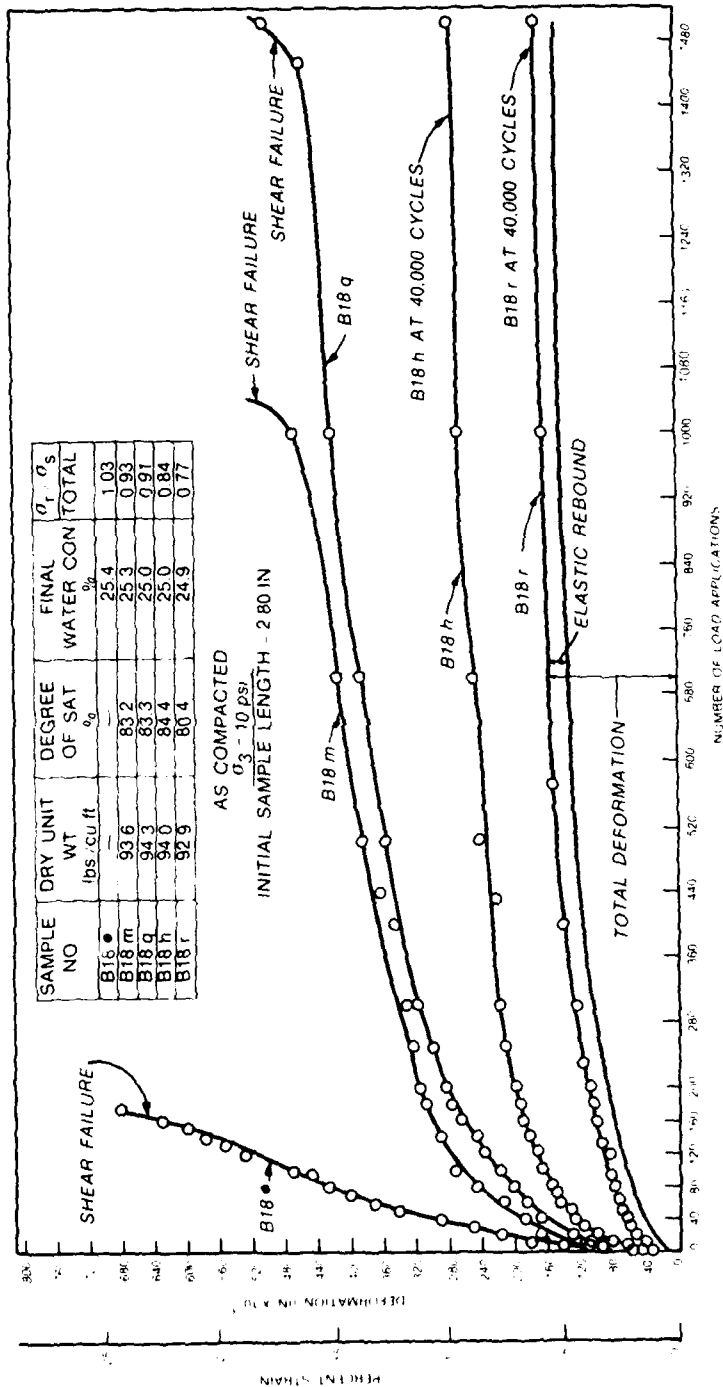
Larew<sup>18</sup> concluded that for the test conditions employed and the particular soils tested,

A critical level of repeated deviator stress,  $\Delta\sigma_r$ , exists at which the slope of the deformation versus number of repetitions curve is constant after the first few load applications. For levels of deviator stress in excess of this critical value, the deformation curves eventually turn concave upward, their slopes increase and the soil fails either in shear or by excessive deformation. For levels of deviator stress less than the critical value, the deformation curves eventually approach a horizontal asymptote.

The relationships between the ratio of the strength under repeated loads to the strength under static loads and dry unit weight, moisture content, compactive effort, and confining pressure are complex and no well-defined relationships could be determined from the tests performed.

The only values of critical stress ratio reported directly for a particular soil were for the limestone residual soil. These values of critical stress ratio ranged from 0.84 to 0.91.

Brown, LaShine, and Hyde<sup>20</sup> conducted repeated load tests on a compacted silty clay, termed Keuper Marl, that was back-pressure-saturated prior to testing. Tests were carried out in undrained conditions with pore pressures monitored. Overconsolidation ratios (OCR's) ranged from 2 to 20 and cyclic deviator stress ranged from 22.5 to 40.6 psi (155.12 to 279.89 kPa) with confining pressures ranging from 5.5 to 55 psi (37.92 to 379.17 kPa). Duplicate specimens were statically loaded to failure under similar confining conditions to determine



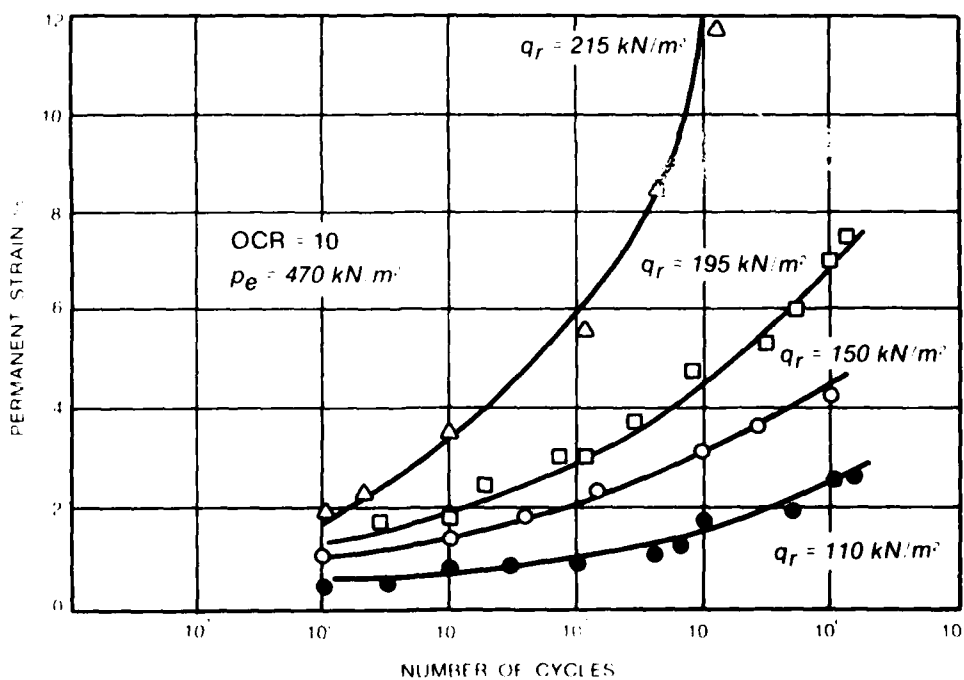
(Reprinted from a paper entitled "A Strength Criterion for Repeated Loads" by H. G. Larew and G. A. Leonards with permission granted by the Transportation Research Board)

Figure 3. Deformation versus number of load applications, limestone residual soil (1 lb/cu ft = 16.02 kg/m<sup>3</sup>; 1 psi = 6.89 kPa; 1 in. = 2.54 cm)

the ratio of the cyclic deviator stress to the deviator stress at failure under static load conditions. A typical set of curves of permanent axial strain versus number of repeated load cycles for an OCR of 10 is shown in Figure 4.

From Figure 4, it may be observed that there is a steady, distinct upturn of each curve for each repetitive stress level. The investigators<sup>20</sup> reported that in general there was a continued increase in permanent axial strain response even after one million strain repetitions and observed only three specific cases of apparent development of failure. They also stated in regard to the ratio of the repeated stresses to the static stress that a cyclic stress value in excess of 90 percent of the single load value may be required to include failure.

Townsend and Chisolm<sup>21</sup> studied the plastic and resilient properties of Vicksburg buckshot clay under repeated loading. Soil specimens



(Reprinted from a paper entitled "Repeated Load Triaxial Testing of a Silty Clay" by S. F. Brown, A. K. F. Shine, and A. F. L. Hyde with permission granted by the Institution of Civil Engineers)

Figure 4. Permanent axial strain versus number of load cycles (OCR = 10) ( $1 \text{ kN/m}^2 = 0.145 \text{ psi}$ )

were molded wet of optimum at densities at and below the maximum dry density obtained using the CE 12 compaction effort (12,000 ft-lb/ft<sup>3</sup> of compaction energy). Confining pressures were 2, 4, and 6 psi (13.79, 27.58, and 41.36 kPa) and repeated axial stress varied from less than 2 psi (13.79 kPa) to over 22 psi (151.67 kPa). The values of the repetitive axial stress were selected based on the unconfined compressive strength of the soil. Usually the repetitive axial stress levels applied to replicate specimens represented roughly 15, 35, 55, or 70 percent of the unconfined compressive strength, although the exact percentages varied somewhat. The laboratory tests were conducted in two phases. In the Phase I tests, only 1,000 load repetitions were applied to each specimen, whereas in the Phase II tests, 50,000 stress cycles were applied. An example of the test results for one group of Phase II tests is shown in Figure 5. The specimens are identified in terms of the CBR of the molded soil.

Since the primary objective of that investigation was to examine the effect of the CBR of the soil on the relationship between the elastic and the plastic strain, little of the analysis of the test data was applied specifically to the plastic response alone. Of primary interest are the general shapes of the curves of plastic strain versus number of load repetitions, as shown in Figure 5, and the relationship between stress ratio and "failure" of the test specimens under repetitive loading. For this study, "failure" is defined qualitatively as "when the rate of permanent strain increased with each additional load repetition, i.e., the curve approached the vertical." Based on this definition, it could be assumed from Figure 5 that for none of the curves shown was failure of the specimen observed, although the curve for the specimen tested at 55 percent of the unconfined compressive strength does indicate some increase in rate of permanent strain with increase in load applications. The investigators<sup>21</sup> indicated that no failures were observed in any of the tests, even up to a stress ratio of 70 percent.

Monismith, Ogawa, and Freeme,<sup>22</sup> in studying the contribution of subgrade deformation to rutting in a flexible pavement, tested a California silty clay subgrade material in repetitive loading. Specimens

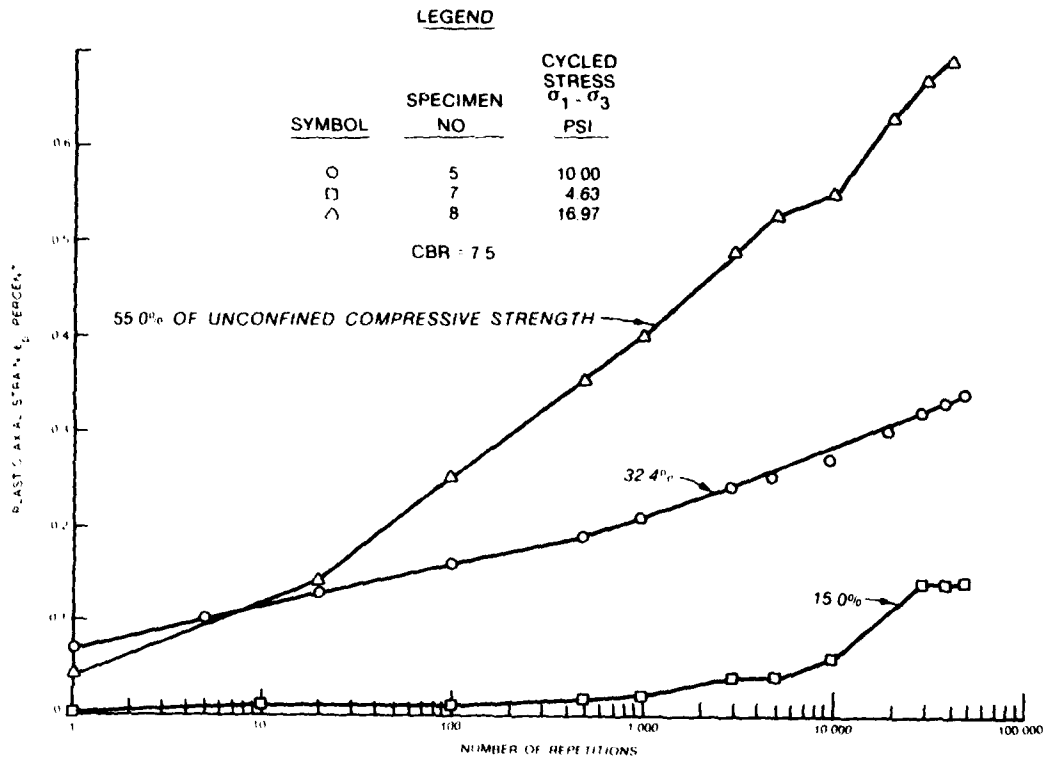


Figure 5. Effect of number of cycles on plastic axial strain for CBR = 7.5, Phase II tests (from Townsend and Chisolm<sup>21</sup>) (1 psi = 6.89 kPa)

were tested at dry densities of 90 to 95 percent of the maximum modified AASHTO dry density and at water contents from 16 to 20 percent. Optimum moisture content for this soil compacted using modified AASHTO effort was about 13 percent. All specimens were tested at confining pressures of 5 psi (34.47 kPa). The repeated axial deviator stress varied from 5 to 20 psi (34.47 to 137.88 kPa). Most specimens were tested to 10,000 cycles, although in some cases up to 100,000 load cycles were applied. Test data were presented in terms of plots of permanent axial, radial, and volumetric strain versus number of load repetitions. These investigators also presented a relationship between permanent axial strain and number of load repetitions. The general form of the equation, which

potentially may be used as a predictive basis for the estimation of rutting potential in the subgrade, is

$$\epsilon_a^P = AN^b \quad (1)$$

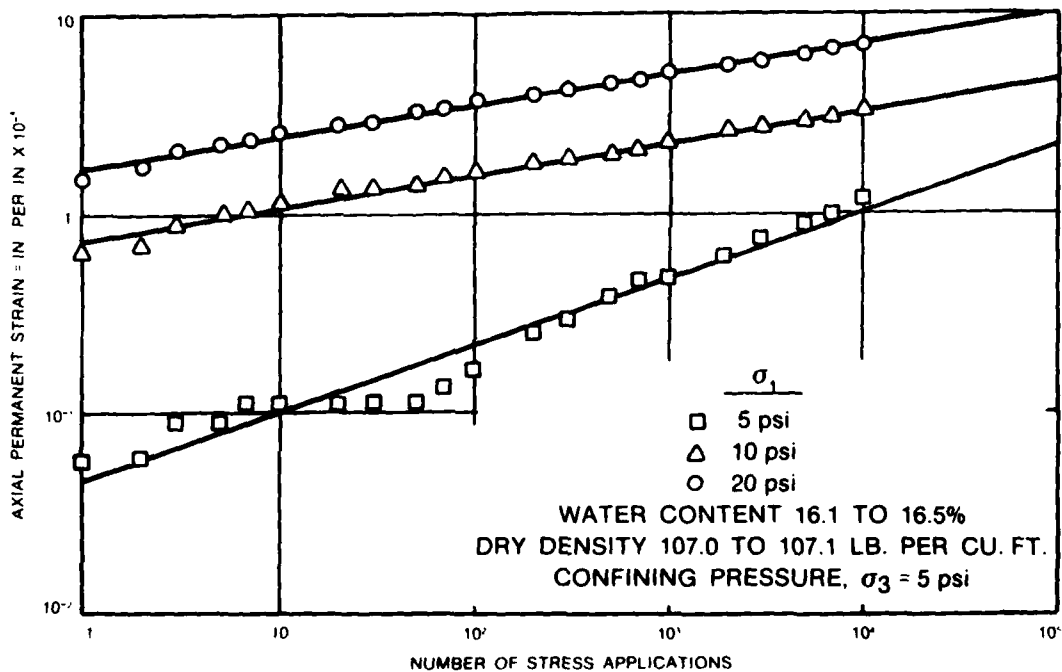
where

$\epsilon_a^P$  = permanent axial strain

N = number of stress applications

A, b = experimentally determined coefficients

Examples of the experimentally developed data along with the respective statistical log-log type relationships are shown in Figure 6.



(Reprinted from a paper entitled "Permanent Deformation Characteristics of Subgrade Soils Due to Repeated Loading" by C. L. Monismith, N. Ogawa, and C. R. Freeme with permission granted by the Transportation Research Board)

Figure 6. Axial permanent strain versus number of load applications, experimental data and statistical relationship (1 in. = 2.54 cm; 1 psi = 6.89 kPa; 1 lb/cu ft = 16.02 kg/m<sup>3</sup>)

Since the strain response depends not only on load repetition level but also is a function of the repeated axial stress, the following expression relating permanent axial strain and repeated axial stress was also presented.

$$\Delta\sigma_a = \frac{\epsilon_a^p}{l + m\epsilon_a^p} \quad (2)$$

where

$\Delta\sigma_a$  = repeated axial stress

$\epsilon_a^p$  = cumulative permanent axial strain at a specific number of stress applications

$l, m$  = experimentally determined coefficient

It may be noted that Equation 2 takes the general form of a hyperbola. This relationship is based on concepts presented by Kondner<sup>23</sup> using static load triaxial tests on fine-grained soils and work by Barksdale<sup>24</sup> using repeated load tests on granular soils.

Brown and Bell,<sup>25</sup> in a study on the permanent deformation characteristics of asphalt pavements, tested Keuper Marl, a silty clay subgrade soil, which was similar to the material investigated by Brown, LaShine, and Hyde earlier.<sup>20</sup> These two investigators characterized the relationship between the permanent vertical strain of specimens tested in repetitive loading and the number of load cycles as a semilog function as follows:

$$\epsilon_{vp} = b \log N \quad (3)$$

where

$\epsilon_{vp}$  = permanent vertical strain

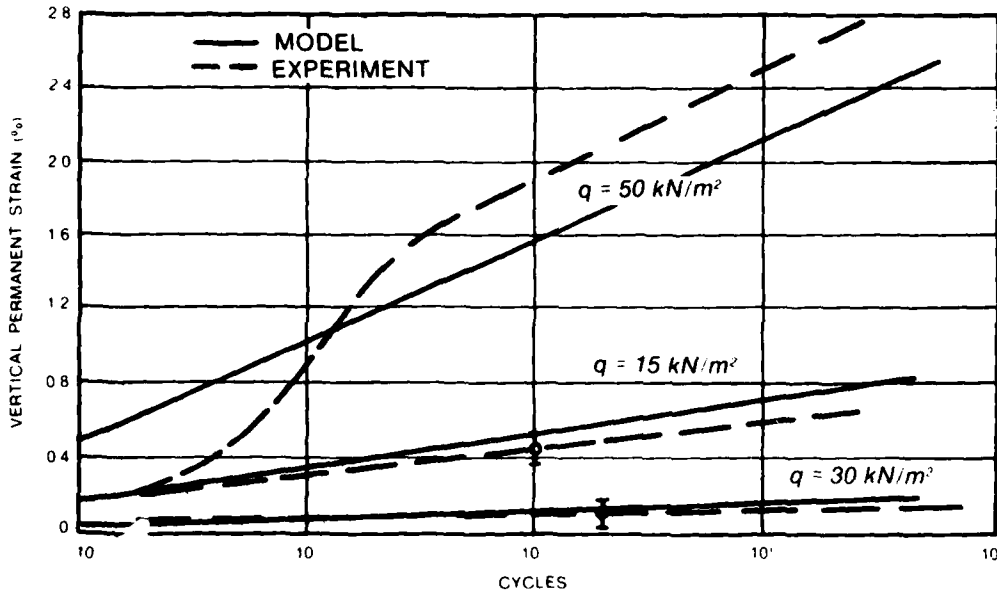
$N$  = number of load cycles

$b$  = a constant that was a function of the repeated deviator stress  $q$

They also noted that the relationship between the constant  $b$  and the deviator stress  $q$  depended on the moisture content and density of the soil. They further reported that for the main test program the soil was tested at an average water content of 17.4 percent and that the resulting equation for permanent strain is

$$\epsilon_{vp} = \left(\frac{q}{70}\right)^2 \log N \quad (4)$$

It was noted that Equation 4 was valid for values of  $q$  up to  $40 \text{ kN/m}^2$  ( $5.8 \text{ psi}$ ). Figure 7 is a comparison of test data for the Keuper Marl clay with curves generated from Equation 4.



(Reprinted from a paper entitled "The Prediction of Permanent Deformation in Asphalt Pavements" by S. F. Broun and C. A. Bell with permission granted by the Association of Asphalt Paving Technologists)

Figure 7. Comparison of test data for Keuper Marl clay and curves generated from Equation 4

## SELECTION OF TEST PARAMETERS

### SOIL TYPES

In determining the types of soils to be evaluated in this study, it was decided that the soils should vary with respect to grain-size and plasticity characteristics; however, all should be representative of typical subgrade materials. Three materials were selected: a silty clay (CL),\* a plastic clay (CH) termed buckshot clay,\* and a silty sand (SM).\* Although all materials were obtained in the Warren County, Mississippi area, each soil was of a different geological origin with varying engineering characteristics.

#### SILTY CLAY

The silty clay (CL) was a light tan loess material found in abundance in the uplands of Warren County. Origin of the soil is described by Snowden and Priddy:<sup>27</sup>

The Mississippi loess detritus was: (a) derived from outwash carried down the major glacier-draining stream valleys, (b) deposited on the Pleistocene Mississippi-Ohio Valley flats by outwash-choked braided streams, and (c) picked up and carried eastward by the prevailing winds, where it slowly settled on the dissected uplands.

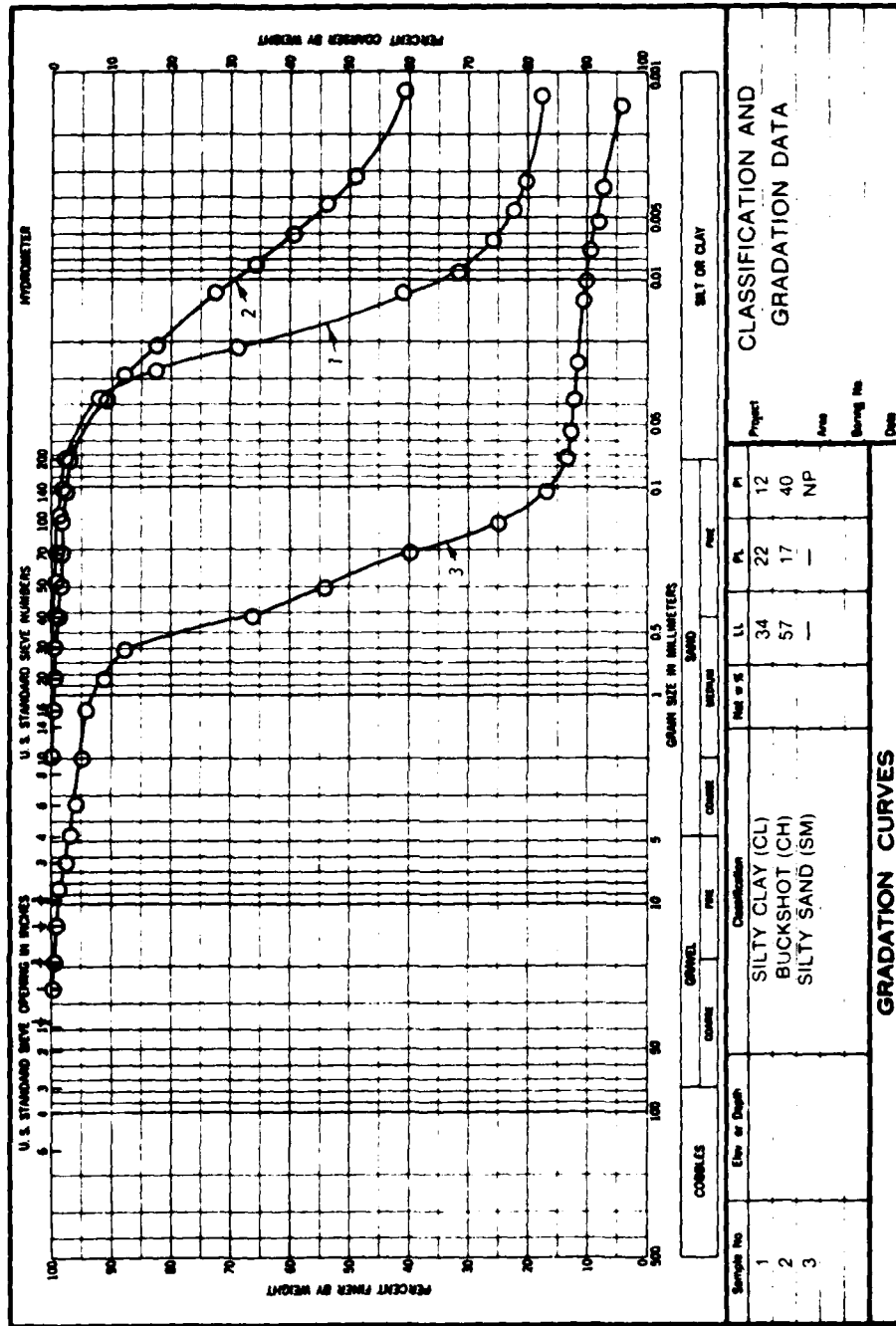
Gradation and classification data for the silty clay are shown in Figure 8. The soil was of low plasticity, having a liquid limit (LL) of 34, plastic limit (PL) of 22, and plasticity index (PI) of 12 percent.

#### BUCKSHOT CLAY

Buckshot clay (CH) is a highly plastic soil, so named locally because of its tendency upon drying to break into small cubes, which may become rounded by abrasion and thus tend to resemble a grouping of buckshot. The soil is dark brown and is found in backswamp deposits in the floodplain of the Mississippi River; thus it is a recent alluvium. The particular soil used in this study was obtained from deposits in the eastern margin of the Mississippi River floodplain.

---

\* Soils classified using ASTM Designation: D 2487.<sup>26</sup>



ENG FORM  
1 MAY 55 2087

Figure 8. Gradation and classification data for silty clay, buckshot clay, and silty sand soils (1 in. = 25.4 mm)

Gradation and classification data for this soil are also shown in Figure 8. The soil has a LL of 57, PL of 17, and PI of 40 percent.

#### SILTY SAND

The silty sand was a reddish brown nonplastic material found in the uplands of Warren County. The deposits from which the material was obtained were originally overlain by a blanket of loess 10 to 30 ft (3.05 to 9.14 m) thick that had been stripped away for access to the underlying sands and gravels which are controversially termed Citronelle formation and thought to be early Pleistocene or possibly Pliocene deposits.<sup>28</sup>

Classification and gradation data for the silty sand are shown in Figure 8. The material is fairly uniformly graded with over 70 percent of the soil particles being in the 0.1- to 0.5-mm (0.004- to 0.02-in.) range. Fines content, i.e., amount of soil passing the No. 200 sieve, was about 13 percent. As indicated, the minus 40 fraction was found to be nonplastic.

#### SOIL DENSITY AND MOISTURE CONTENT

In order to determine moisture content and density values at which soil specimens were to be molded for testing, current FAA compaction criteria were first reviewed. As indicated earlier, it was decided that test densities should be representative of values at the lower end and below those found in the criteria. Therefore, it was determined that target densities for the cohesive soils, CL and CH, would be 90, 85, and 80 percent of the maximum ASTM D 1557<sup>6</sup> laboratory dry density, and for the noncohesive soil, SM, target density values were 95, 90, and 85 percent.

In selecting appropriate values of moisture content at which the test specimens were to be molded, general field practice was followed; i.e., the specimens were to be molded to a moisture content as close as possible to the optimum moisture content. Therefore, the procedure followed for each soil was to first develop a "family" of moisture density curves from which a line of optimums could be defined. Then, based

on the specific target density, the appropriate moisture content could be determined at the line of optimums.

#### MOISTURE-DENSITY RELATIONS

Three different compaction efforts were used to develop a family of curves for the moisture-density relations. These were: the standard ASTM D 1557<sup>6</sup> procedure involving a compaction effort of 56,000 ft-lb/ft<sup>3</sup> (2688 kJ/m<sup>3</sup>) of energy for each specimen; a second relationship using an effort of 26,000 ft-lb/ft<sup>3</sup> (1248 kJ/m<sup>3</sup>); and a third relationship using 12,000 ft-lb/ft<sup>3</sup> (576 kJ/m<sup>3</sup>), which is similar to Standard AASHTO. All specimens were prepared using impact molding procedures with a 10-lb (4.54-kg) hammer having an 18-in. (45.72-cm) drop in a 6-in.- (15.24-cm-) diam by 4-1/2-in.- (11.43-cm-) high cylindrical mold.

#### INITIAL TARGET DENSITIES-- SILTY CLAY

Moisture-density relations for the silty clay soil are shown in Figure 9. Based on these relations, a line of optimums was developed by passing a line as closely as possible through the point of maximum density for each moisture-density curve. For this soil, the line of optimums represents a degree of saturation of about 87 to 88 percent. The maximum ASTM D 1557<sup>6</sup> density for this soil was 115.6 pcf (1851.73 kg/m<sup>3</sup>) at the optimum moisture content of 14.8 percent. As indicated previously, target density values for the cohesive soils were 90, 85, and 80 percent of the maximum ASTM D 1557 density. Therefore, specific target density values for this soil were 104.0, 98.3, and 92.5 pcf (1665.92, 1574.61, and 1481.71 kg/m<sup>3</sup>). Based on the position of these density values with respect to the line of optimums, the corresponding target moisture content values were 19.4, 22.2, and 25.3 percent. As can be seen, a density value of 90 percent represents a compaction effort considerably less than 12,000 ft-lb/ft<sup>3</sup> (576 kJ/m<sup>3</sup>). Therefore, in order to establish target density values of 85 and 80 percent, it was necessary to extend the line of optimums beyond that indicated on Figure 9. Therefore, these points are not shown. Target density and moisture content values are summarized in Table 2.

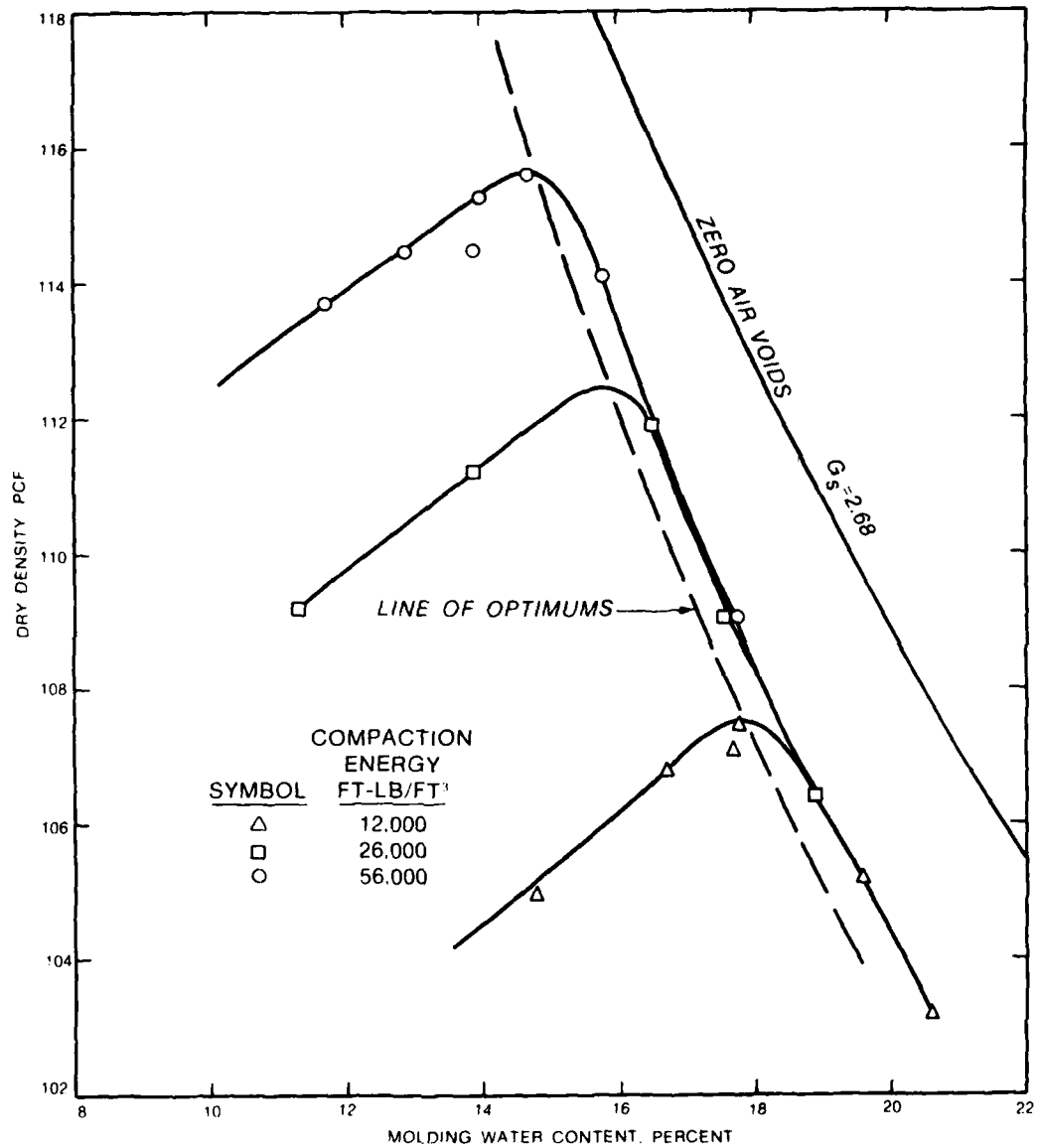


Figure 9. Moisture-density relations for silty clay  
 (1 pcf = 16.02 kg/m<sup>3</sup>; 1 ft-lb/ft<sup>3</sup> = 0.048 kJ/m<sup>3</sup>)

Table 2. Target Density and Moisture Content -  
Silty Clay

Density		Moisture Content percent
Percent ASTM D 1557	Actual pcf	
90	104.0	19.4
85	98.3	22.2
80	92.5	25.3

Note: 1 pcf = 16.02 kg/m<sup>3</sup>.

INITIAL TARGET DENSITIES -  
BUCKSHOT CLAY

Moisture-density relations for the buckshot clay soil are shown in Figure 10. The position of the line of optimums for this soil was determined using procedures previously described for the silty clay soil. The line of optimums for the buckshot clay represents a saturation value of about 87 to 90 percent. The maximum ASTM D 1557<sup>6</sup> density for this soil was 113.8 pcf (1823.08 kg/m<sup>3</sup>) at the optimum moisture content of 15.8 percent. Target density and moisture content values for this soil are indicated in Table 3.

Table 3. Target Density and Moisture Content -  
Buckshot Clay

Density		Moisture Content percent
Percent ASTM D 1557	Actual pcf	
90	102.4	21.0
85	96.7	23.7
80	91.1	26.1

Note: 1 pcf = 16.02 kg/m<sup>3</sup>.

INITIAL TARGET DENSITIES--  
SILTY SAND

Moisture-density relations for the silty sand are shown in Figure 11. For this soil, the position of the line of optimums was also determined graphically and represents a saturation value of about 70 to 75 percent. The maximum ASTM D 1557<sup>6</sup> density was 125.2 pcf

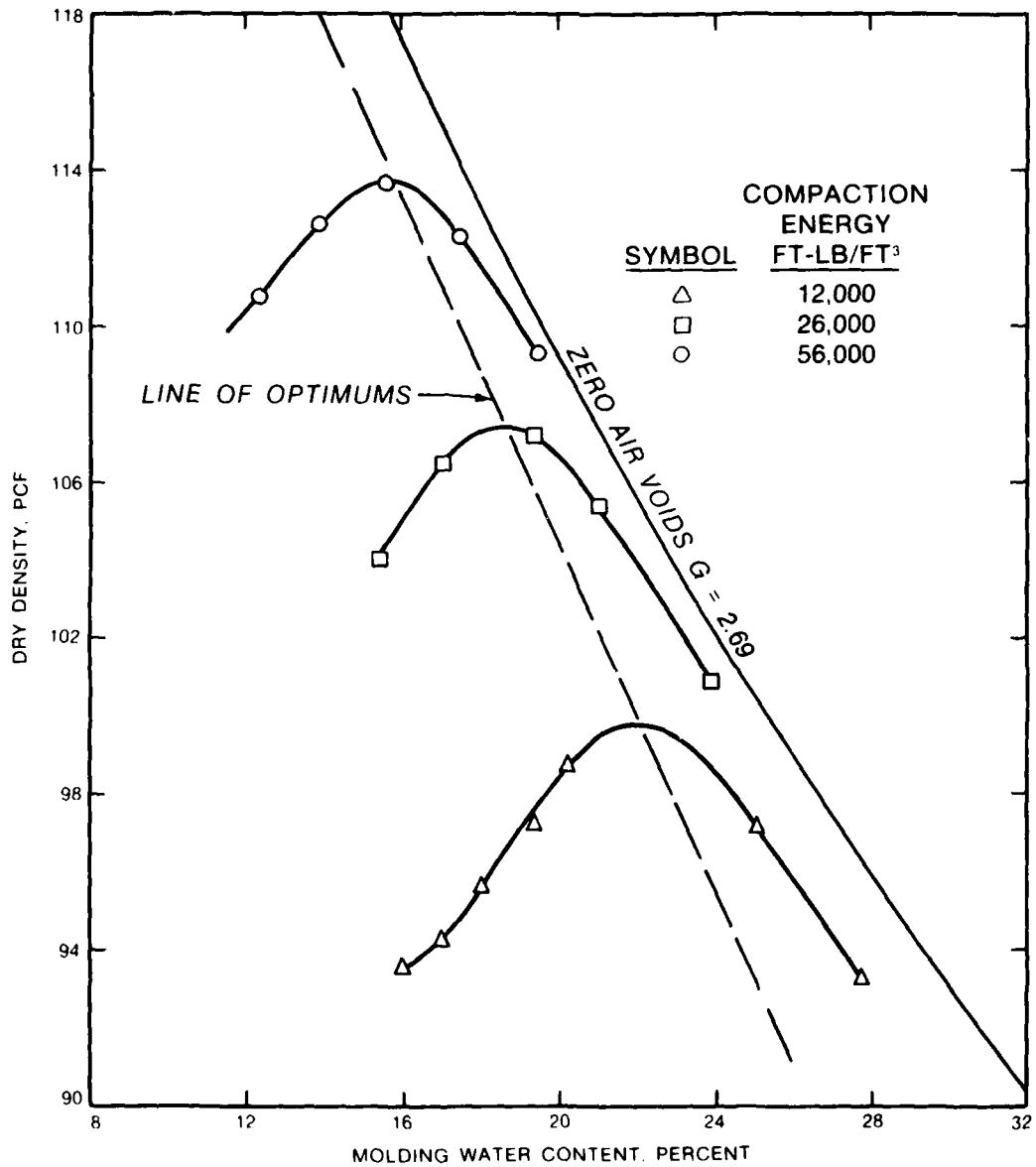


Figure 10. Moisture-density relations for buckshot clay  
 (1 pcf = 16.02 kg/m<sup>3</sup>; 1 ft-lb/ft<sup>3</sup> = 0.48 kJ/m<sup>3</sup>)

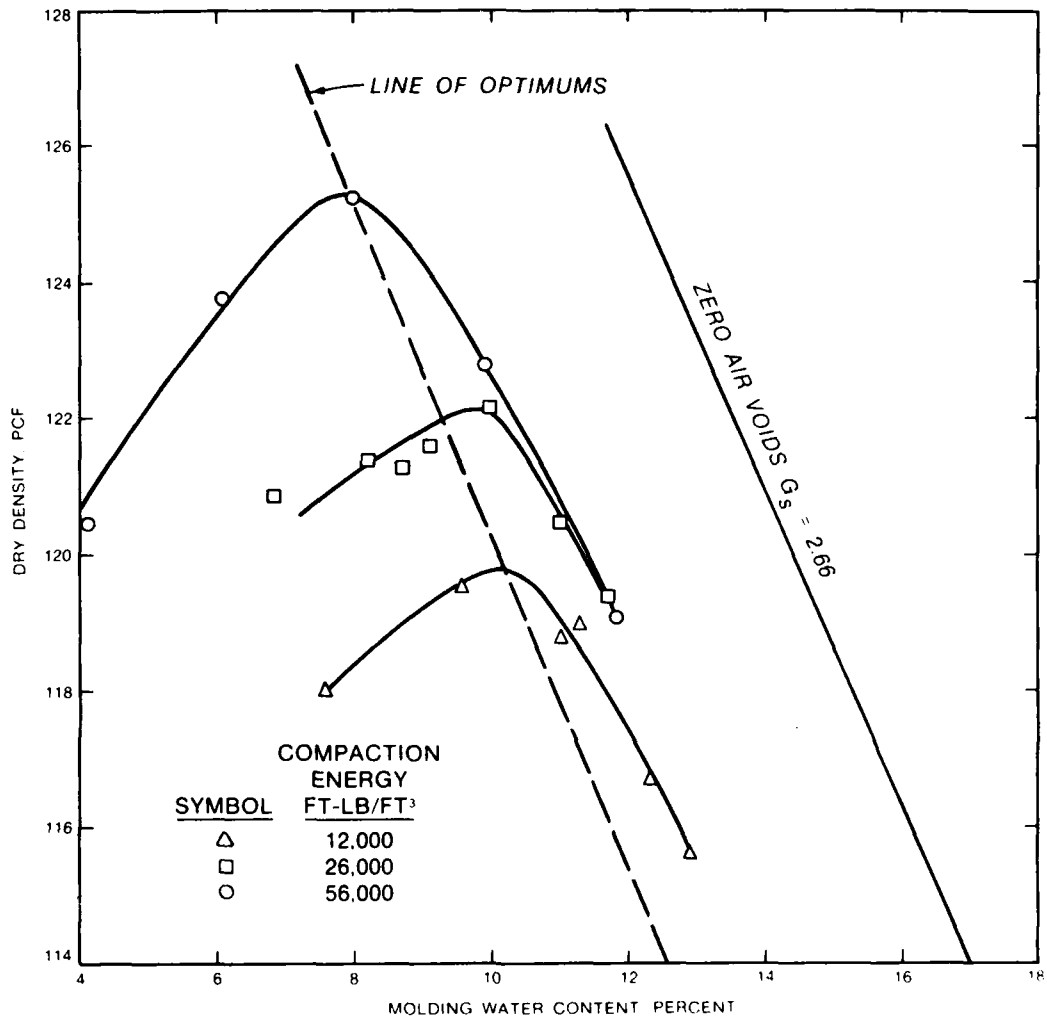


Figure 11. Moisture-density relations for silty sand  
 (1 pcf = 16.02 kg/m<sup>3</sup>; 1 ft-lb/ft<sup>3</sup> = 0.48 kJ/m<sup>3</sup>)

(2005.7 kg/m<sup>3</sup>) at the optimum moisture content of 7.9 percent. For the sandy soil, target density values were based on 95, 90, and 85 percent of the maximum value. The line of optimums was extended to determine the 90 and 85 percent density values. Target densities and moisture contents are indicated in Table 4.

Table 4. Target Density and Moisture Content - Silty Sand

Density		Moisture Content percent
Percent ASTM D 1557	Actual pcf	
95	118.9	10.6
90	112.7	13.1
85	106.4	15.7

Note: 1 pcf = 16.02 kg/m<sup>3</sup>.

#### REVISED TARGET DENSITIES

The repetitive load tests were conducted on a specimen-by-specimen basis. For each soil, the specimens having the highest target density were tested first, followed by those having the intermediate and lowest densities. During the course of the repetitive load test program, premature failure of the test specimens developed for two particular cases, the silty clay and the silty sand at the lowest target densities. Premature failure is defined as development of permanent axial strain exceeding 10 percent at less than 5000 load repetitions. In order to ensure that meaningful data would be produced, therefore, the target density array was revised to reflect an increase in these values. As will be shown later, it also became necessary to revise the applied repetitive stress levels for the silty sand tested at the lowest target density.

The revised target density and moisture content values for each soil are shown in Table 5. Target moisture contents are based on line-of-optimum values. The only revisions to the original target values are as follows: for the silty clay, the lowest target density was increased from 80 to 83 percent; and for the silty sand, the 85 percent target density was deleted and a revised target density of 92.5 percent was added.

Table 5. Revised Target Density and Moisture Content

Soil	Density		Moisture Content percent
	Percent ASTM D 1557	Actual pcf	
CL	90.0	104.0	19.4
	85.0	98.3	22.2
	83.0	96.0	24.5
CH	90.0	102.4	21.0
	85.0	96.7	23.7
	80.0	91.1	26.1
SM	95.0	118.9	10.6
	92.5	115.8	11.8
	90.0	112.7	13.1

Note: 1 pcf = 16.02 kg/m<sup>3</sup>.

#### STRESS STATES

Since one of the objectives of the study was to evaluate subgrade soil response under realistic levels of repeated stress, some means of estimating subgrade stress was first required. For this purpose, it was decided to develop structural designs for hypothetical rigid and flexible airport pavements and then, using the appropriate pavement response model, determine subgrade stress values. It was felt that the pavement designs should reflect a typical modern-day airport pavement subject to high volumes of heavy-load aircraft.

#### STRUCTURAL DESIGN OF PAVEMENTS

Hypothetical pavement designs were developed for both flexible- and rigid-type pavements based on design data for the Dallas-Fort Worth (DFW) Regional Airport.<sup>29</sup> Aircraft traffic data, based on a 20-year forecast, used in the design are presented in Table 6. These data indicate the estimated departures of different types of aircraft expected on one particular area of the airport. Departure data for the mixed aircraft assemblage were converted to equivalent departures of a design aircraft, the DC-8-61F, based on the relationship

$$\text{Log } R_1 = \text{log } R_2 \left( \frac{w_2}{w_1} \right)^{1/2} \quad (5)$$

where

$R_1$  = equivalent departures of the design aircraft

$R_2$  = departures of aircraft under consideration

$w_1$  = single-wheel load of design aircraft

$w_2$  = single-wheel load of aircraft under consideration

Table 6. Design Traffic\*

<u>Aircraft</u>	<u>Departures</u>
B707	266,742
B720	40,442
B727	705,691
B737	92,892
B747STR	207,758
DC-8-61F	55,881
DC-9	595,315
DC-10-CF	442,781
L-100-30	57,780
L-1011-1	7,446
L-500	85,483
CV580	40,515
CF880	1,752
Concorde	78,694

Note: Equivalent departures of DC-8-61F  
= 1,659,193.

\* Data taken from Reference 29.

Single-wheel load data for all aircraft were taken from Reference 30. The design traffic level of equivalent departures of the DC-8-61F was 1,659,193. The design subgrade strength, based on the DFW design data, was 5 CBR.

From these data, hypothetical designs for a flexible and a rigid pavement were developed, as shown in Figures 12 and 13, respectively. Both pavements were designed using current FAA procedures. The flexible pavement design required a total pavement thickness of 55 in. (139.7 cm) based on the subgrade CBR of 5. The rigid pavement thickness, based on a modulus of subgrade reaction  $k$  of 82 pci ( $227.14 \times 10^4 \text{ kg/m}^3$ ) and plain portland cement concrete (PCC) slab, was 20 in. (50.8 cm). As shown in Figure 13, for purposes of computation of subgrade stress, the rigid pavement was assumed to have a keyed joint as it was felt that

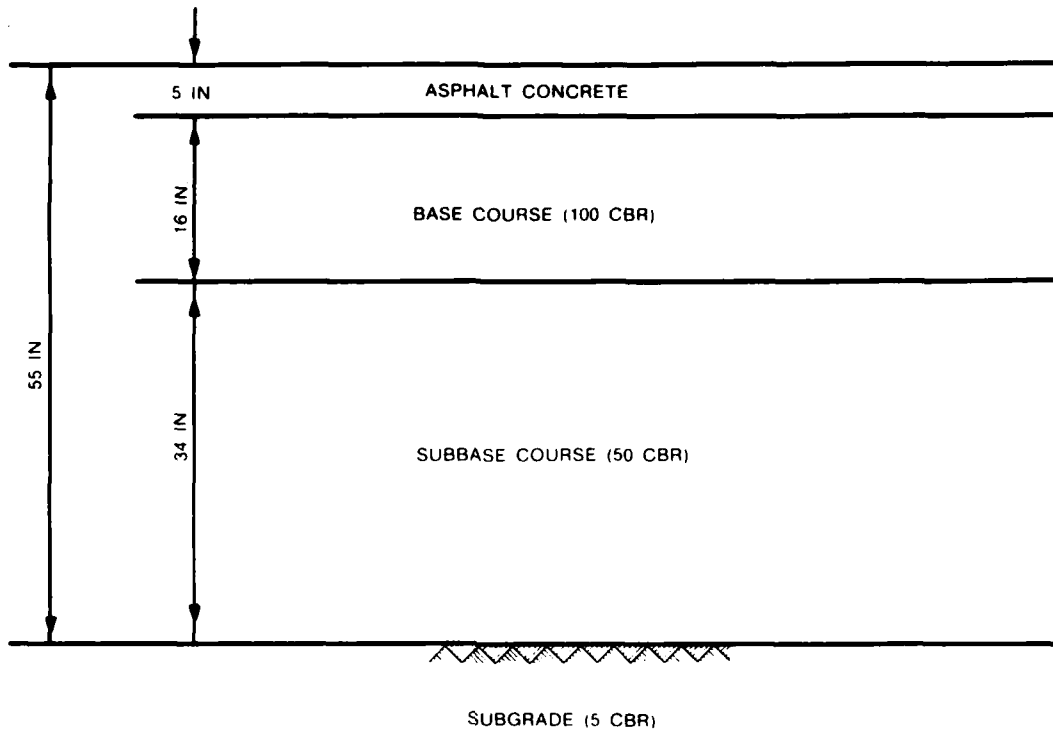


Figure 12. Flexible pavement design (1 in. = 2.54 cm)

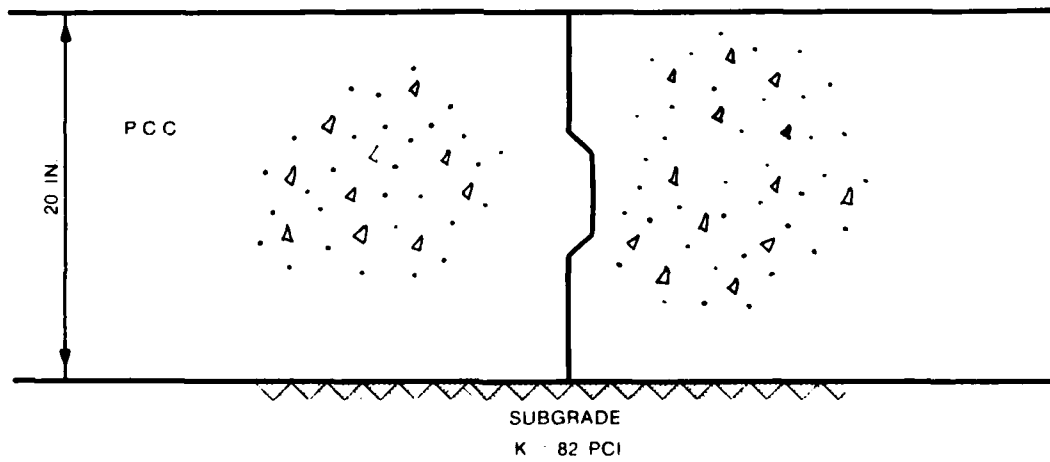


Figure 13. Rigid pavement design (1 in. = 2.54 cm;  
 $1 \text{ pci} = 2.77 \times 10^4 \text{ kg/m}^3$ )

this condition on the interior of a runway would result in higher subgrade stresses.

#### PAVEMENT RESPONSE MODELS

Two different computer codes were used in calculation of subgrade stress. For the flexible pavement, the BISAR<sup>31</sup> program was used, while the AFPVAV<sup>32</sup> code was used for the rigid pavement.

The BISAR model is layered elastic, with the pavement considered to be composed of horizontal layers of homogeneous, isotropic, elastic material that extend infinitely in the horizontal direction with each layer having a finite thickness except the bottommost layer which also extends infinitely downward. Inputs required are the structural characteristics and thickness of each layer, the load data, and the tire and assembly geometry. Material structural characteristics are expressed in terms of modulus of elasticity  $E$  and Poisson's ratio  $\nu$ . Wheel loads at the surface of the pavements are represented as circular plates of uniform pressure. The area of each plate is equal to that of the tire print for the particular wheel under consideration. For multiple-wheel loads, the center-to-center spacing of each plate is determined based on the geometry of the actual assembly configuration. Output of the program includes vertical and horizontal stresses, strain, and displacement at selected points in the pavement.

The AFPVAV code is a three-dimensional finite element computer program, which models a pavement system as an assemblage of prismatic solids. The program is based on a finite element code developed by Herrmann for elastic analysis of periodically (spatially) loaded solids.<sup>33</sup> For this program, a prismatic solid is defined as a body having a finite cross-sectional area (X, Y direction) but extending infinitely in the longitudinal (Z) direction, whose cross section is identical for all values of Z, and whose material properties do not vary in the Z direction.<sup>34</sup> The program may be used in the analysis of flexible, rigid, or composite pavements and was selected for computation of stresses in the rigid pavement because of the capability of incorporating discontinuities, such as joints, in the finite element grid. Unlike the layered

elastic codes, the pavement configuration using the AFPV has finite dimensions at the sides and bottom of the grid where they are confined by rollers and supports, respectively. Loading at the surface is effected by applying forces at the appropriate surface nodal points to simulate the contact pressure of an aircraft tire. Input to the program involves loading parameters, pavement geometry, and elastic constants,  $E$  and  $\nu$ , of the pavement materials. Output includes vertical and horizontal stress, strain, and displacement values. Computer work with the AFPV program was conducted by the Eric H. Wang Civil Engineering Research Facility, Albuquerque, New Mexico.

#### COMPUTATION OF STRESS VALUES

Loading data. Although structural design of pavements is based on a design aircraft that is usually representative of the majority of the types of aircraft expected on a runway, compaction criteria generally are based on the heaviest aircraft using the runway. Projected traffic data for the DFW design indicated that the Boeing 747 aircraft would probably be the aircraft having the largest gross weight of all expected aircraft. Reference 29 indicates that a current maximum gross weight for this aircraft is 778,000 lb (352,894.89 kg); however, the aircraft industry has for years speculated on future development of a 1,000,000-lb (453,592.4-kg) jumbo jet. Therefore, it was decided that the loading configuration for calculation of subgrade stresses would be that of a main landing gear of a Boeing 747 having an assembly load of 240,000 lb (1067.52 kN) and a gross aircraft weight of approximately 1,027,000 lb (465,839.39 kg). Wheel spacings and tire print data for this assembly are shown in Figure 14.

As can be seen, the assembly has a twin-tandem configuration with lateral and longitudinal (direction of traffic) spacing of 44 by 58 in. (111.76 by 147.32 cm). Based on test track data from past tests involving a similar full-scale assembly at the U. S. Army Engineer Waterways Experiment Station (WES),<sup>35</sup> a tire contact area of 286 sq in. (1845.16 sq cm) was assumed. With each wheel having an individual load of 60,000 lb (266.88 kN), the resulting contact pressure at the pavement surface would be about 210 psi (1447.74 kPa).

LOADING DATA

ASSEMBLY TYPE: TWIN-TANDEM  
ASSEMBLY LOAD: 240,000 LB  
WHEEL LOAD: 60,000 LB  
CONTACT AREA: 286 SQ IN  
RADIUS: 9.54 IN  
SPACING: 44 IN. x 58 IN

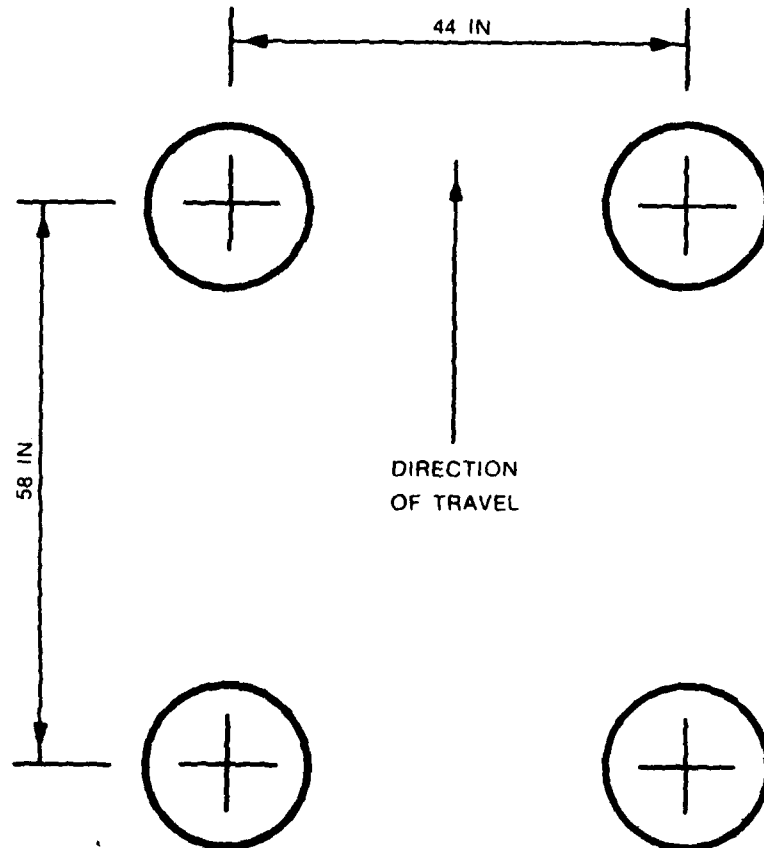


Figure 14. Loading configuration (1 lbf = 0.00444 kN;  
1 sq in. = 6.45 sq cm; 1 in. = 2.54 cm)

Materials characterization. Input to the BISAR program, which was used to calculate stresses in the flexible pavement, requires values of  $E$  and  $\nu$  for the subgrade and each of the materials comprising the pavement structure. For the subgrade, the values of the elastic modulus were selected based on the expression

$$E \text{ (in psi)} = 1500 \times \text{CBR} \quad (6)$$

which was developed by Heukelom and Klomp<sup>36</sup> from a study involving correlation between dynamic modulus and CBR. Thus, for a 5-CBR subgrade, a value of 7500 psi (51.71 MPa) was used for the subgrade modulus. A value of 0.4 was selected for Poisson's ratio. For the granular base and sub-base course materials, a procedure developed by WES personnel was used to determine appropriate values for E-modulus.<sup>11</sup> In this procedure, the base and sub-base course layers are divided horizontally into sublayers of approximately equal thickness. The modulus of each sublayer is dependent on the modulus of the layer below it and is determined using relationships that express the modulus of the layer in question as a function of the layer thickness and of the modulus of the layer directly below. Two such expressions are involved, one for base course materials and a second for subbase course materials. The relationship for base course materials is

$$E_n = E_{n+1} (1 + 10.52 \log t - 2.10 \log E_{n+1} \log t) \quad (7)$$

and the relationship for subbase course materials is

$$E_n = E_{n+1} (1 + 7.18 \log t - 1.56 \log E_{n+1} \log t) \quad (8)$$

where

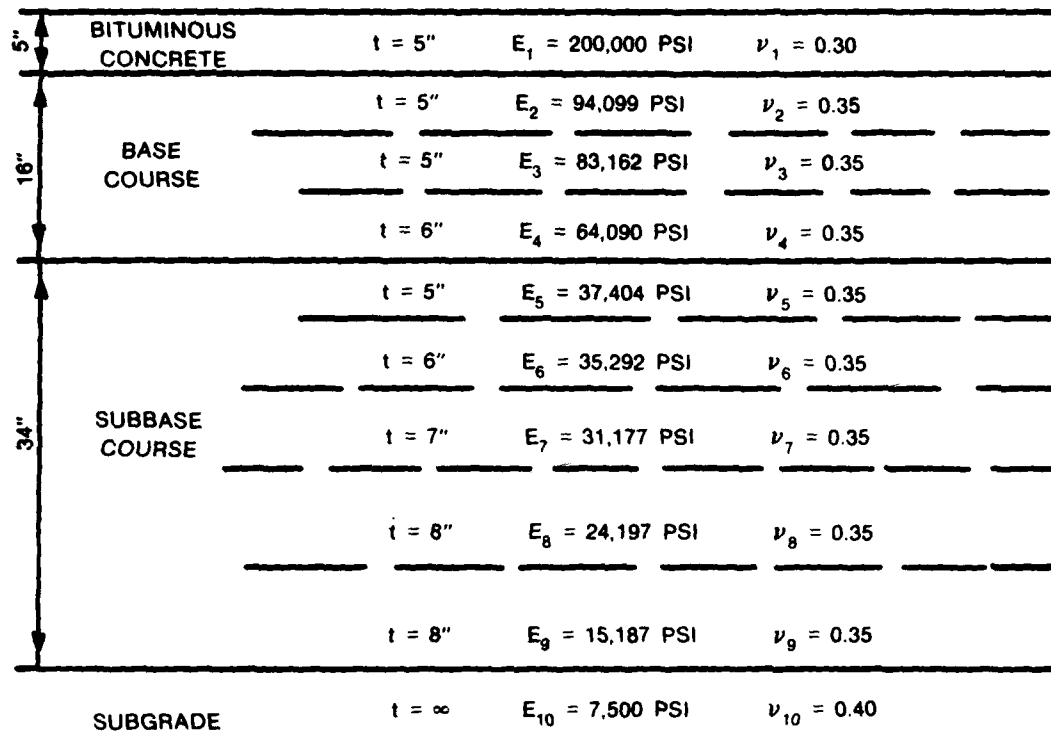
- $E_n$  = elastic modulus of layer in question
- $E_{n+1}$  = elastic modulus of underlying layer
- $t$  = thickness of layer in question

As shown in Figure 15a, the base and subbase courses were first divided into sublayers 5, 6, 7, and 8 in. (12.7, 15.24, 17.78, and 20.32 cm) thick. Then, beginning with the subgrade modulus (7,500 psi (51.71 MPa)) and using Equation 8, the modulus of the first sublayer in the subbase course was computed as 15,187 psi (104.71 MPa). This procedure was then repeated through the subbase course. The modulus of the lowest layer in the base course (64,090 psi (441.88 MPa)) was computed with Equation 7 based on the modulus of the underlying subbase course sublayer, 37,404 psi (257.89 MPa). The modulus of the remaining sublayers in the base course was then computed using Equation 7. For all base and subbase course layers, a value of 0.35 was used for Poisson's ratio.

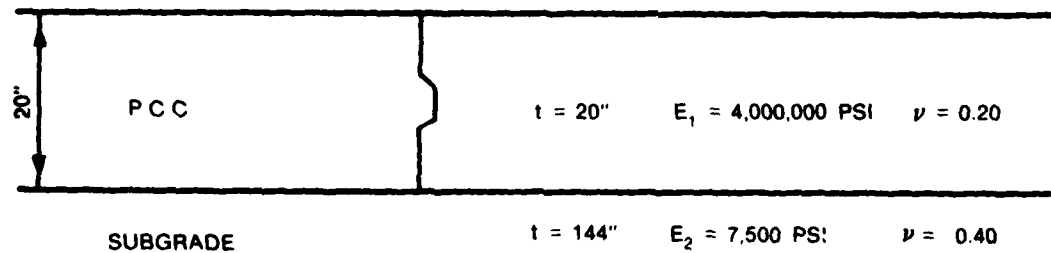
For the bituminous concrete, a value of 200,000 psi (1378.95 MPa) was used based on an average ambient temperature condition of about 80°F (27°C) since the stiffness of this material is temperature dependent. A value of 0.3 was used for Poisson's ratio.

The rigid pavement analysis, which was conducted with the AFPAV program, involved only two sets of elastic constants, one set for the subgrade and another set for the PCC slab. Values for  $E$  and  $\nu$  for the subgrade again were 7500 psi (51,71 MPa) and 0.4, respectively. Values of elastic constants for the PCC were selected based on those commonly used for concrete, i.e.,  $E = 4,000,000$  psi (27,579.03 MPa) and  $\nu = 0.20$ , as shown in Figure 15b.

Target stress conditions. Plots of maximum vertical stress versus depth for the rigid and flexible pavements are shown in Figure 16. An examination of these plots reveals that for the flexible pavement the computed stress at the top of the subgrade is about 9 psi (62.05 kPa), with uniform attenuation thereafter. At a depth of 95 in. (241.3 cm) below the surface, stress drops to less than 6 psi (41.37 kPa). For the rigid pavement, the computed stress at the surface of the subgrade was about 11 psi (75.84 kPa), with attenuation to about 7.5 psi (51.71 kPa) at 50 in. (127.0 cm). At a depth of 70 in. (177.8 cm), a stress value of 7 psi (48.24 kPa) is shown with very little stress attenuation indicated.



a. Flexible pavement



b. Rigid pavement

Figure 15. Elastic constants for flexible and rigid pavements (1 in. = 2.54 cm; 1 psi = 0.00689 MPa)

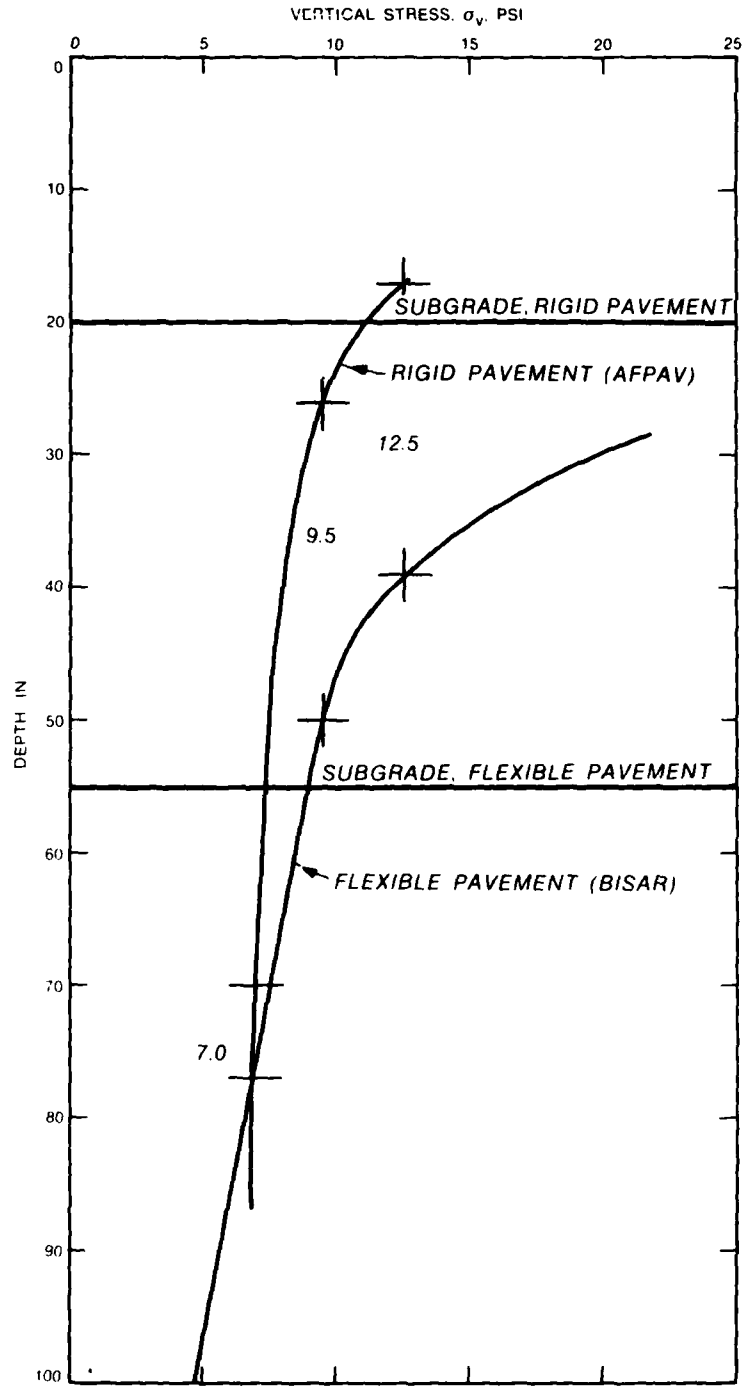


Figure 16. Vertical stress-depth relation for flexible and rigid pavements (1 in. = 2.54 cm; 1 psi = 6.89 kPa)

In selecting the appropriate stress levels for the laboratory tests, there were two particular items of concern: first, that the test stress values should if possible bracket those computed for the subgrade; and second, that the repetitive axial stress should be sufficiently high to produce meaningful permanent deformation in the laboratory soil specimens. Therefore, in order to satisfy these criteria, and based on the computed stress patterns indicated in Figure 16, it was decided that the laboratory tests would be conducted using repeated axial stress levels of 12.5, 9.5, and 7.0 psi (86.18, 65.50, and 48.24 kPa).

In addition to repetitive stress, it is also necessary to consider the in situ stress levels that are present in a subgrade under a pavement structure. Based on the depth in the pavement at which the stress levels selected for repetitive loading occurred, as well as on overburden forces and lateral earth pressure, specific values of vertical and lateral static pressure to be associated with each repetitive load were determined.

It was anticipated that in the laboratory tests the static lateral stress would be simulated by using a confining or chamber pressure of equal magnitude. By ensuring that an all-around confining pressure was employed, the vertical static stress could then be effected by applying a seated load equal to the difference between the lateral and the vertical static stress. A summary of the various stress conditions is shown in Table 7.

Table 7. Summary of Estimated In Situ and Target Stress Conditions

Test Condition	Estimated In Situ Stresses, psi		Static Stress for Tests, psi		Repeated Stress, psi $\sigma_r$
	$\sigma_v$ Vertical	$\sigma_H$ Horizontal	$\sigma_c$ Confining	$\sigma_s$ Seating	
1	3.5	2.0	2.0	1.5	12.5
2	4.5	2.5	2.5	2.0	9.5
3	5.5	3.0	3.0	2.5	7.0

Note: 1 psi = 6.89 kPa.

## WAVE FORMS

In most previous studies involving repetitive load testing, full sine, haversine, or square wave forms were used. In this investigation, it was desired to duplicate as closely as possible the stress patterns of rise, peak, and decay that a point in the subgrade would experience as an aircraft landing gear approaches, passes over, and departs from a position on the pavement surface directly above the subgrade point. In order to develop appropriate wave forms, computations were made, using the BISAR program and the flexible pavement design, of vertical stress at three points in the pavement and subgrade with the B747 load assembly at incremental distances from the point, proceeding from a distance 12.5 ft (3.81 m) away to a position directly over the point. Due to the symmetry of the stress patterns of rise and decay, computations for only one side from the point, or one-half of the total distance of 25 ft (7.62m) traveled, were required. In order to transfer the wave form from a spatial to a time frame, a situation was assumed wherein a taxiing aircraft would have a speed of about 15 mph (24.14 km/hr) or 22 ft/sec (6.7 m/sec). Therefore, total load/unload time of 1 sec was used for each pattern. Depths for each point at which wave forms were developed were selected based on the locations of the peak stress values of 12.5, 9.5, and 7.0 psi (86.18, 65.50, and 48.24 kPa) (Figure 17). From this figure, it can be seen that for the peak stress of 12.5 psi (86.18 kPa), the effects of the tandem wheels have not yet converged and a double-peak wave form is indicated. Convergence is shown for the other two wave forms. Figure 18 shows conceptually the axial static and repeated stress conditions applied to a typical soil specimen.

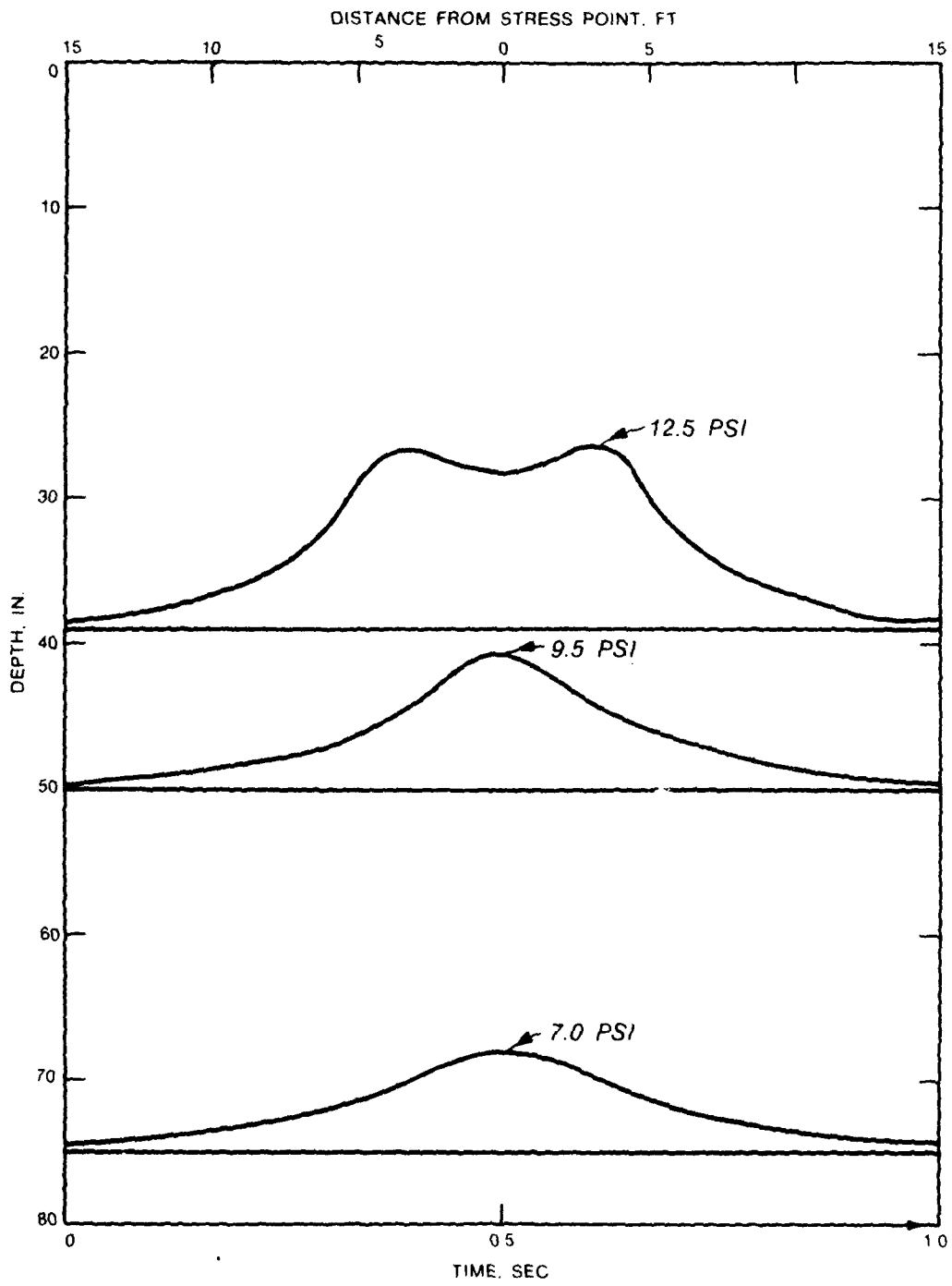


Figure 17. Stress wave forms used in repetitive load tests  
 (1 in. = 2.54 cm; 1 ft = 0.3048 m; 1 psi = 6.89 kPa)

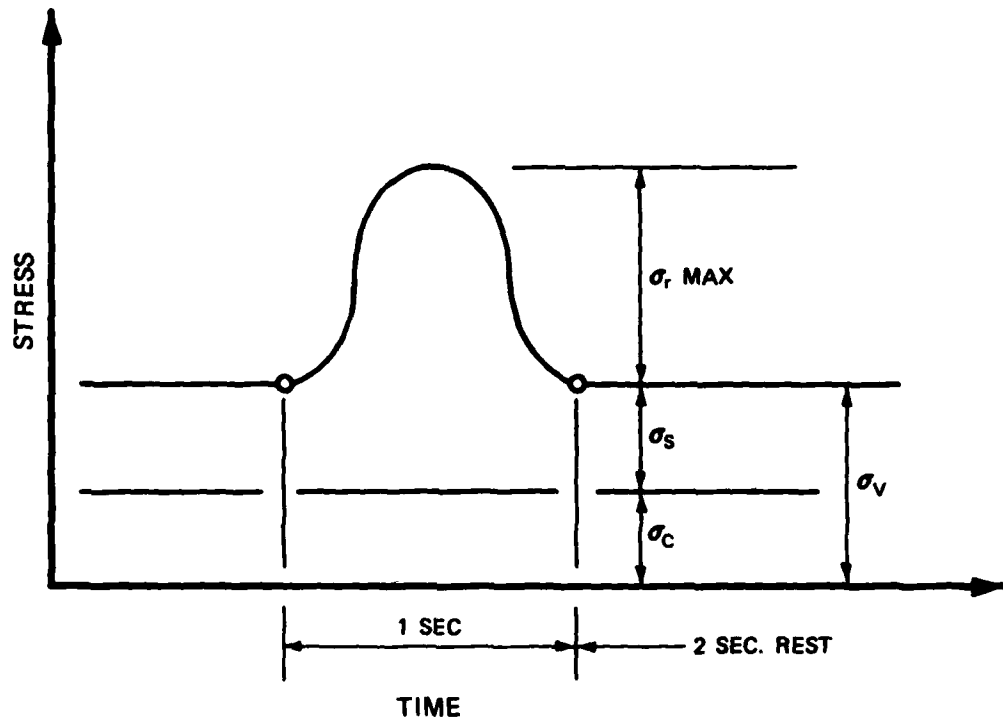


Figure 18. Axial stress conditions for typical repeated load test

PREPARATION OF SOIL SPECIMENS, REPETITIVE LOAD  
EQUIPMENT, AND TEST PROCEDURES

PREPARATION OF SOIL SPECIMENS

Quantities of all three soils were originally stored in 55-gal ( $0.21\text{-m}^3$ ) drums prior to processing. The silty clay soil was processed and tested first, followed by the buckshot clay and the silty sand. The first step in preparing the soils was to break the larger particles into smaller sizes to facilitate uniform moisture distribution. The soil was processed into smaller sizes by forcing batches of the silty clay and buckshot clay first through a screen of No. 4 hardware cloth ( $1/4\text{-in.} + 6.35\text{-mm} +$ ) opening) repeatedly until 100 percent of the material passed through and then through a No. 10 screen. The silty sand was processed only through the No. 4 hardware cloth in similar fashion.

The next step was to adjust the moisture content of the soil to the target value. For each target water content, an amount of soil estimated to be sufficient to prepare four specimens (about 4000 g (140.8 oz)) was processed. The dry soil was first placed in a stainless steel bowl, and water was added incrementally while the soil and water were mixed in a rotary blender. The prepared soil was then placed in a plastic container, which was sealed, and the soil was allowed to equilibrate for about 24 hr. After initial equilibration, the water content of the soil was again taken and any final adjustments in water content were then made. If a reduction in water content was required, the soil was aerated by forcing the material through a screen several times to facilitate drying. For soils requiring an increase in water content, additional water was mixed with the soil in the blender. After the final adjustment in water content, the soil was again allowed to equilibrate in sealed containers for 24 hr. It was desired that the final water content be within  $\pm 0.5$  percent of the target value.

The next step involved molding of the soil specimens. For the cohesive materials, procedures were developed by which one specimen was being tested while the next successive specimen was being molded, thus

providing minimum delay in the testing sequence. However, it was necessary to mold the silty sand specimens directly on the base of the repetitive load apparatus.

All soil specimens were cylindrical, having a diameter of 2.8 in. (7.11 cm) and a height of 6.0 in. (15.24 cm), and were molded using kneading compaction techniques.

For the cohesive soils, the specimens molded at the two higher target densities were prepared using a pneumatic kneading tamper while the specimens having the lowest target density were prepared by hand tamping. Specimen preparation consisted of first taking from the batched material an amount of processed soil slightly in excess of that needed to achieve the target density and then molding the soil in a split cylindrical mold in six layers of equal thickness. After compaction, the excess soil extended slightly above the top of the mold and was screeded off to provide a smooth, flat surface.

The pneumatic tamper (Figure 19) consisted of an air-driven ram to which was attached a circular steel piston having an end area of 1.54 sq in. (9.94 sq cm). The foot pressure and number of tamps per layer were varied to obtain the target density based on prior experimentation with both soils. The general objective was to have, as closely as possible, equal thickness among the six compacted layers and to obtain a specimen having a uniform density within  $\pm 1.0$  pcf ( $16.02 \text{ kg/m}^3$ ) of the target density.

For the silty clay, 10 and 20 tamps per layer were used for the intermediate and higher target densities with foot pressures varying from 3 to 10 psi (20.67 to 68.94 kPa). The buckshot clay specimens were prepared using 10 tamps per layer with foot pressures ranging from 9.5 to 17 psi (65.50 to 117.21 kPa).

Due to the higher water content and workability of both soils at the lowest target density, it was found that hand compaction was more suitable in order to control foot pressure and stroke length of the tamper. For these procedures, the hand tamper shown in Figure 20 was used. This tamper also has a contact foot area of 1.54 sq in. (9.94 sq cm). In this procedure also, the general object was to obtain layers of equal

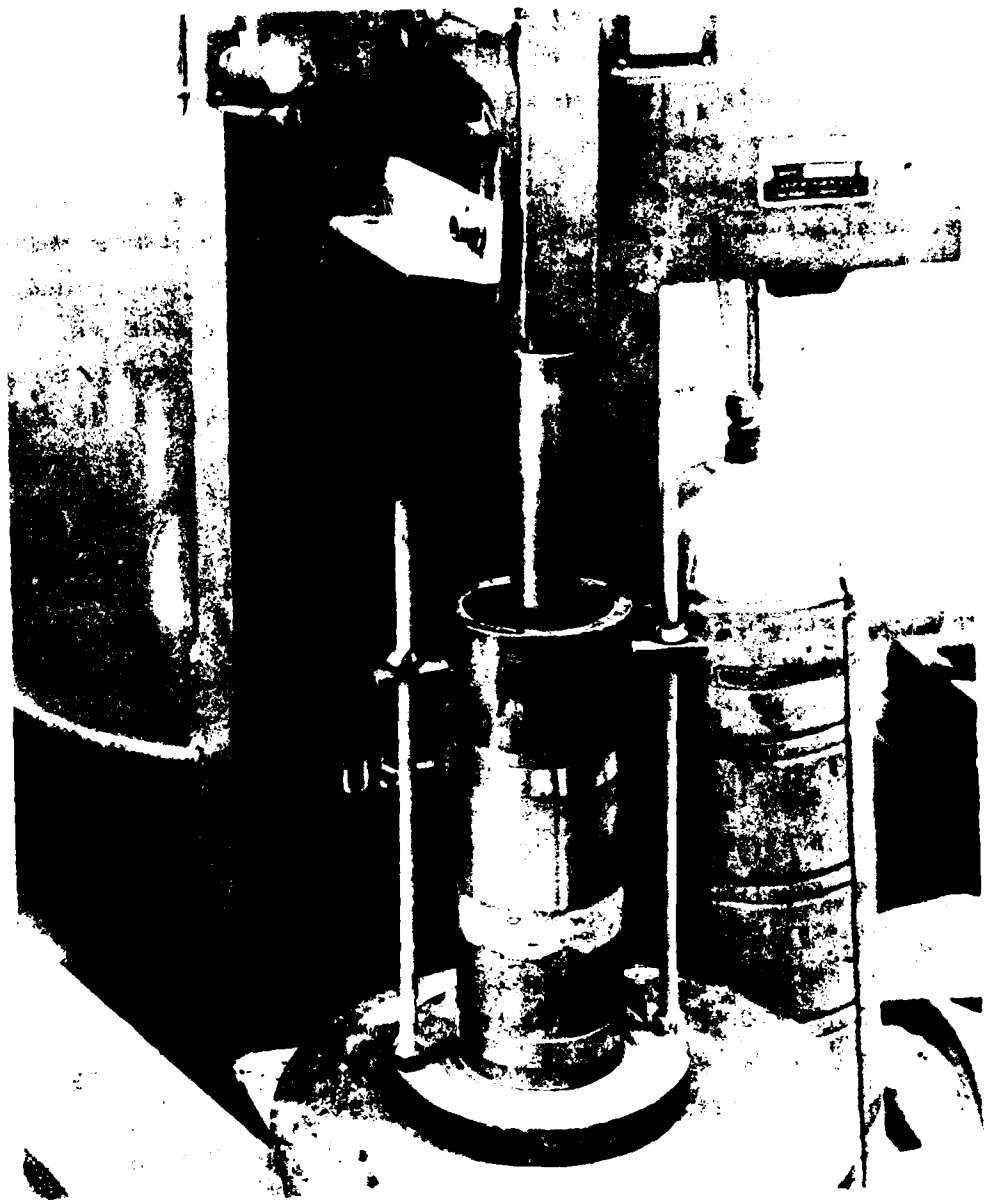


Figure 19. Pneumatic tamper

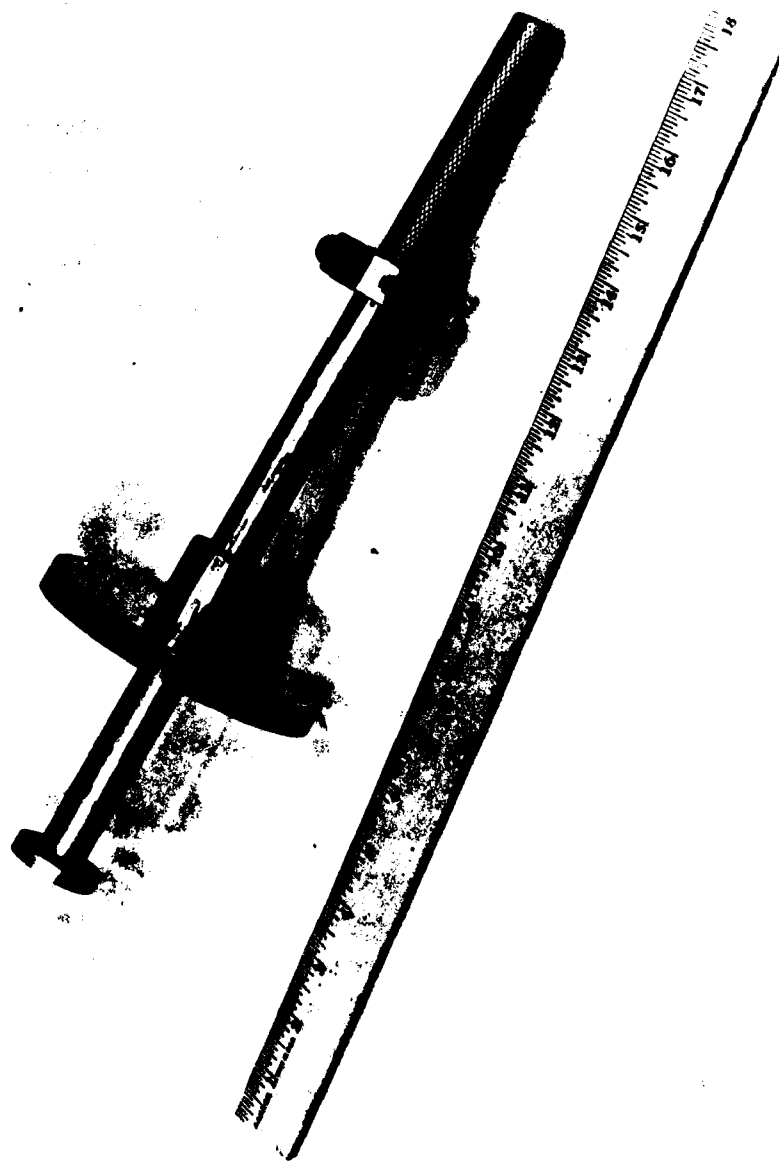


Figure 20. Manual tamper

thickness using the proper weight of soil to achieve the desired target density. Based on prior experimentation, about 18 to 24 tamps per layer were required for both materials.

After each soil specimen had been molded by either procedure, the split mold was removed and the specimen carefully wrapped in plastic wrap and coated with paraffin. The specimen was then placed in a humid room at 68° to 72°F (20° to 22.2°C) and 95 to 100 percent relative humidity and allowed to stand at least 24 hr in order to undergo any significant thixotropic strength gain.

Specimens of the silty sand were hand compacted in place on the base of the repetitive load triaxial chamber shown in Figure 21. Specimen compaction was accomplished as follows (Figure 22): First, an open end rubber membrane was secured to the base pedestal with a neoprene O-ring. The split cylindrical mold was placed over the pedestal resting on the base, with the membrane passing up through the mold and the upper end of the membrane being lapped over the top edge of the mold. A collar was then placed on the mold to contain soil overflow. A vacuum was applied, pulling the membrane tightly against the side of the mold to prevent formation of voids or irregular areas on the surface of the specimen. The soil specimen was then molded in six equal layers using hand tamping procedures and equipment previously described. About 20 to 24 tamps per layer were required.

After the sand specimens had been molded, the collar was removed. A top cap was then placed on top of the specimen, and the membrane was pulled up over the cap to which it was secured with a neoprene O-ring. A vacuum equal to the test confining pressure was then applied through the top cap and the split mold was removed, leaving the specimen standing in place.

Next, the specimen dimensions were taken. The specimen height was determined by measuring the distance from the baseplate to the top of the upper cap and subtracting from this measurement the thickness of the pedestal and cap. The diameter was calculated by measuring the diameter of the jacketed specimen with a pi-tape and subtracting twice the wall thickness of the membrane.

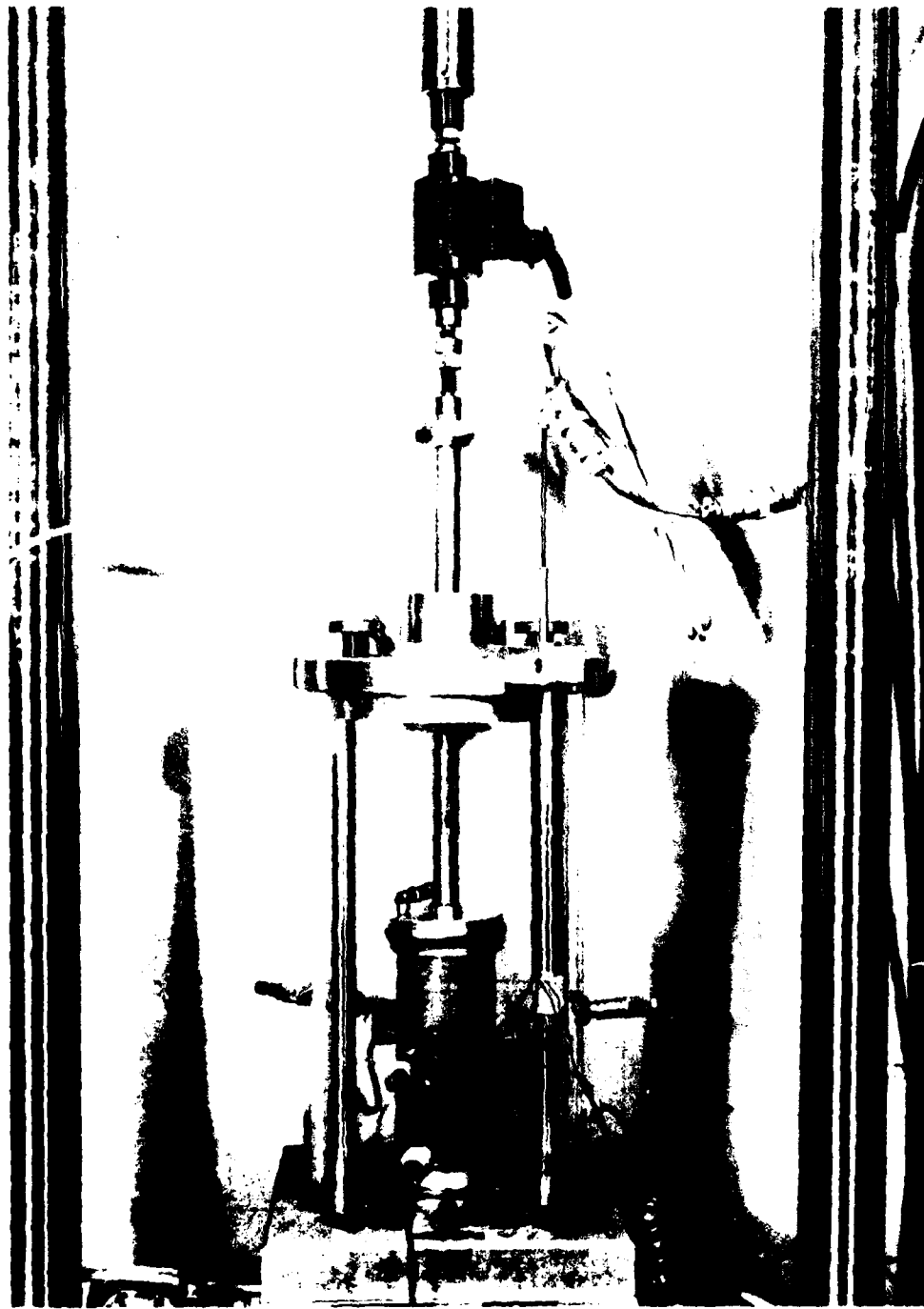


Figure 21. General view of repetitive load chamber

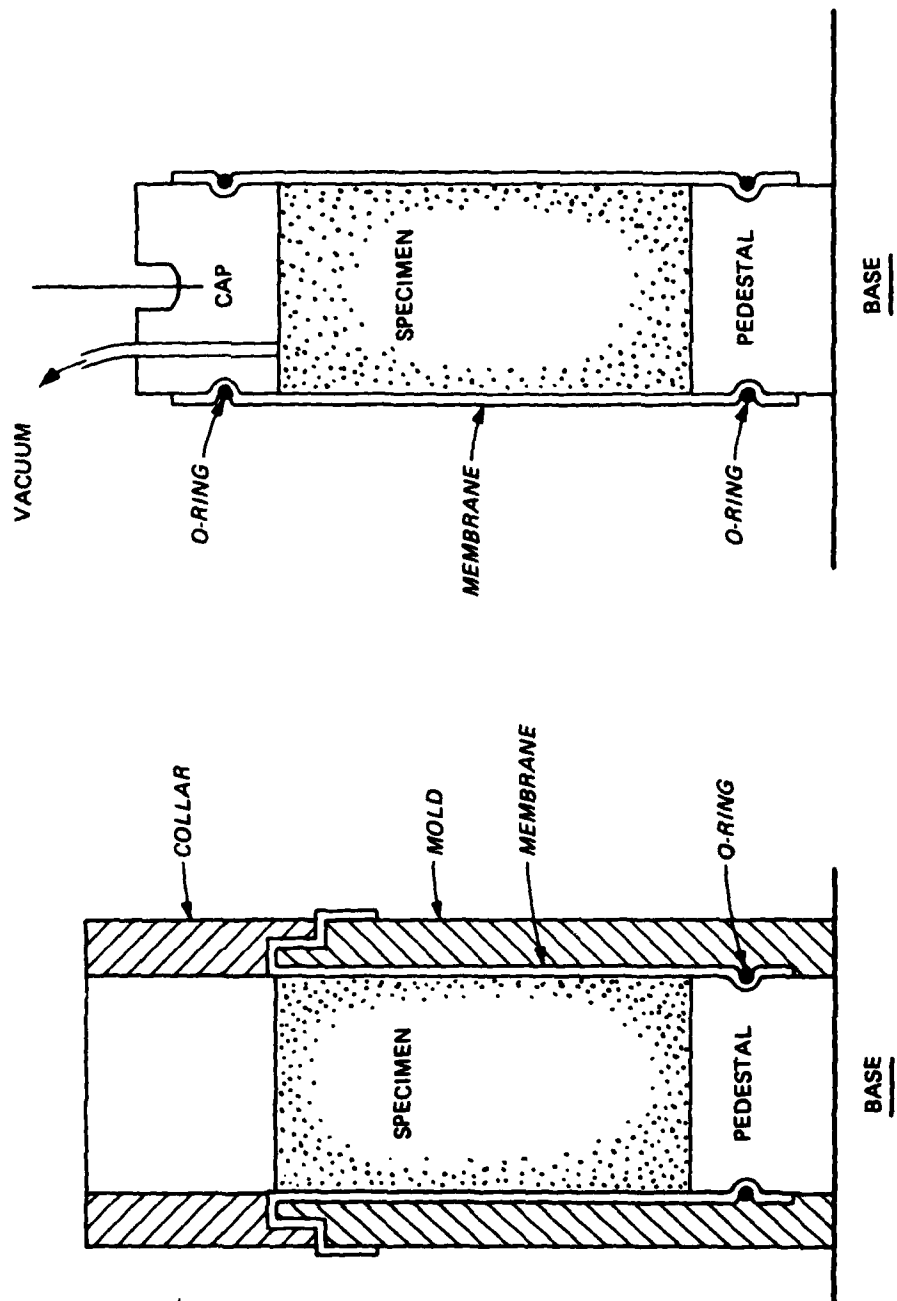


Figure 22. Method of preparation on base of triaxial chamber specimen

Metallic targets that were made of brass shim stock and measured 1 by 1 by 0.003 in. (25.4 by 25.4 by 0.08 mm) thick were then temporarily secured to the midsection of the sand specimen at third points around the circumference. A second membrane was then secured around the pedestal, after which the first membrane was pierced with a needle uniformly around the specimen surface. During this procedure, the vacuum was maintained and adjusted as necessary to maintain the desired value. The second membrane was pulled up around and secured to the top cap, and the vacuum was again maintained. As a result of the penetrations in the interior membrane, it was possible to apply the vacuum through the original connections. This procedure allowed for the second membrane to be pulled tight against the specimen, thus holding the targets more securely in place and ensuring their conformity with the specimen surface. Since thixotropy was not of concern with the silty sand, the repetitive load test was generally started immediately after molding.

#### REPETITIVE LOAD EQUIPMENT

The equipment with which the repetitive load tests were conducted consisted of the repetitive loading system, the triaxial cell containing the soil specimen, and the associated controlling, monitoring, display, and recording devices. The basic repetitive load system was manufactured by MTS Systems Corporation. A schematic drawing of the closed-loop system is shown in Figure 23. Functioning of the system is initiated with the wave form generator, which sends a signal to the controller indicating the time rate of loading and unloading. For this study, the load/unload time was 1 sec with a 2-sec delay between signals. Each wave form was repeated every 3 sec, resulting in a load application rate of 20 repetitions per minute. Also input to the controller was a load command signal, which limits the magnitude of the peak force applied to the specimen. Based on the estimated specimen diameter, the maximum axial stress, or the peak stress, may therefore be limited to the desired value. The peak load and wave form signals then pass to a servovalve that controls the load actuator. This device is basically a vertical piston linked to the hydraulic power system that provides the driving

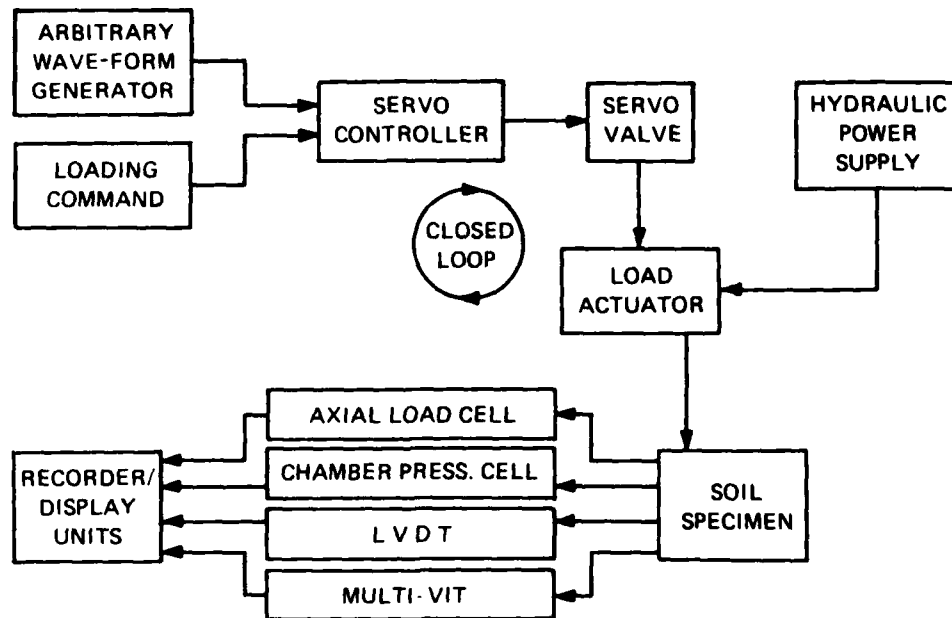


Figure 23. Schematic drawing of closed-loop electrohydraulic repetitive load system

force for loading and unloading the soil specimen positioned in the triaxial chamber directly below the actuator.

The triaxial chamber with the soil specimen is shown in Figure 24. The chamber wall consists of a 16-in.- (40.64-cm-) high acrylic cylinder having an 8-in. (20.32-cm) outside diameter and 1/2-in. (12.7-mm) wall thickness. An extension of the load piston from the actuator enters the chamber through a sealed bearing in the top plate and transmits the load to the specimen through a cap positioned on top of the specimen. The force on the specimen was monitored by means of a load cell, which was mounted in the piston stem between the actuator and triaxial cell. Chamber pressure was obtained with compressed air and was maintained at a constant level. Chamber pressure was monitored by means of a pressure transducer located in the base plate of the chamber.

Axial deformation of the specimens was measured by means of a linear variable differential transducer (LVDT). The LVDT barrel was mounted at the top of the chamber frame while the LVDT core, which moves within the barrel, was mounted on a steel arm that is fixed to, and

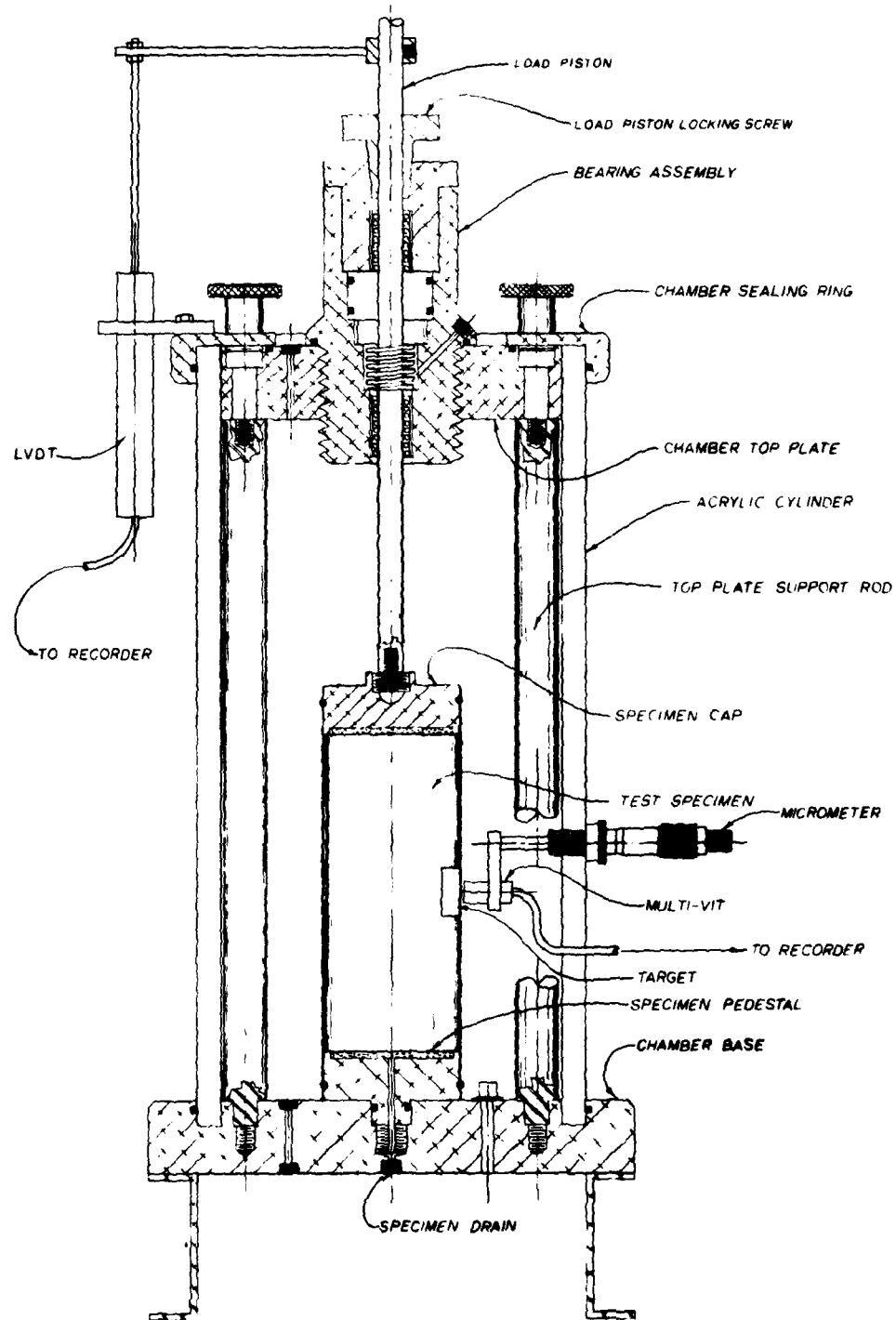


Figure 24. WES triaxial compression chamber

moves with, the load piston. Thus, the chamber frame served as a fixed reference, and the axial deformation of the specimens was measured by relative movement between the load piston and the chamber frame. Lateral deformation was measured at the middle of the specimen using three non-contact inductance devices known as multipurpose variable impedance transducers (MULTI-VIT). The MULTI-VIT's were mounted at third points around the chamber wall. Metallic targets made of brass shim stock were mounted on the soil specimen opposite each MULTI-VIT. The basic principle on which the system operates is that the output voltage of each unit is proportional to the distance between the face of the sensor and the metallic target. Thus, any lateral displacement of the specimen was detected by a change in output voltages.

Output signals from the axial load cell were transmitted to the recorder and display units and to the controller, which compared the input load signal to the output load signal going to the servovalve for compliance. Outputs from the LVDT and MULTI-VIT units and the chamber pressure transducer response were also transmitted to the recorder and display units (Figure 25). The test data monitored included axial load, chamber pressure, axial deformation, lateral deformation from each MULTI-VIT, and the averaged data from all three MULTI-VIT units. These data were recorded permanently in analog fashion using a moving strip chart recorder having scaled heat-sensitive paper on which each signal was traced by means of heated stylus points. Each signal could also be monitored digitally at selected repetition levels by means of a channel selector and digital display units.

## TEST PROCEDURES

### REPETITIVE LOAD TESTS

One of the objectives of the laboratory test phase of this study was to ensure that enough load repetitions were applied to each specimen to develop a characteristic curve of permanent axial strain versus number of load repetitions. This objective was sought to explore the possibility of defining the relationship in more precise mathematical terms than had been previously presented. Based on a review of previous

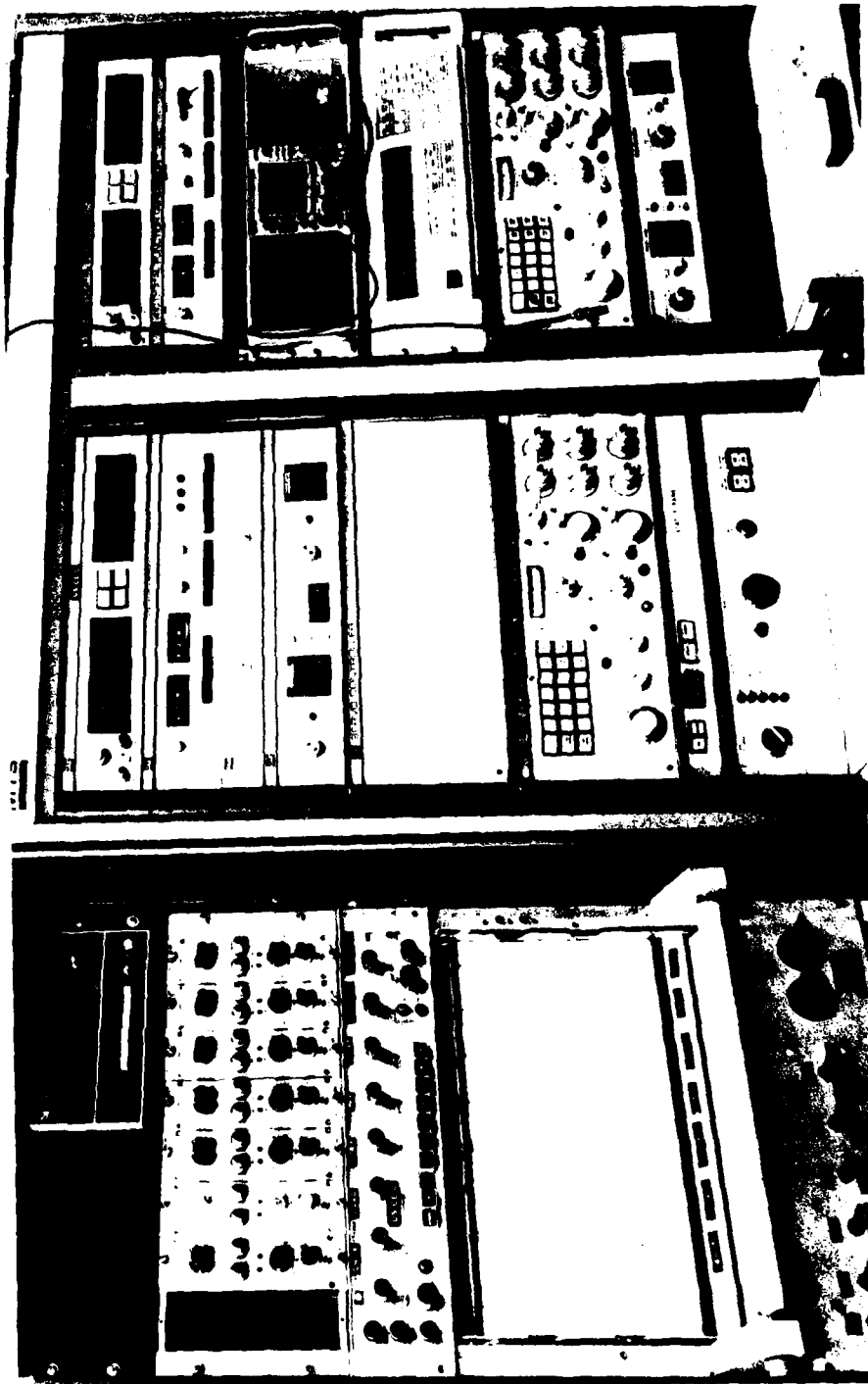


Figure 25. General view of controller-recorder-display console

work, it was determined that up to 70,000 to 100,000 load repetitions could be required to develop a characteristic pattern, depending on the ratio of the applied deviator stress to the failure deviator stress under static loading. A review of the literature did not reveal uniformity in findings concerning the criticality of this ratio with respect to number of strain repetitions. Therefore, it was decided that to consider a test successful a minimum of 10,000 repetitions must be applied without the permanent axial strain exceeding 10 percent.

Based on a mean application of 80,000 repetitions per specimen, at 3 sec per application, it would theoretically take 2.8 days to complete the repetitive loading for each test. Therefore, to compensate for equipment set-up time, loss time, etc., 4 days per specimen were allowed.

As noted earlier, specimens of the cohesive soil were molded at least 24 hr prior to initiation of testing and were sealed and stored in a humid room. To prepare the specimen for testing, the paraffin coating and plastic wrap were carefully removed to avoid damage, and the specimen was placed on the chamber pedestal (Figure 26). The diameter and height of the specimen were then measured carefully. Four measurements were taken for each dimension, and the average value was used for actual specimen dimensions. A rubber membrane that previously had been secured to the pedestal by means of a neoprene O-ring was then pulled up over the specimen and a cap was placed on top of the specimen. The upper part of the membrane was pulled up around the cap to which it was secured with a neoprene O-ring. A vacuum, somewhat less in magnitude than the test confining pressure, was then applied through the top cap to pull the membrane tight around the specimen. Metallic targets and a second membrane were then installed on the specimen following procedures previously described for preparation of the silty sand specimens. After installation of the second membrane, a vacuum was maintained during assembly of the chamber.

As previously noted, the silty sand specimens were molded in place, after which the specimen dimensions were taken and the metallic

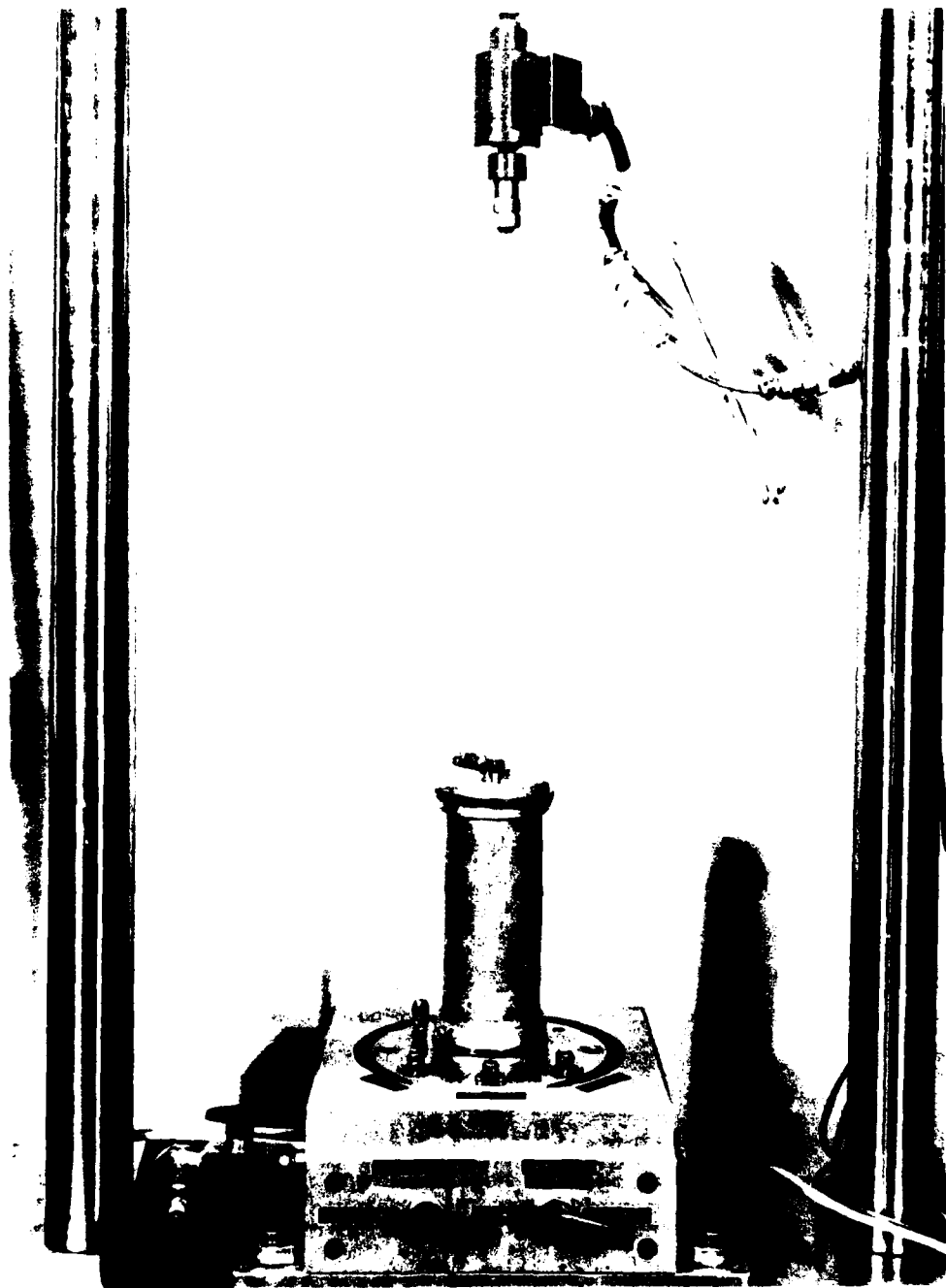


Figure 26. Specimen mounted on base

targets and second membrane were installed prior to conduct of the repetitive load test.

With the appropriate specimen so mounted, the acrylic cylinder that formed the chamber walls was placed on the base. At the base of the apparatus, the cylinder fits into a circular groove equipped with an O-ring on the exterior wall to seal the chamber. The top plate, similarly equipped with a groove and an O-ring, was then placed on the top of the cylinder. Vertical support rods inside the cylinder that serve to pull the top and bottom plates together were then secured tightly, and the load piston was passed through an air seal in an opening in the center of the top plate to complete the sealed chamber.

All electronic connections to the vertical LVDT, MULTI-VIT units, and axial load and chamber pressure transducers were then completed, and the monitoring units were calibrated. The chamber pressure was next applied and adjusted to the proper level, replacing the vacuum pressure. The vertical LVDT was positioned at some arbitrary position of travel near the center point of the core stem, while each MULTI-VIT, using the micrometer adjustments, was positioned radially toward the specimen so that the face of the unit prior to initiation of testing was about 0.075 in. (1.91 mm) from the specimen target. The load piston was adjusted vertically downward into a recess in the top cap, and the desired seating pressure was applied. All tests were made in a drained condition through porous caps and outlet tubing at the bottom of the specimen. With the desired wave form and peak load programmed into the command signal package, the repetitive load test was then started.

In general, it was desired to obtain data readings at or near the following repetition levels: 1, 2, 5, 10, 20, 50, 100, 200, 500, 1,000, 2,000, 5,000, 10,000, 20,000, 50,000, and 100,000 cycles, or at any interval within this range of values at the termination of testing. In most cases, data were taken at the desired repetition level up to 5000 cycles. Thereafter, however, data were taken at various intervals generally dictated by the hour at which readings could feasibly be taken. Data were recorded in two forms. At the selected time, the strip chart

was turned on to obtain an analog recording after which the same data were recorded digitally.

#### STATIC LOAD TESTS

Unconsolidated-undrained standard triaxial compression tests were conducted on duplicate specimens to determine the compressive strength of each soil at each condition. Specimens were molded in a manner previously described for the repetitive load triaxial tests. The static load tests were conducted using a chamber having a diameter of 7-3/4 in. (19.69 cm) and height of 11-1/2 in. (29.21 cm). The tests were conducted using standard procedures. Strain rates for the silty clay and silty sand were about 1 percent per minute and for the buckshot clay were about 0.5 percent per minute. Each test was conducted until a minimum axial deformation of 15 percent had been reached. Failure stress was determined from the axial load value at 15 percent strain unless a higher or peak value was obtained at a lower strain value. Chamber pressure for each specimen was the same as that for the repetitive load triaxial tests.

#### DATA COLLECTION AND REDUCTION

Raw data monitored and recorded for each repetitive-load test included permanent and resilient axial and radial deformation, static chamber pressure, static axial load in excess of chamber pressure, and peak cyclic load. These data, along with specimen geometry, were processed through a specially developed computational program, which calculated and tabulated for selected repetition levels values of peak repetitive axial stress and static chamber pressure in psi, peak resilient axial and radial strain in in./in., resilient modulus in psi, resilient Poisson's ratio, and maximum permanent axial, radial, and volumetric strain in percent. Resilient modulus is defined as the peak repetitive axial stress divided by the maximum resilient axial strain. Also calculated were values of permanent volumetric strain defined as

$$\epsilon_v = \epsilon_1 - \epsilon_3 \quad (9)$$

where

$\epsilon_v$  = permanent volumetric strain

$\epsilon_1$  = permanent axial strain

$\epsilon_3$  = permanent radial strain

The purpose in collecting and assembling such a voluminous data file was based on several considerations. First, the computational program used to process the broad band of response data was readily available, and it was felt to be, without preselection of specific parameters, more advantageous to acquire as much potentially useful response data as practical initially for a thorough analysis. Second, it could not be known in advance which response parameters would evolve as being the most significant or whether the resilient or the permanent response data would be more relevant. Therefore, a broad array of response data was recorded.

For the static load tests, the primary response of interest was the maximum deviator stress on the specimen at failure.

## TEST RESULTS AND DISCUSSION

### TEST RESULTS

#### GENERAL

During the course of the laboratory test program, a total of 45 individual tests were attempted, 28 of which were considered successful. The primary causes of failures were mechanical and electrical outages and, in several instances, overstressing of the test specimen. In one case involving the buckshot clay, the data from two individual tests (23 and 24) conducted under the same test conditions were averaged, thus resulting in the reporting of 28 data sets. These data are presented in Appendix A.

Table 8 gives a summary of actual test conditions including soil dry density and water content values, test stresses, and the total number of repetitions at the termination of each test. As can be seen, target values of density and water content were generally met. Actual values of axial stress varied from the target values somewhat, more often being slightly lower than the desired value, mainly because the axial stress actually achieved was a function of specimen response within the time frame of loading and unloading. As was indicated earlier, the target values of density were revised upward for the silty clay and silty sand in order to maintain the target stress regime. However, as shown in Table 8, axial stress values applied to the silty sand at the lower target densities were also reduced to prevent premature failure.

Table 9 presents a summary of test results for the static load triaxial tests. This summary includes data on specimen water content and density, deviator stress at failure  $\sigma_{Df}$ , confining pressure, and deviator stress for the associated repetitive load test  $\sigma_{Dr}$  conducted with a similar specimen. Also shown is a column of mean failure deviator stress values  $\bar{\sigma}_{Df}$ . These values represent the numerical mean of the three failure stresses obtained for each specimen having similar densities and water contents. A review of the failure values obtained

Table 8. Summary of Test Conditions for Repetitive Load Tests

Soil Type	Test No.	Dry Density pcf	Percent Max ASTM D 1557	Water Content percent	Repeated		Confining Pressure $\sigma_c$ , psi	Seating Pressure $\sigma_s$ , psi	Total No. of Repetitions
					$\sigma_D$ , psi	Deviator Stress			
Silty clay (CL)	2	103.7	89.7	20.0	12.90	2.0	1.5	72,050	
	3	104.2	90.1	20.1	9.20	2.5	2.0	85,360	
	5	104.3	90.2	19.9	7.10	3.0	2.5	83,030	
	6	98.0	84.8	22.2	12.40	2.0	1.5	107,890	
	7	99.0	85.6	22.1	9.30	2.5	2.0	75,000	
	8	98.9	85.5	22.1	7.20	3.0	2.5	85,840	
	27	96.3	83.3	24.3	11.80	2.0	1.5	85,462	
	26	95.7	82.8	24.2	9.20	2.5	2.0	88,500	
	25	96.6	83.6	23.9	6.80	3.0	2.5	83,150	
	Buckshot clay (CH)	15	103.0	90.5	20.3	12.70	2.0	1.5	90,049
13		101.2	88.9	21.2	9.40	2.5	2.0	107,225	
12		101.7	89.4	20.8	7.00	3.0	2.5	83,455	
22		98.6	86.1	23.4	12.70	2.0	1.5	60,000	
17		95.6	84.1	23.4	9.60	2.5	2.0	85,000	
16		96.2	84.5	23.2	6.80	3.0	2.5	84,290	
23/24		90.9	79.9	26.4	12.40	2.0	1.5	81,543	
21		90.6	79.6	26.1	9.50	2.5	2.0	80,080	
19		91.1	80.1	26.6	6.90	3.0	2.5	85,975	
Silty sand (SM)		31	118.4	94.6	10.8	12.30	2.0	1.5	83,102
	30	118.7	94.8	10.8	9.77	2.5	2.0	82,250	
	29	120.7	96.4	10.9	7.35	3.0	2.5	61,400	
	39	115.7	92.4	11.9	10.20	2.0	1.5	24,800	
	36	116.0	92.7	11.4	9.52	2.5	2.0	63,400	
	35	115.2	92.0	12.0	7.20	3.0	2.5	60,000	
	33	112.9	90.2	13.2	9.20	2.5	2.0	27,113	
	34	112.9	90.2	13.2	7.23	3.0	2.5	107,430	
	40	112.7	90.0	13.2	5.07	3.5	2.5	61,580	

Note: 1 pcf = 16.02 kg/m<sup>3</sup>; 1 psi = 6.89 kPa.  
\* Estimated.

Table 9. Summary of Test Data for Static Load Triaxial Tests

Soil Type	Applicable Repetitive Load Test	Dry Density pcf	Water Content percent	Failure Deviator Stress $\sigma_{Df}$ , psi	Confining Pressure $\sigma_c$ , psi	Avg Failure Deviator Stress $\bar{\sigma}_{Df}$ , psi	Applicable Repetitive Stress $\sigma_{Dr}$ , psi	Stress Ratio $\Delta\sigma = \sigma_{Dr} / \bar{\sigma}_{Df}$
Silty clay (CL)	2	104.7	20.0	43.2	2.0	40.7	12.9	0.317
	3	104.7	20.3	39.5	2.5	40.7	9.2	0.226
	5	104.9	20.3	39.5	3.0	40.7	7.1	0.175
	6	97.7	22.1	15.8	2.0	19.0	12.4	0.653
	7	98.0	21.9	18.6	2.5	19.0	9.3	0.490
	8	98.8	21.9	22.7	3.0	19.0	7.2	0.379
	27	96.1	23.9	11.8	2.0	12.1	11.8	0.975
	26	95.8	24.0	11.4	2.5	12.1	9.2	0.760
	25	95.9	24.0	13.2	3.0	12.1	6.9	0.562
	Buckshot clay (CH)	15	102.0	21.0	66.0	2.0	67.0	12.7
13		102.4	21.1	64.0	2.5	67.0	9.4	0.140
12		102.0	20.9	70.9	3.0	67.0	7.0	0.105
22		96.0	23.5	35.2	2.0	36.5	12.7	0.348
17		96.2	23.4	37.1	2.5	36.5	9.6	0.263
16		96.2	23.4	37.1	3.0	36.5	6.8	0.186
23/24		90.9	26.4	23.6	2.0	23.5	12.4	0.528
21		91.8	26.3	24.0	2.5	23.5	9.5	0.404
19		91.8	26.3	23.0	3.0	23.5	6.9	0.294
Silty sand (SM)		31	119.3	10.8	23.1	2.0	21.9	12.8
	30	119.4	10.6	18.7	2.5	21.9	9.8	0.448
	29	119.6	10.8	23.8	3.0	21.9	7.4	0.338
	39	115.1	11.7	17.5	2.0	17.9	10.2	0.570
	36	115.3	11.7	18.1	2.5	17.9	9.5	0.531
	35	115.5	11.9	18.2	3.0	17.9	7.2	0.402
	33	113.4	13.0	11.2	2.6	13.0	9.2	0.708
	34	113.2	13.0	11.4	2.5	13.0	7.2	0.554
	40	112.7	13.4	16.5	3.0	13.0	5.1	0.392

Note: 1 pcf = 16.02 kg/m<sup>3</sup>; 1 psi = 6.89 kPa.

for each set of specimens for all soils indicates that there was little influence of the confining pressure on the failure stress; therefore, the mean value was used to represent the failure stress for each set of specimens. Finally, the ratio of the repetitive deviator stress to the mean failure deviator stress,  $\Delta\sigma$ , is shown for each test condition.

#### RESILIENT STRAIN

Although there is some variation in the resilient response of soil specimens during the course of a repetitive load test in the laboratory, it is often considered that a steady response state develops after the first 1000 or so cycles of loading. Based on this premise, a review of the resilient response data was conducted from which single point values of resilient axial strain and resilient modulus associated with each test were determined. These values are indicated in Table 10. The strain values were selected as being representative of each test, and the resilient modulus was calculated using the actual repeated axial stress value and the resilient strain. Plots of resilient axial strain versus repeated deviator stress are shown in Figures 27, 28, and 29.

In general, the resilient response data indicate that the silty sand soil demonstrated the highest stiffness and lowest strain values while the silty clay indicated the largest strain response with corresponding lower modulus values. The magnitudes of the resilient strain values appear to be somewhat small compared with similar data obtained in this type test, and the resilient modulus values appear to be somewhat higher than expected. For the silty clay, strain values ranged from  $0.5 \times 10^{-3}$  to  $2.5 \times 10^{-3}$  in./in. The buckshot clay indicated a range in strain from  $0.2 \times 10^{-3}$  to  $2.1 \times 10^{-3}$  in./in. There was little variation in the strain values indicated for the silty sand. These values ranged from  $0.3 \times 10^{-3}$  to  $0.7 \times 10^{-3}$  in./in. with seven of the nine strain values being in the range of  $0.4 \times 10^{-3}$  to  $0.6 \times 10^{-3}$  in./in.

#### PERMANENT STRAIN

The primary permanent strain responses of significance were the

Table 10. Summary of Resilient Axial Strain and Resilient Modulus

Soil	Test No.	Resilient Axial Strain in./in. $\times 10^{-3}$	Resilient Modulus psi
Silty clay (CL)	2	1.6	8,063
	3	0.9	10,222
	5	0.5	14,200
	6	2.1	5,905
	7	1.3	7,154
	8	0.8	9,000
	27	2.5	4,720
	26	1.6	5,750
	25	1.1	6,182
	Buckshot clay (CH)	15	0.8
13		0.6	15,500
12		0.2	35,000
22		1.0	12,900
17		0.6	16,000
16		0.4	17,000
23/24		2.1	5,904
21		1.1	8,636
19		0.6	11,500
Silty sand (SM)	31	0.6	20,500
	30	0.5	19,600
	29	0.4	18,500
	39	0.7	14,571
	36	0.5	19,000
	35	0.4	18,000
	33	0.6	15,333
	34	0.4	18,000
	40	0.3	17,000

Note: 1 psi = 6.89 kPa; 1 in. = 2.54 cm.

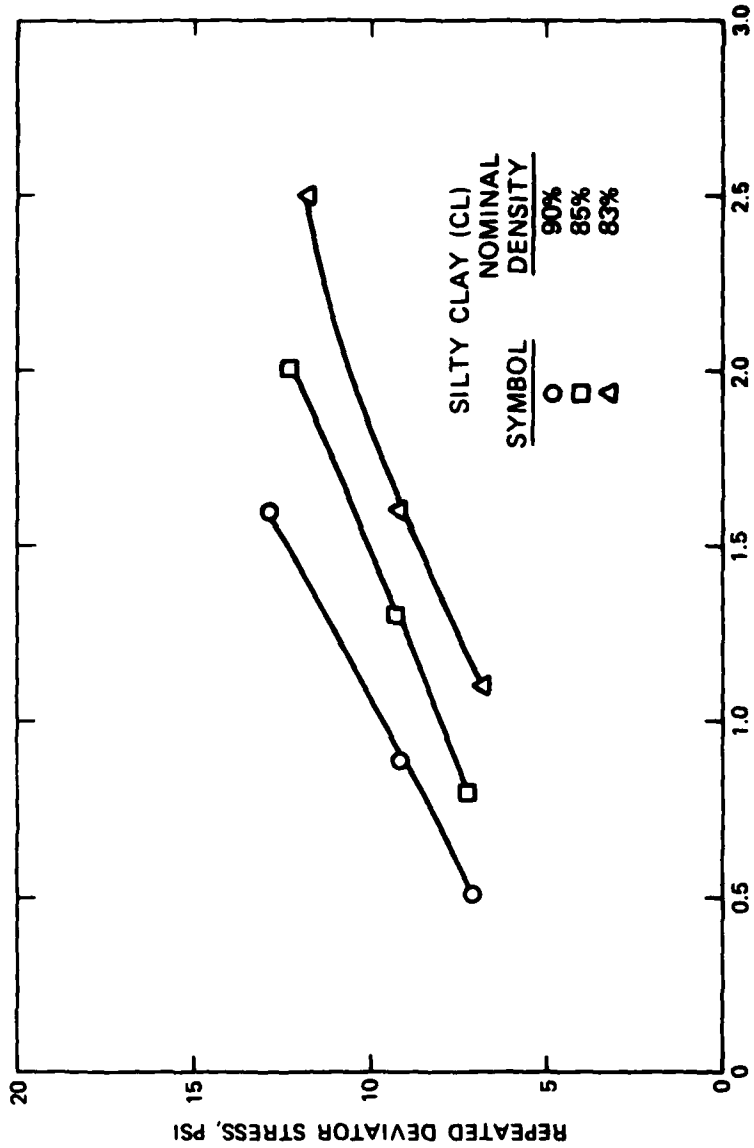


Figure 27. Resilient axial strain versus repeated deviator stress for silty clay (1 psi = 6.89 kPa; 1 in. = 2.54 cm)

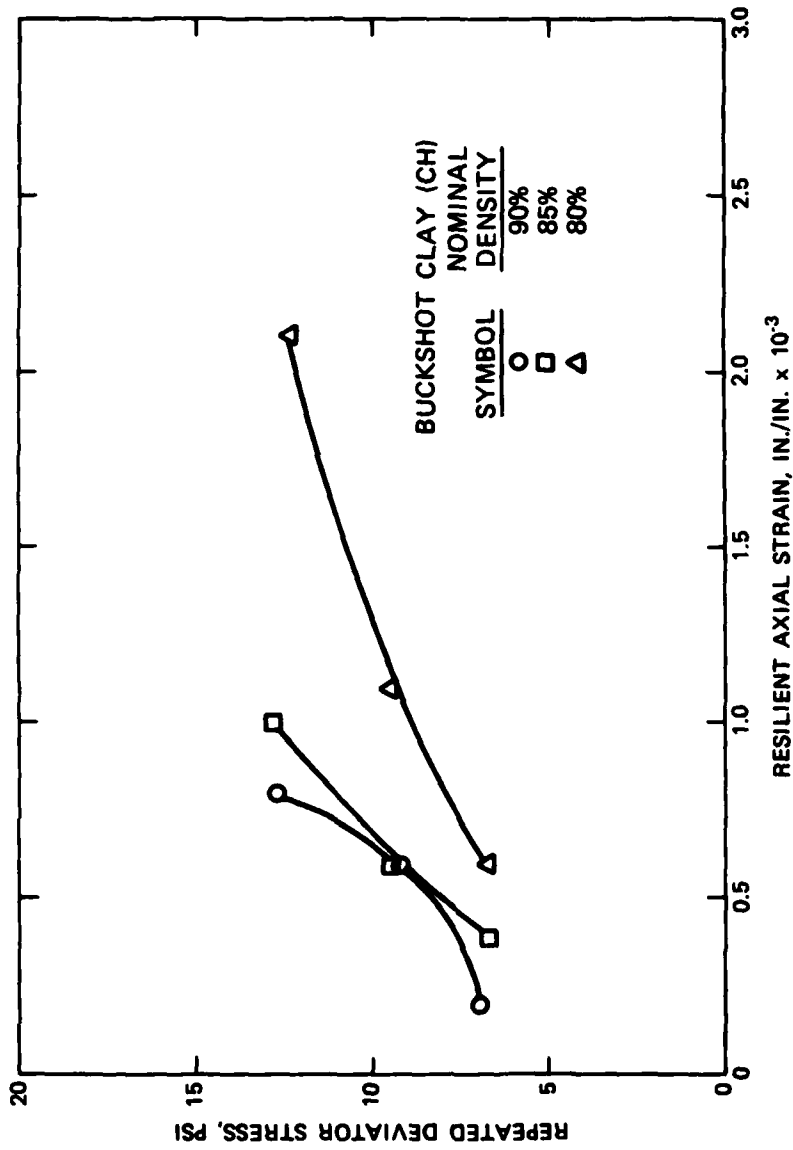


Figure 28. Resilient axial strain versus repeated deviator stress for buckshot clay (1 psi = 6.89 kPa; 1 in. = 2.54 cm)

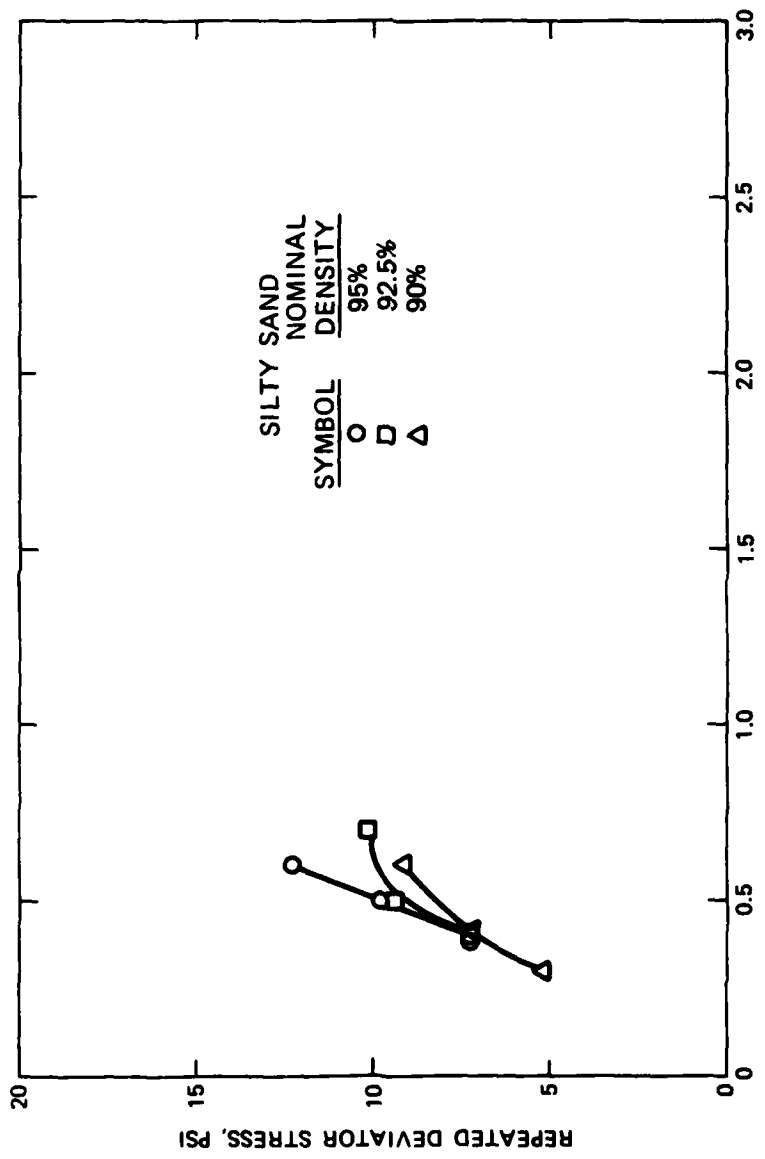


Figure 29. Resilient axial strain versus repeated deviator stress for silty sand (1 psi = 6.89 kPa; 1 in. = 2.54 cm)

axial strain values. The radial strain data in some cases were negligible or erratic and, therefore, could not be used to define overall soil deformation patterns. The permanent axial strain data are presented in two types of plots: first, in a semilog plot with the number of load repetitions on a logarithmic scale and the permanent axial strain on an arithmetic scale (Figures 30-38); and second, with both values plotted on an arithmetic scale (Figures 39-47). The first type of plot is presented in order to enable comparison of the data with those of other researchers whose data are similarly presented. This type of plot also indicates much better the behavior of the specimen during the first 1000 load repetitions. The second (or arithmetic plot), on the other hand, presents an undistorted pattern of the test data. In these plots, some of the data points between repetition 1 and repetition 5000 have been omitted for clarity without changing the basic shape of the curve.

Silty clay. The semilog and arithmetic plots of percent permanent axial deformation versus number of load repetitions for the silty clay soil are presented in Figures 30-32 and 39-41, respectively. In all cases where the data are plotted in semilog form, the characteristic reverse shape curve is indicated. This form has been observed by other researchers. The data presented in Figures 30 and 39 represent tests 2, 3, and 5, which were conducted at stress ratios of 0.317, 0.226, and 0.175, respectively, on specimens compacted to 90 percent nominal density. From Figure 39, it may be observed that, for the range of load repetitions for which test 2 was conducted, there appears to be a decrease in rate of strain with load repetitions. For tests 3 and 5, the rate of strain appears to become constant after 25,000-35,000 repetitions. In Figure 31, which represents tests 6, 7, and 8 conducted at stress ratios of 0.653, 0.490, and 0.379 on the silty clay at a nominal density of 85 percent, there is less pronounced curvature in the semilog plots. These same data, in arithmetic form (Figure 40), indicate that the rate of strain decreases significantly at some point in each test although at different end repetition levels. The general trend appears to be that the point at which the strain rate essentially becomes constant varies with the stress ratio, being at higher repetition levels

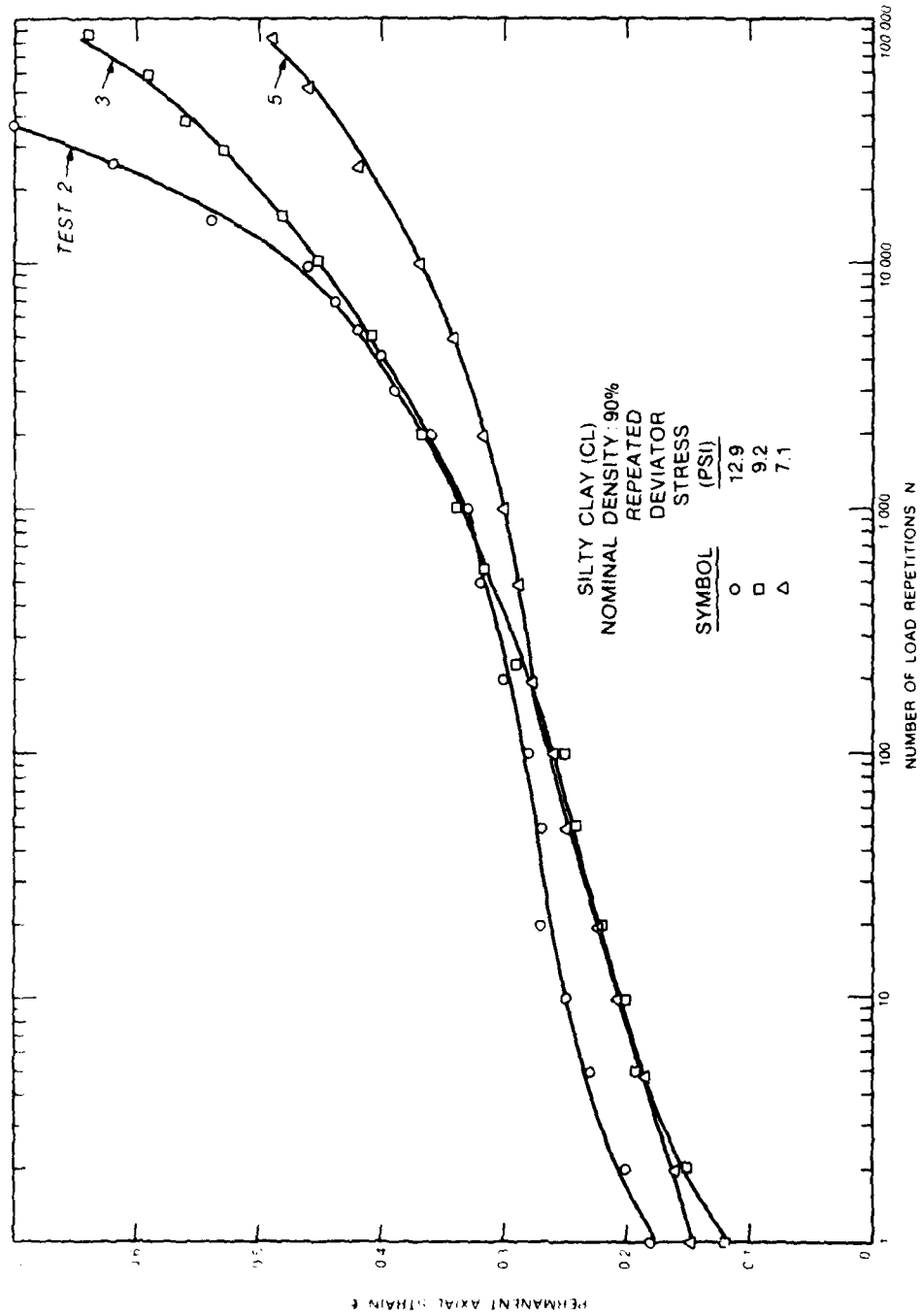


Figure 30. Permanent axial strain versus number of load repetitions (semilogarithmic), tests 2, 3, and 5 (1 psi = 6.89 kPa)

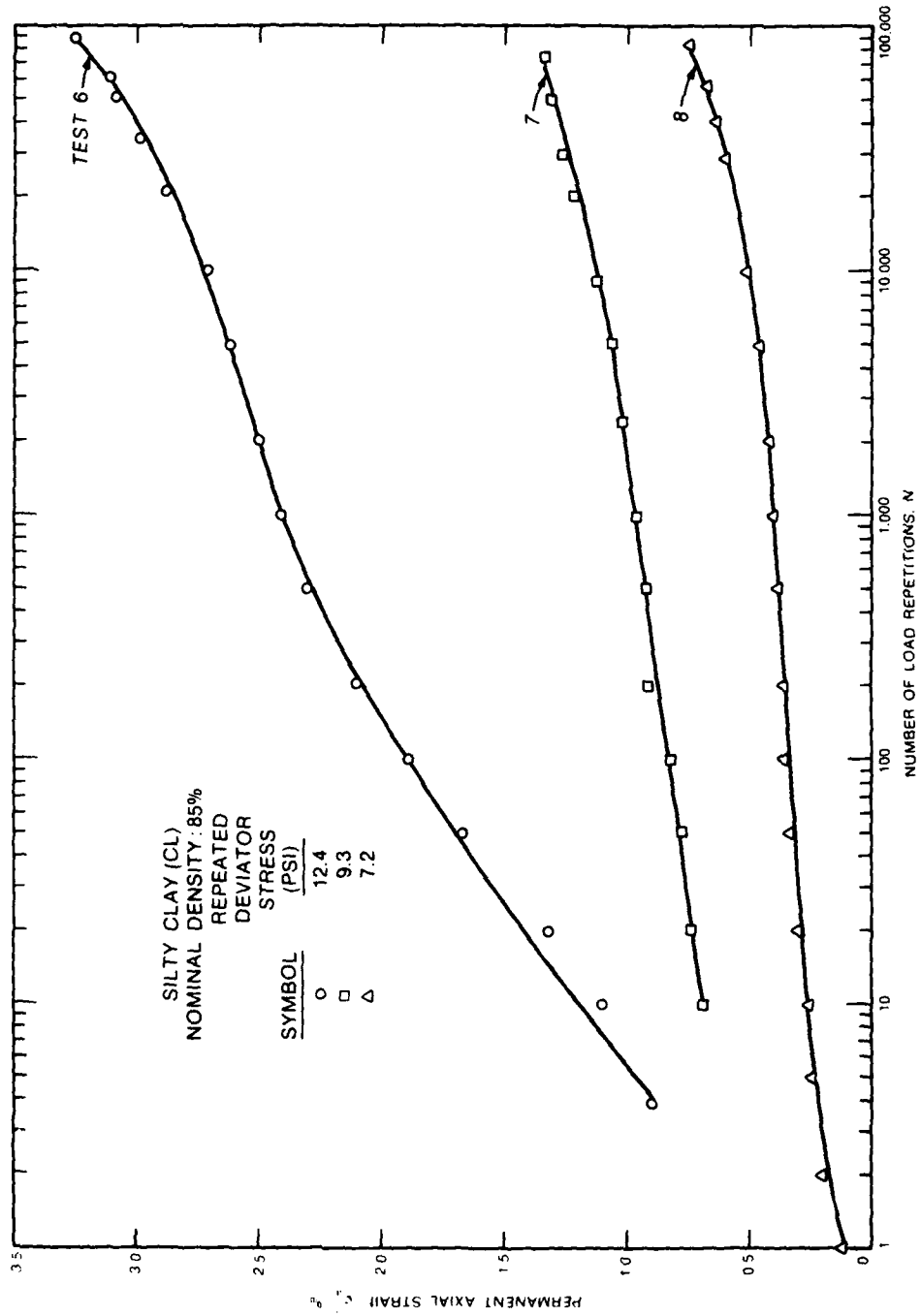


Figure 31. Permanent axial strain versus number of load repetitions (semilogarithmic), tests 6, 7, and 8 (1 psi = 6.89 kPa)

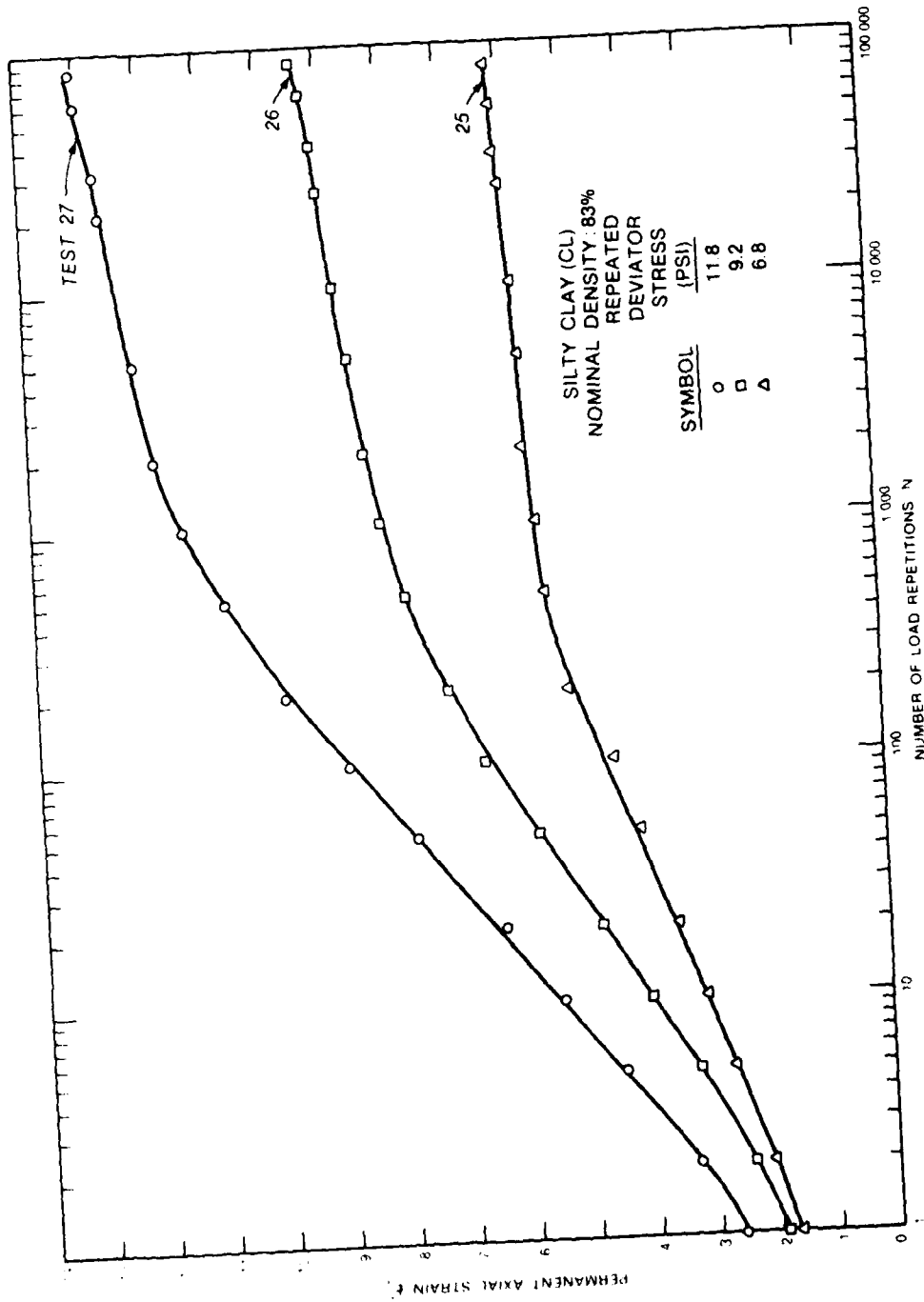


Figure 32. Permanent axial strain versus number of load repetitions (semilogarithmic), tests 25, 26, and 27 (1 psi = 6.89 kPa)

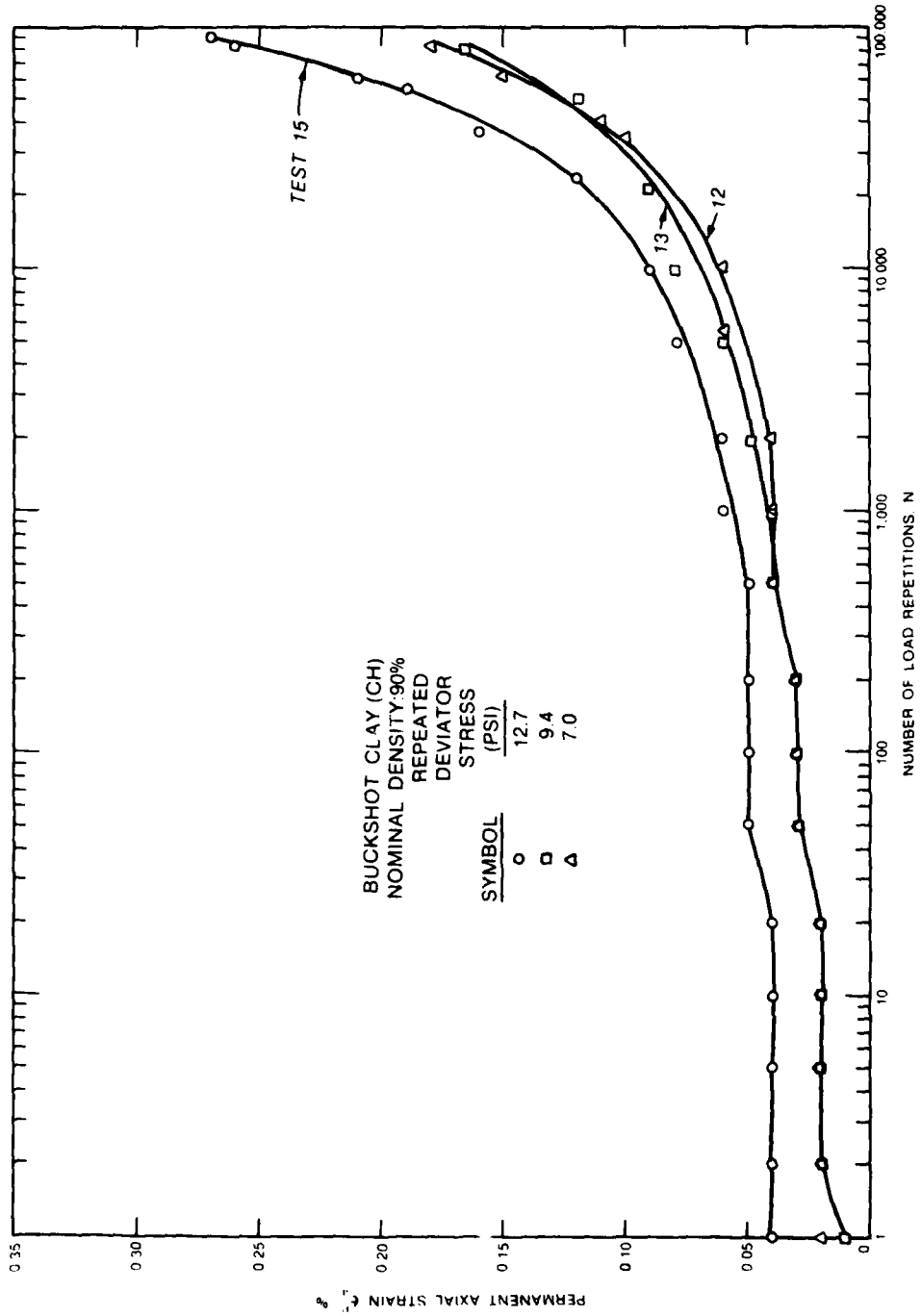


Figure 33. Permanent axial strain versus number of load repetitions (semilogarithmic), tests 12, 13, and 15 (1 psi = 6.89 kPa)

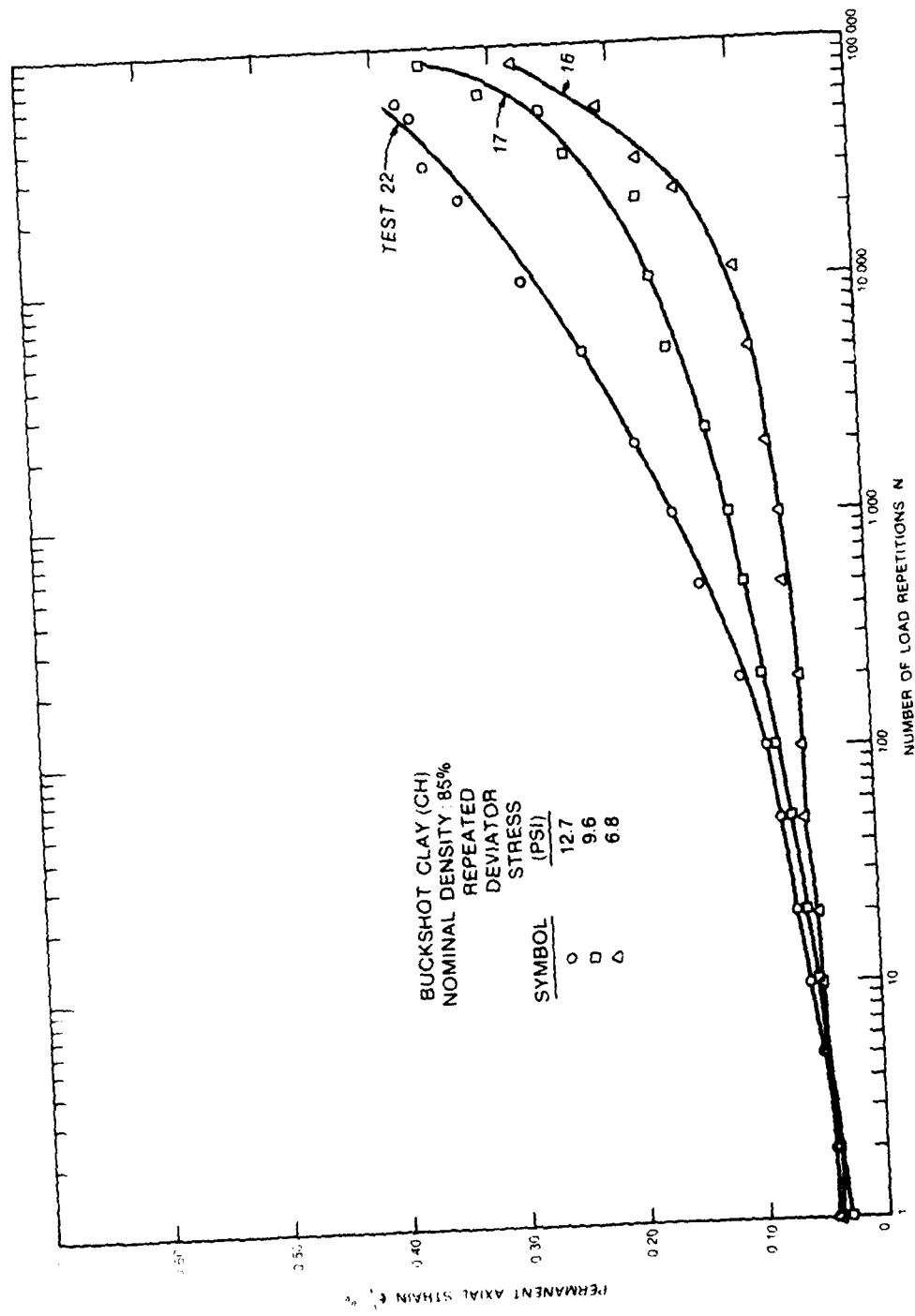


Figure 34. Permanent axial strain versus number of load repetitions (semilogarithmic), tests 16, 17, and 22 (1 psi = 6.89 kPa)

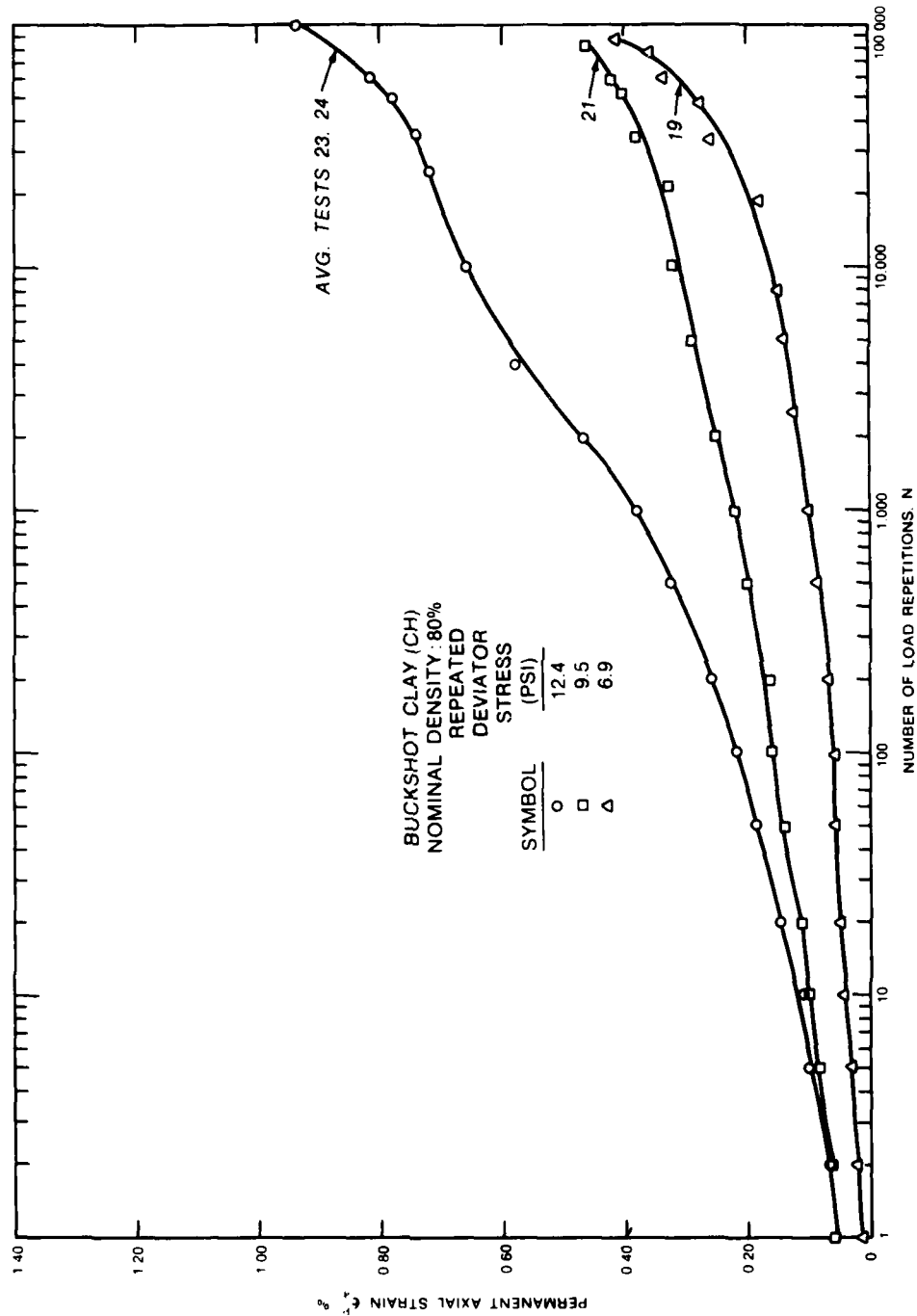


Figure 35. Permanent axial strain versus number of load repetitions (semilogarithmic), tests 19 and 21 and average data from tests 23 and 24 (1 psi = 6.89 kPa)

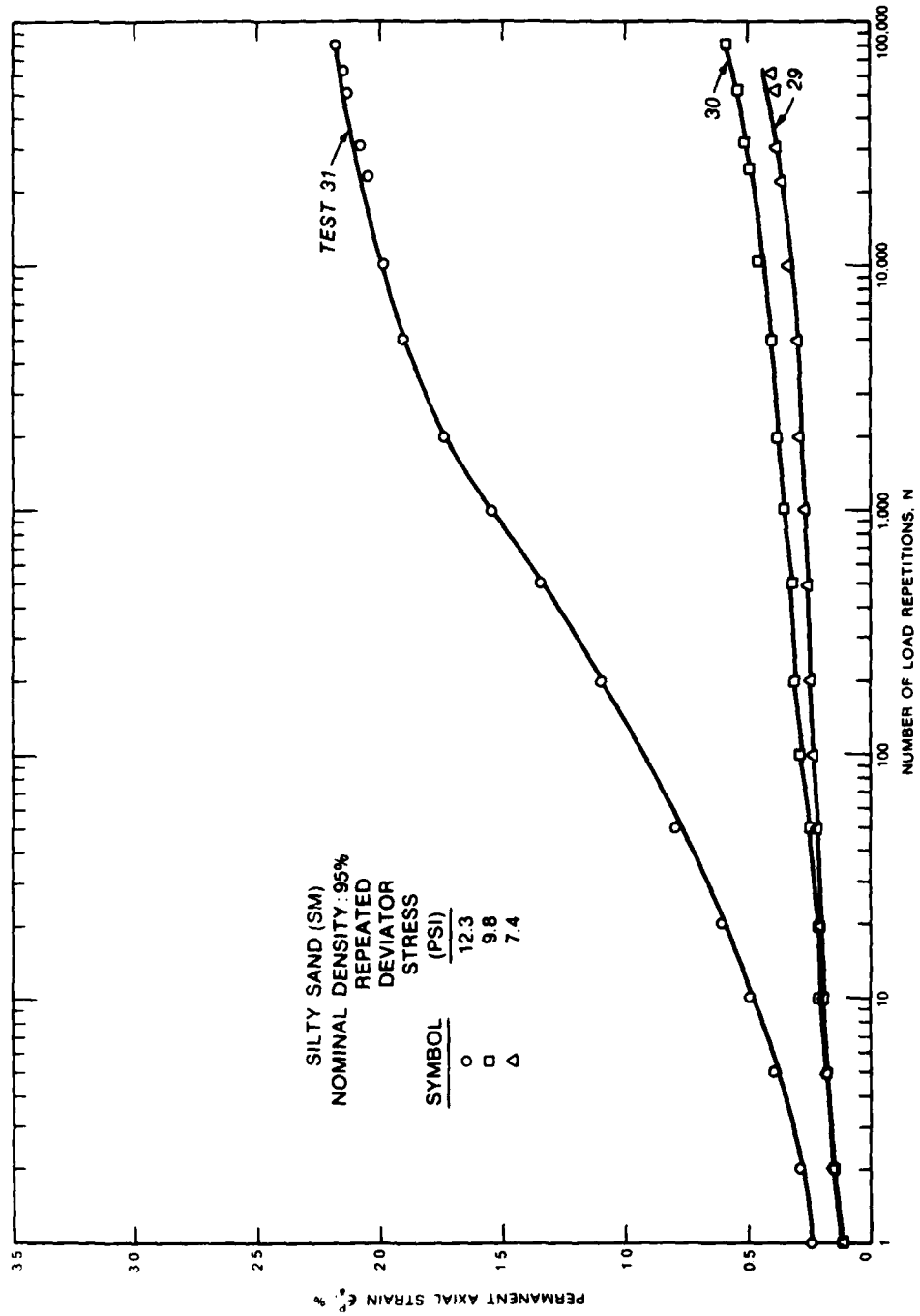


Figure 36. Permanent axial strain versus number of load repetitions (semilogarithmic), tests 29, 30, and 31 (1 psi = 6.89 kPa)

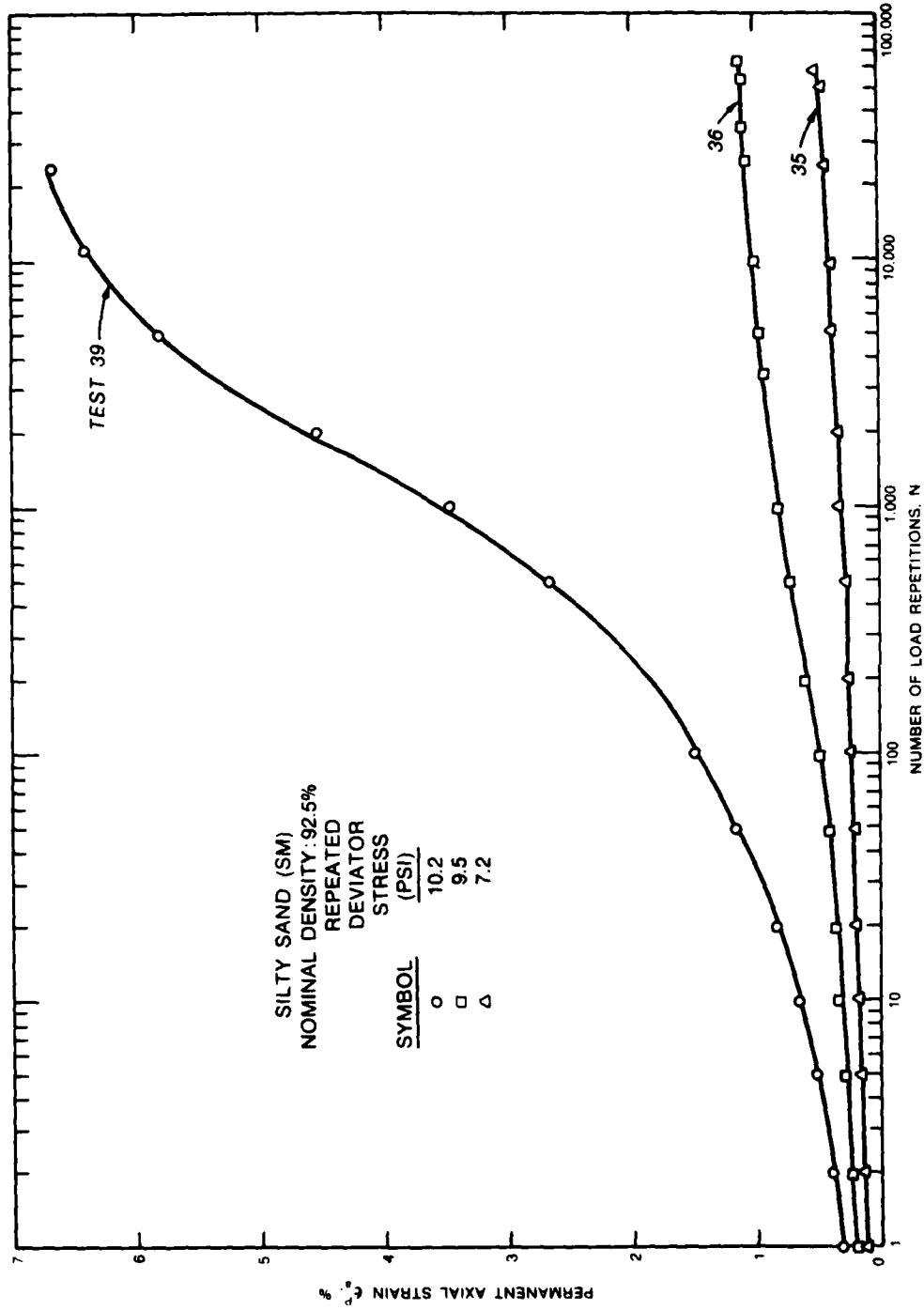


Figure 37. Permanent axial strain versus number of load repetitions (semilogarithmic), tests 35, 36, and 39 (1 psi = 6.89 kPa)

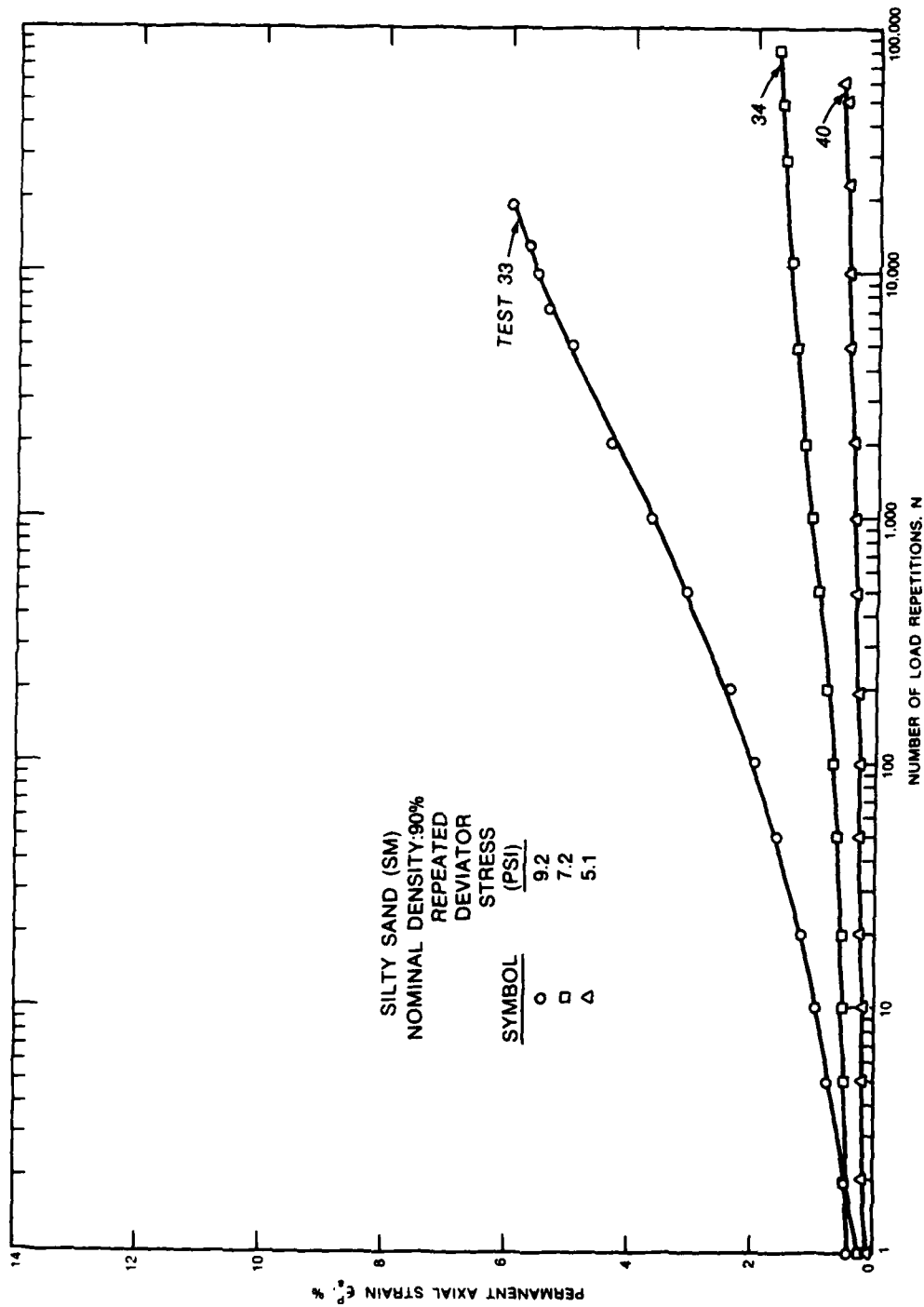


Figure 38. Permanent axial strain versus number of load repetitions (semilogarithmic), tests 33, 34, and 40 (1 psi = 6.89 kPa)

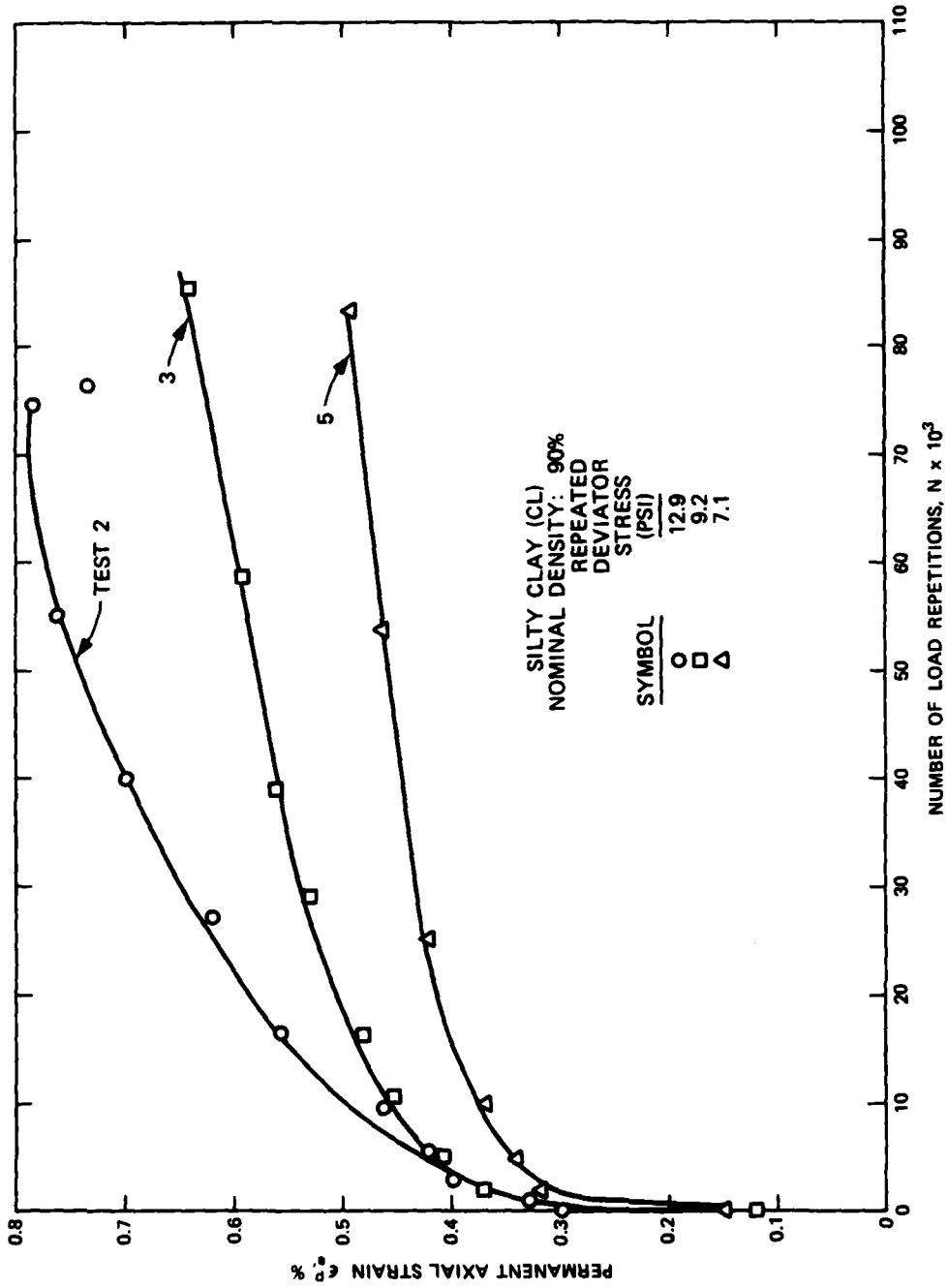


Figure 39. Permanent axial strain versus number of load repetitions (arithmetic), tests 2, 3, and 5 (1 psi = 6.89 kPa)

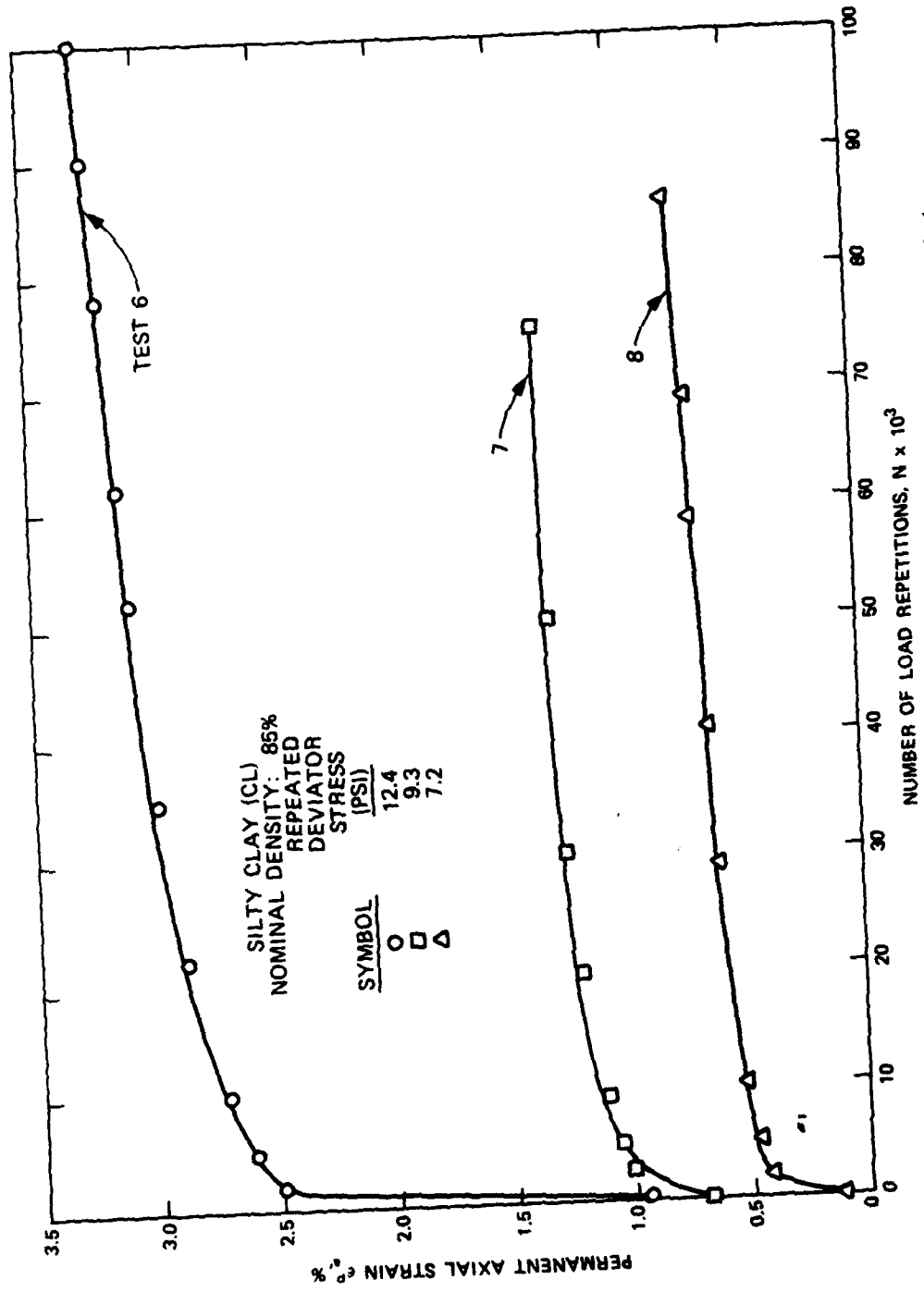


Figure 40. Permanent axial strain versus number of load repetitions (arithmetic), tests 6, 7, and 8 (1 psi = 6.89 kPa)

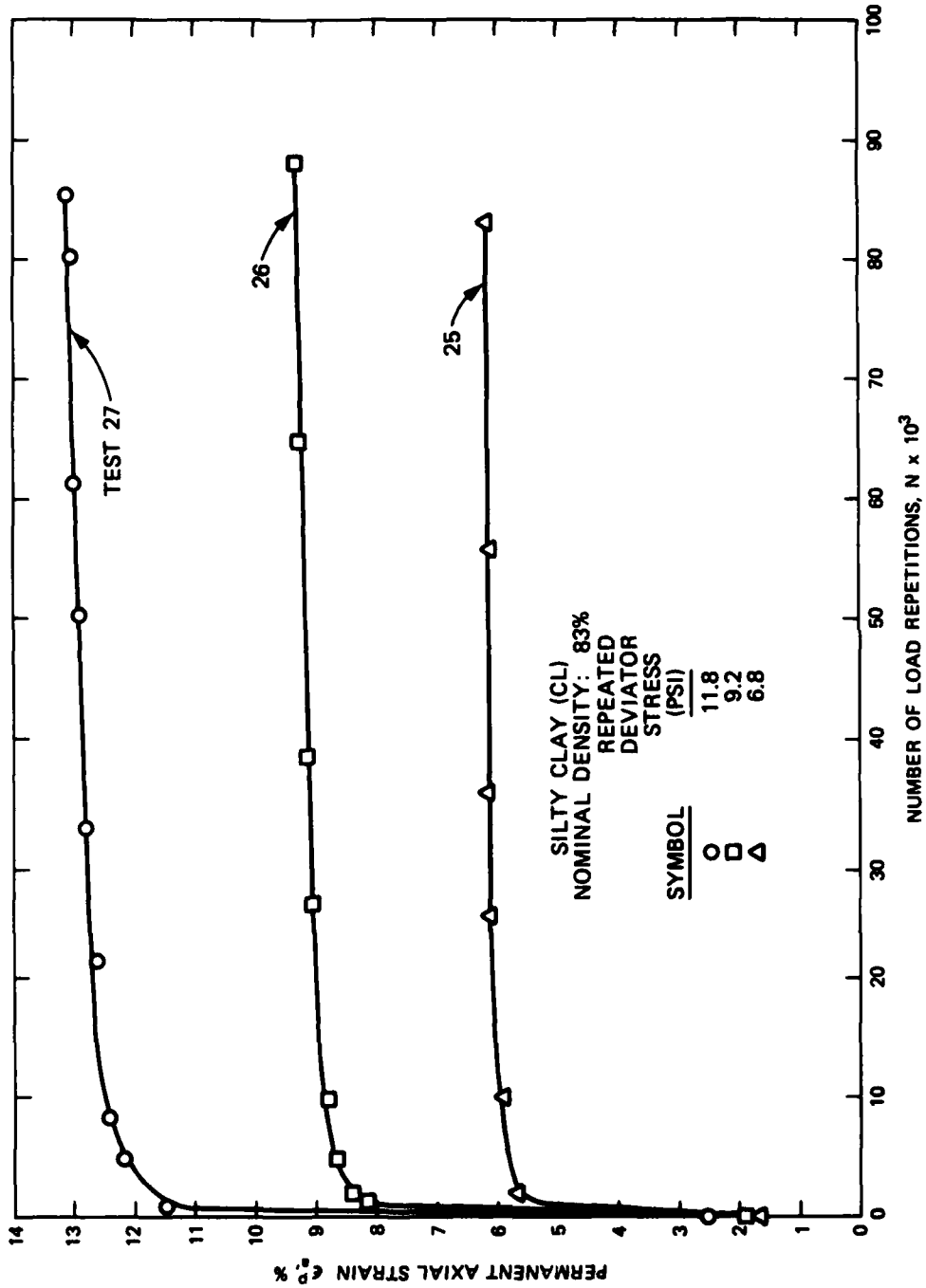


Figure 41. Permanent axial strain versus number of load repetitions (arithmetic), tests 25, 26, and 27 (1 psi = 6.89 kPa)

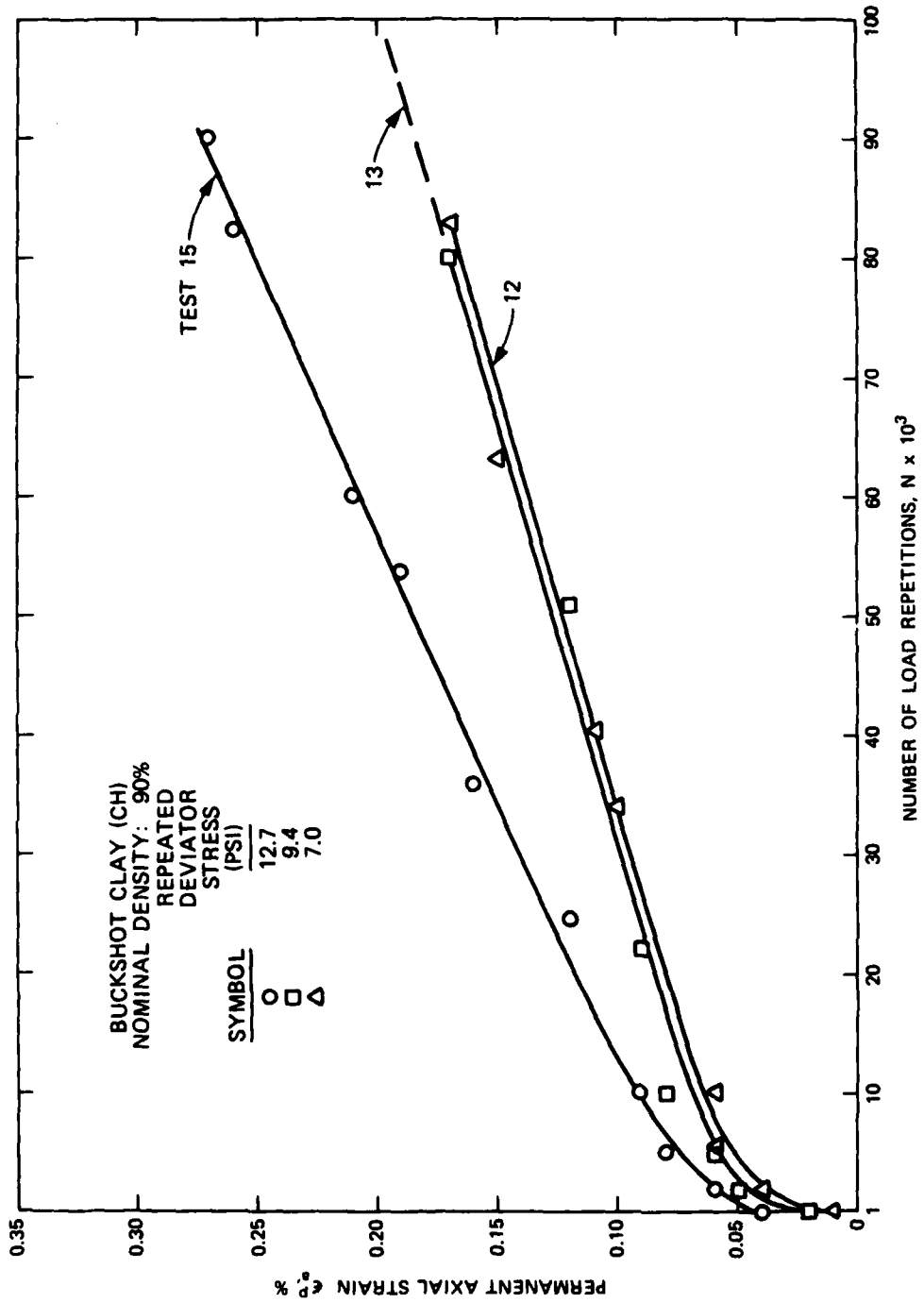


Figure 42. Permanent axial strain versus number of load repetitions (arithmetic), tests 12, 13, and 15 (1 psi = 6.89 kPa)

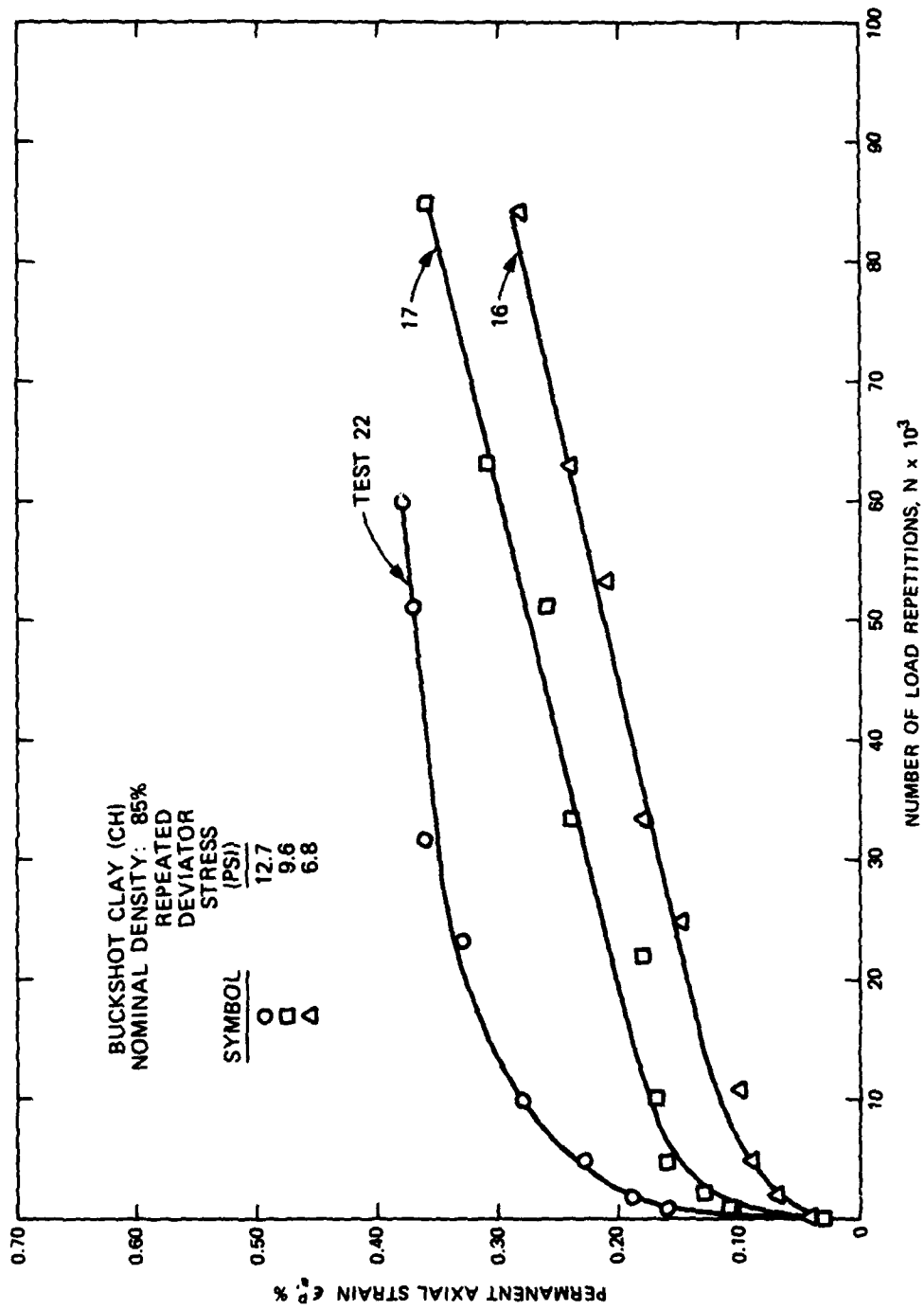


Figure 43. Permanent axial strain versus number of load repetitions (arithmetic), tests 16, 17, and 22 (1 psi = 6.89 kPa)

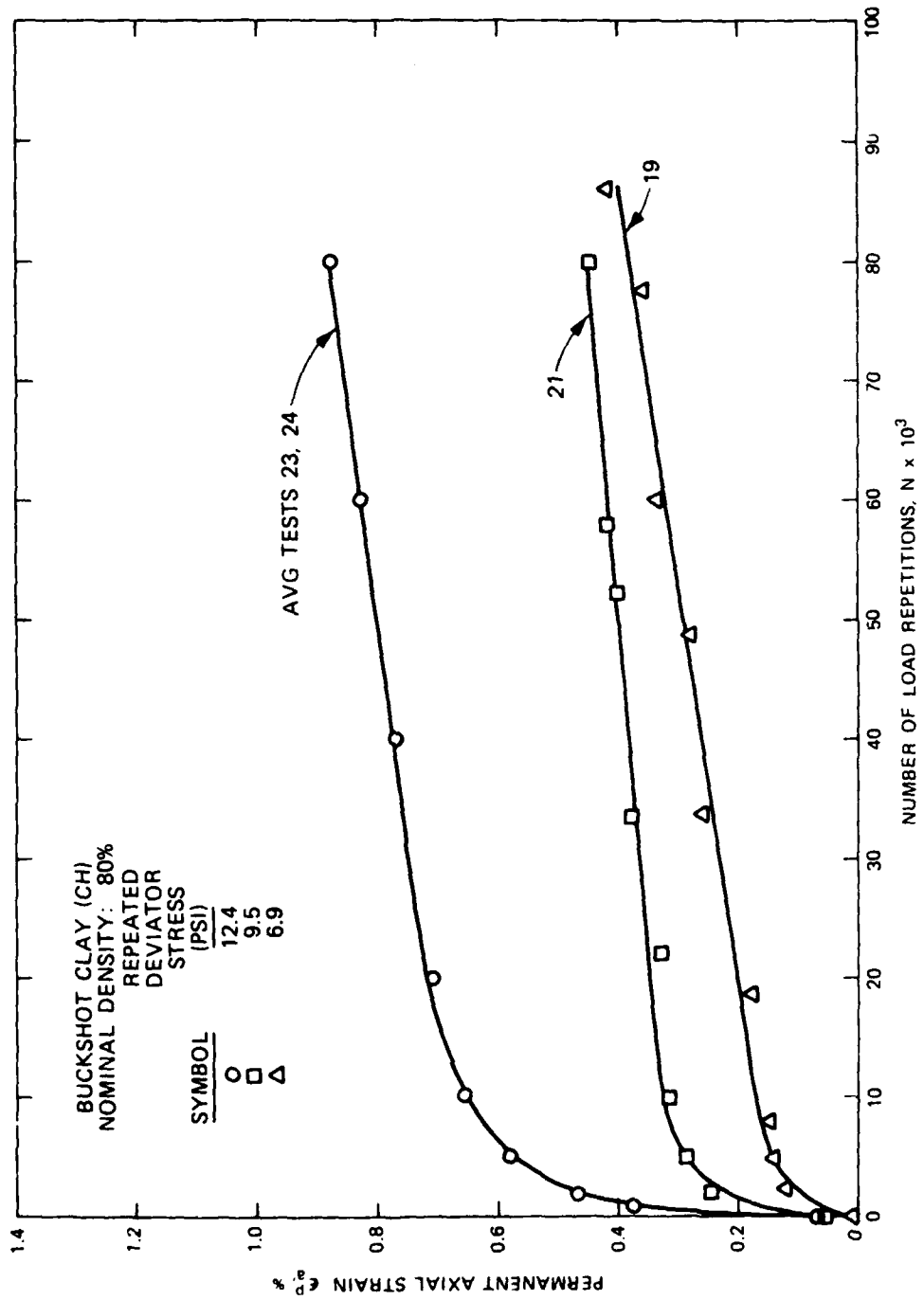


Figure 44. Permanent axial strain versus number of load repetitions (arithmetic), tests 19 and 21 and average data from tests 23 and 24 (1 psi = 6.89 kPa)

AD-A108 518

ARMY ENGINEER WATERWAYS EXPERIMENT STATION VICKSBURG--ETC F/G 8/13  
INVESTIGATION OF COMPACTION CRITERIA FOR AIRPORT PAVEMENT SUBGR--ETC(U)  
OCT 81 W N BRABSTON DOT-FA78WA1-876  
WES/TR/GL-81-11 FAA/RD-81/48 NL

UNCLASSIFIED

2.2

2.2

2.2

2.2

2.2

2.2

2.2

2.2

2.2

2.2

2.2

2.2

2.2

2.2

2.2

2.2

2.2

2.2

2.2

2.2

2.2

2.2

2.2

2.2

2.2

2.2

2.2

2.2

2.2

2.2

2.2

2.2

2.2

2.2

2.2

2.2

2.2

2.2

2.2

2.2

2.2

2.2

2.2

2.2

2.2

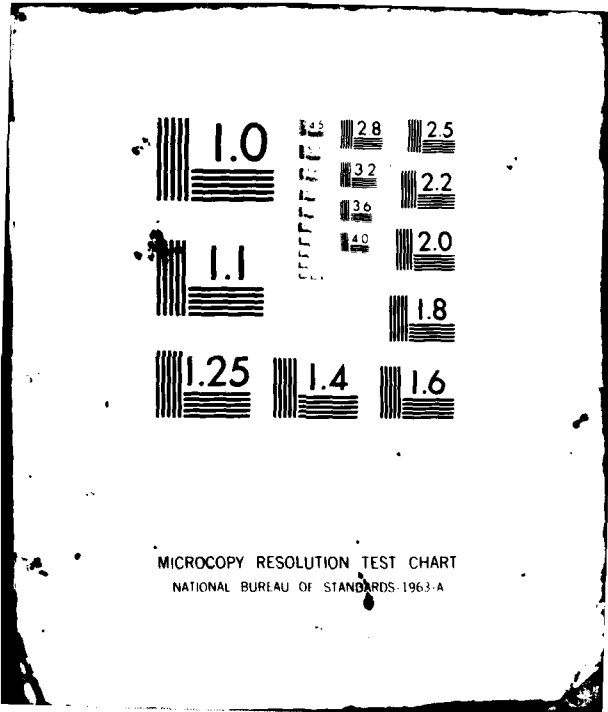
2.2

2.2

2.2

2.2

END  
DATE  
FILMED  
1 82  
DTIC



MICROCOPY RESOLUTION TEST CHART  
NATIONAL BUREAU OF STANDARDS-1963-A

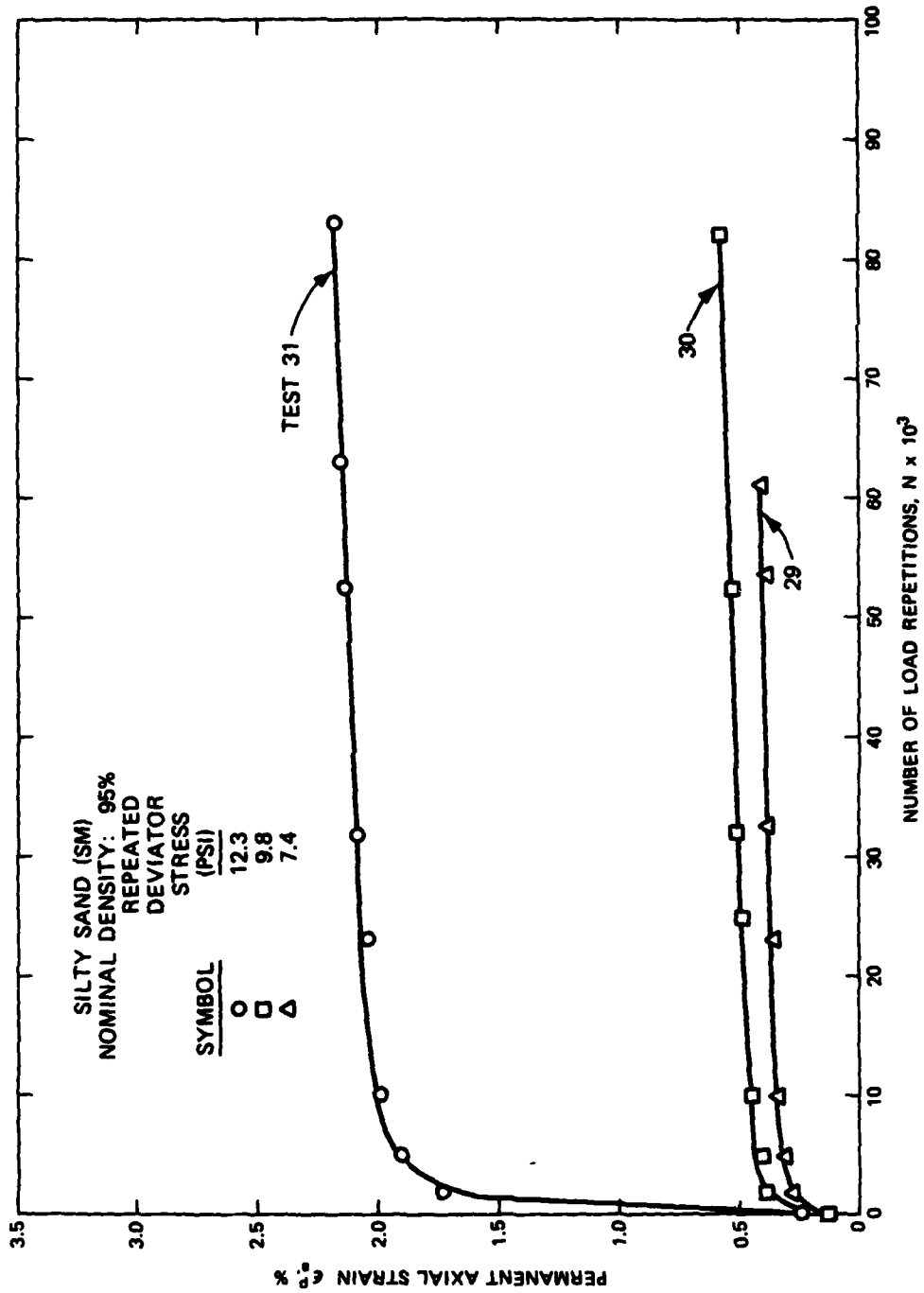


Figure 45. Permanent axial strain versus number of load repetitions (arithmetic), tests 29, 30, and 31 (1 psi = 6.89 kPa)

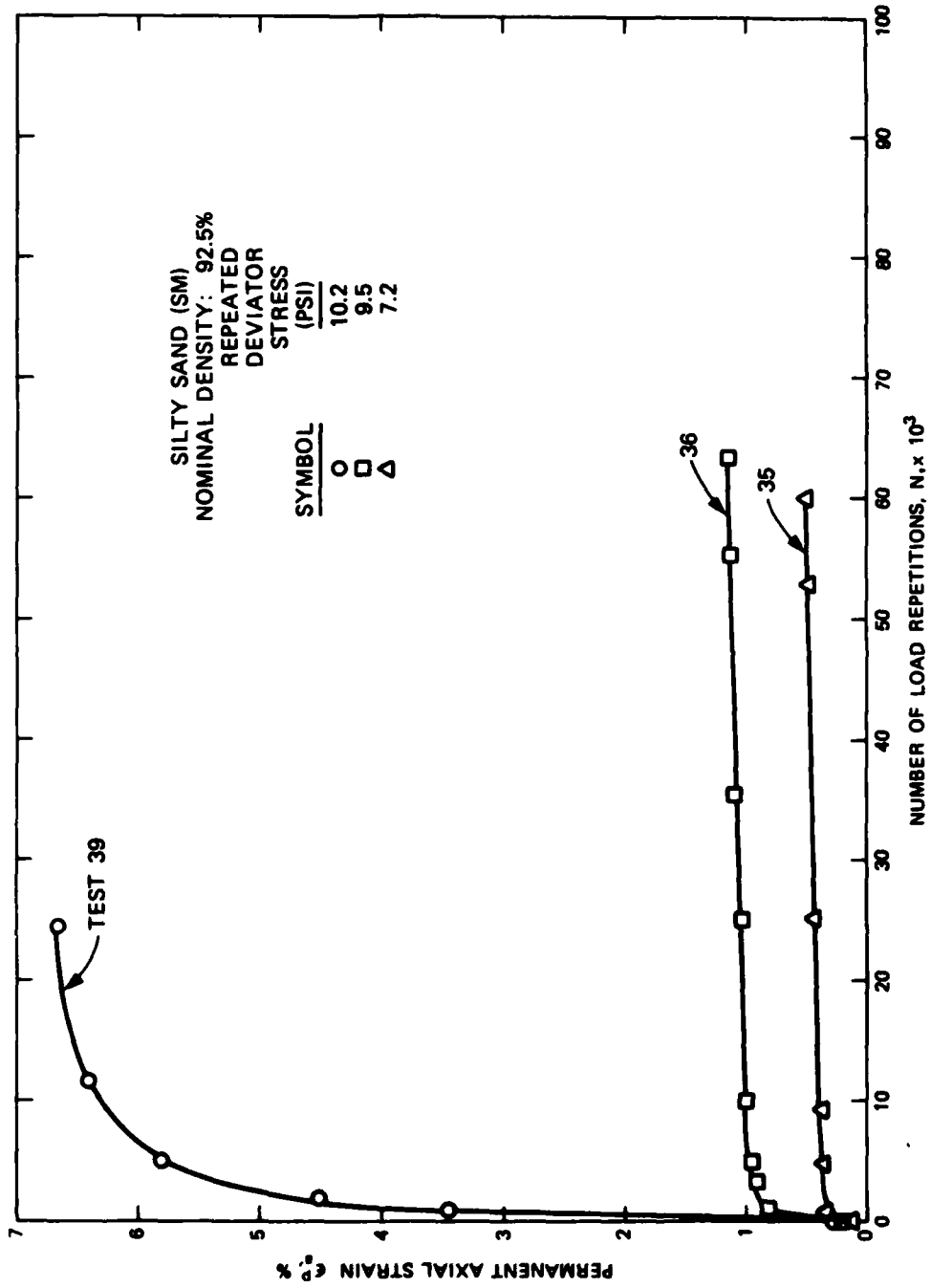


Figure 46. Permanent axial strain versus number of load repetitions (arithmetic), tests 35, 36, and 39 (1 psi = 6.89 kPa)

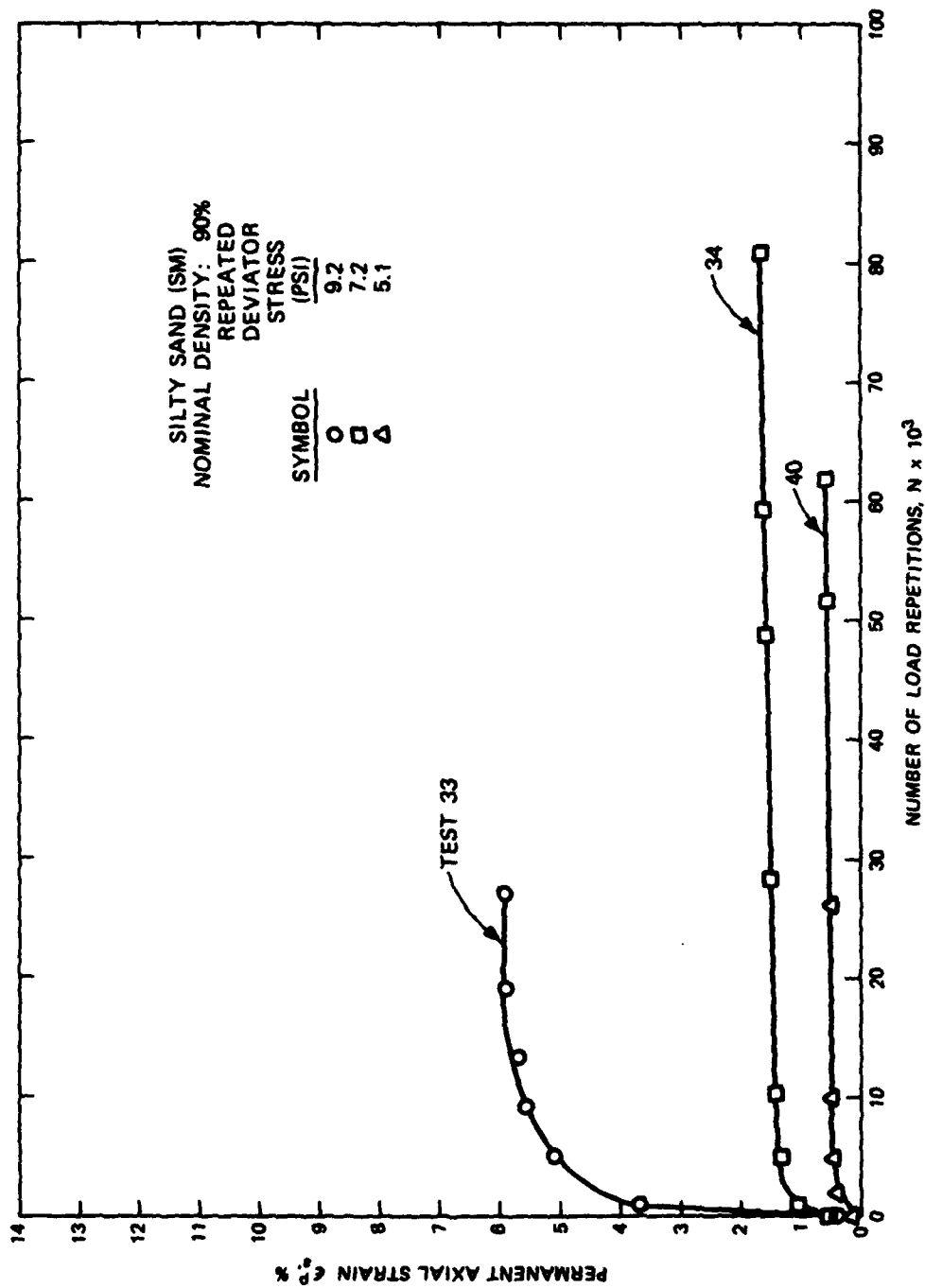


Figure 47. Permanent axial strain versus number of load repetitions (arithmetic), tests 33, 34, and 40 (1 psi = 6.89 kPa)

for higher stress ratios. This pattern is also evident for tests 27, 26, and 25, which were conducted at stress ratios of 0.975, 0.760, and 0.562, respectively, on specimens molded to 83 percent nominal density. These data are presented in Figures 32 and 41. Again, no reversal of shape of the deformation plot is shown on the semilog plot (Figure 32). On the arithmetic plot (Figure 41), it appears that most of the axial deformation developed very early in each test (i.e., 20,000 to 30,000 repetitions), after which there was very little additional permanent deformation.

Buckshot clay. Semilog and arithmetic plots of permanent axial deformation for the buckshot clay are shown in Figures 33-35 and 42-44, respectively. In all cases, the semilog plots indicate an upward turn typical of repetitive load data so presented. However, the degree of curvature becomes significantly less pronounced with decrease in density. These data shown in Figures 33 and 42 represent tests 15, 13, and 12, which were conducted on specimens molded to 90 percent nominal density and at respective stress ratios of 0.190, 0.140, and 0.105. In Figure 42, the rate of strain appears to become constant in the 15,000- to 20,000-repetition range and remains so until termination of testing. A similar pattern is observed for the buckshot clay tested at 85 percent nominal density. These data are indicated on Figures 34 and 43, which represent tests 22, 17, and 16 conducted at strain ratios of 0.348, 0.263, and 0.186, respectively. Again, for these tests it appears that the strain rates become constant for each test in the 15,000- to 25,000-repetition level range. Data for tests 21 and 19 and average data from tests 23 and 24 are indicated in Figures 35 and 44. These tests were conducted on the soil at 80 percent nominal density at stress ratios of 0.528 (tests 23/24) and 0.404 and 0.294 (tests 21 and 19). For these tests, strain patterns similar to those observed in the previous tests with buckshot clay were also found.

Silty sand. Semilog and arithmetic plots of permanent axial deformation versus number of load repetitions for the silty sand are shown in Figures 36-38 and 45-47, respectively. Significantly, there is little evidence of upward curvature of the plots in semilog form,

and all of the plots in arithmetic form indicate that most of the permanent axial deformation occurred very early in the test, after which there was very little additional permanent deformation. Tests 31, 30, and 29 (Figures 36 and 45) were conducted at stress ratios of 0.562, 0.448, and 0.338, respectively, on soil molded to 95 percent nominal density. Tests 39, 36, and 35 were conducted on specimens at 82.5 percent nominal density at stress ratios of 0.570, 0.531, and 0.402, respectively. It may be noted that test 39 was terminated prematurely (24,800 repetitions) and indicated a much higher strain value than the other two tests conducted on specimens at the same density. However, the phenomenon was also observed for the other two sets of tests with the silty sand. The final set of tests involving this material were tests 33, 34, and 40, which were conducted at stress ratios of 0.704, 0.554, and 0.392, respectively, at a nominal density of 90 percent.

#### STATIC LOAD TESTS

Results of the static load triaxial tests are shown in Table 9. Since no replicate specimens were tested simultaneously with the repeated load tests, i.e., these tests were conducted after the repeated load tests were completed, the mean value of the failure deviator stresses for three tests conducted at similar conditions of water content and density were used for calculation of the stress ratio values. For the silty clay at 90, 83, and 80 percent nominal densities, mean deviator stresses at failure were 40.7, 19.0, and 12.1 psi (280.42, 130.91, and 83.37 kPa), respectively. The mean failure deviator stress for the buckshot clay at 90, 85, and 80 percent nominal densities were 67.0, 36.5, and 23.5 psi (461.63, 251.48, and 161.92 kPa), respectively. The silty sand indicated mean failure deviator stresses at nominal densities of 95, 92.5, and 90 percent of 21.9, 17.9, and 13.0 psi (150.89, 123.33, and 89.57 kPa), respectively. In general, the buckshot clay has the highest overall strength value and the silty sand the lowest strength value at the upper density and about the same as the silty clay at the intermediate and lowest density values.

## DISCUSSION

The original purpose of this study was to examine the effect of lowering density requirements for subgrades in airport pavements. The study was accomplished primarily through a laboratory-oriented program in which molded specimens of three different soil types were subjected to repeated axial loads at representative subgrade stress levels and the deformation response of the soils was observed. Two types of soil response data were obtained from the repeated load tests: resilient deformation and permanent deformation, both of which were presented in terms of strain values.

### RESILIENT STRAIN

As was indicated in Table 10, the resilient axial strain values were generally small in magnitude, having mean values of 1.4, 0.8, and  $0.5 \times 10^{-3}$  in./in. for the silty clay, buckshot clay, and silty sand, respectively. The magnitudes of these values were also reflected in the somewhat large resilient modulus values. The range in strain values as reported earlier was largest for the silty clay ( $0.5 \times 10^{-3}$  to  $2.5 \times 10^{-3}$  in./in.) and smallest for the silty sand ( $0.3 \times 10^{-3}$  to  $0.7 \times 10^{-3}$  in./in.). For the buckshot clay, the stress values ranged from  $0.2 \times 10^{-3}$  to  $2.1 \times 10^{-3}$  in./in., respectively. Plots of the resilient strain value associated with each test versus the applied deviator stress are shown in Figures 27, 28, and 29. Since the slopes of these plots represent a modulus value of sorts, additional insight as to the relative properties of each material may also be gained from visual or qualitative observations of each plot. From general observation of the plots, those for the silty sand (Figure 29) have the steepest slopes while those for the silty clay (Figure 27) have the smallest slopes with the slopes of the buckshot clay soil (Figure 28) being of intermediate value. These observations correlate with the magnitudes and ranges of resilient strain for each soil as indicated earlier.

The effect on resilient strain of reduction in density for each soil at a given stress level did not appear to be particularly significant. This fact may be observed from the generally small range found

in strain values for each soil for a decrease in density at each stress level (Table 10). For the silty sand, for example, the entire range in resilient strain over the entire test was from  $0.3 \times 10^{-3}$  to  $0.7 \times 10^{-3}$  in./in. Comparisons with similar resilient strain data from tests conducted on 39 clay soils at the University of Illinois<sup>37</sup> are shown in Table 11. For each case shown, the soil was compacted to 90 percent density prior to testing. Although the stress states differed somewhat, they were generally very similar in magnitude. The values shown for the WES tests are single-point values, while those for the Illinois soils are the mean strain values for the 39 tests. In the Illinois study, only the repeated stress and resilient modulus values were reported; therefore, the individual strain values from which the means were calculated were inferred from the former two values.

Table 11. Summary of Repeated Axial Stress and Resilient Strain Data - WES and University of Illinois Tests

Soil Types	Repeated Axial Stress, psi	Resilient Axial Strain, in./in. $10^{-3}$
WES-Silty clay (CL)	12.9	1.6
	9.2	0.9
	7.1	0.5
WES-Buckshot clay (CH)	12.7	0.8
	9.4	0.6
	7.0	0.2
WES-Silty sand (SM)	12.3	0.6
	9.8	0.4
	7.4	0.3
University of Illinois Mean value, 39 clays	12.5	2.8
	9.5	1.9
	7.0	1.2

Note: 1 psi = 6.89 kPa; 1 in. = 2.54 cm.

As noted in Table 11, the strain levels for the Illinois soils are 1.75, 3.5, and 4.7 times larger than the strain values of the CL, CH, and SM soils at the highest stress levels, respectively; and 2.1, 3.2, and 4.75 times larger at the intermediate stress level; and 2.4, 6.0, and 4.0 times larger at the lowest stress level. Though not shown, similar differences were reflected in the resilient modulus values.

## PERMANENT STRAIN

Strain rate. An examination of the arithmetic plots of number of load repetitions versus permanent axial strain (Figures 39-47) indicate that in none of the tests was there evidence of fatigue, i.e., a pronounced increase in rate of strain with load applications, particularly during the latter portion of the test sequence. In all cases except possibly test 2 of the silty clay, there developed at some point in the test a constant rate of strain, i.e., straight-line portion, although in some cases there was a negligible increase in total strain with load repetitions. For the silty clay and buckshot clay soils, there appeared to be, on a quantitative basis, a decrease in the slope of the straight-line portion with decrease in stress and decrease in density. For the silty clay at 83 percent density, the rate of strain diminished to practically zero for all three stress levels at about 30,000 repetitions or less and continued as such throughout the tests. The buckshot clay indicated steady-state strain increase for all nine tests. Although two tests with the silty sand (39 and 32) were terminated somewhat prematurely, Figures 45, 46, and 47 show that in all tests with the soil, the rate of strain reached a steady state early in the tests after which further increase in strain was very small. For the silty clay, buckshot clay, and silty sand, the maximum strain ratios applied to each soil in any of the tests were 0.975, 0.528, and 0.708, respectively, with mean values of 0.304, 0.273, and 0.501, respectively. As noted in Table 9, most of the values of the stress ratios used in the tests were below 0.75 or 75 percent of the sample failure deviator stress.

Permanent strain versus stress. In order to evaluate the permanent axial strain response of each soil on a mutual basis, the strain values at 75,000 repetitions, actual or extrapolated, was selected for comparison. This load repetition level was selected as being representative of the average terminal point for each test. Values of the terminal permanent axial strain value along with values of repeated deviator stress and stress ratios used in each test are presented in Table 12. Test numbers in this table correspond to those given in Tables 8 and 9.

Table 12. Summary of Stress Ratio and Permanent Axial Strain at 75,000 Repetitions

Soil Type	Test No.	Stress Ratio $\Delta\sigma = \sigma_{D_r} / \sigma_{D_f}$	Permanent Axial Strain @ 75,000 Repetitions percent
Silty clay (CL)	2	0.317	0.80
	3	0.226	0.63
	5	0.175	0.43
	6	0.653	3.20
	7	0.490	1.34
	8	0.379	0.75
	27	0.975	13.10
	26	0.760	9.30
	25	0.562	6.10
Buckshot clay (CH)	15	0.190	0.24
	13	0.140	0.16
	12	0.105	0.16
	22	0.348	0.42
	17	0.263	0.32
	16	0.186	0.26
	23/24	0.528	0.86
	21	0.404	0.44
19	0.294	0.36	
Silty sand (SM)	31	0.562	2.20
	30	0.448	0.60
	29	0.338	0.45
	39	0.570	7.00*
	36	0.531	1.10*
	35	0.402	0.50*
	33	0.708	6.80
	34	0.554	1.60
40	0.392	0.60*	

\* Extrapolated.

Plots of permanent axial strain versus repeated deviator stress for the silty clay, the buckshot clay, and the silty sand are shown in Figures 48, 49, and 50, respectively. An examination of these plots for the silty clay reveals that at 90 percent density there was less than 1 percent strain. At 85 percent density, the strain values ranged from 0.75 to 3.2 percent, and at 83 percent density the permanent axial strain from 6.10 to 13.10 percent. Table 12 also shows that by reducing the density from 90 to 83 percent, the strain increased over 10 times, a significant increase.

A similar plot for the buckshot clay is shown in Figure 49. The permanent axial strain value at 75,000 repetitions at no time exceeded 1 percent. The maximum strain values for this soil at densities of 90, 85, and 80 percent were 0.24, 0.42, and 0.86 percent, respectively. These strain values were observed at the highest repetitive stress levels used. At the lowest stress levels, permanent strain values of 0.16, 0.26, and 0.36 percent were observed for densities of 90, 85, and 80 percent. Therefore, the effect of reducing density from 90 to 80 percent resulted in increase in strain of 3.6 times at the highest stress level and 2.3 times at the lowest repetitive stress level, or an average increase of about 3 times.

The plot of permanent axial strain at 75,000 load repetitions versus repeated deviator stress for the silty sand (Figure 50) indicates high sensitivity to change in stress and density. Strain values for this soil range from 0.45 to 2.20 percent at 95 percent density, 0.50 to 7.00 percent at 92.5 percent, and 0.60 to 6.80 percent at 90 percent. Thus, while the strain figures at 92.5 and 90 percent density are not significantly different (perhaps due to some extrapolation), the significant changes in strain from 2.20 to 7.00 percent with a change in density from 95 to 92.5 percent indicate the extreme sensitivity of the soil.

Permanent strain versus stress ratio. Another means of examining the response of each soil type is found from a plot of permanent axial strain at 75,000 repetitions versus the associated stress ratio for each test. A consolidated plot indicating these relationships for all tests

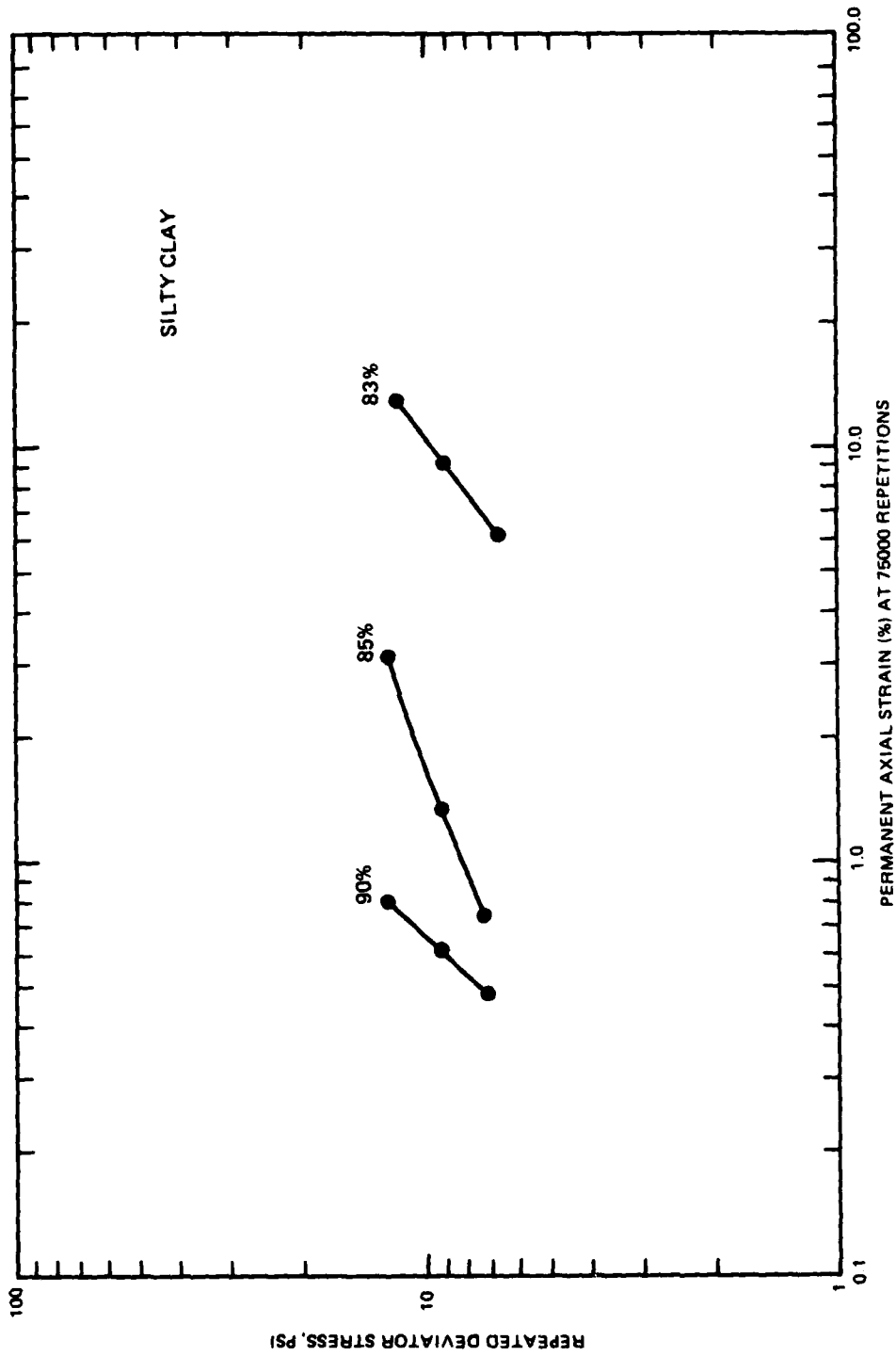


Figure 48. Repeated deviator stress versus permanent axial strain at 75,000 repetitions for silty clay (1 psi = 6.89 kPa)

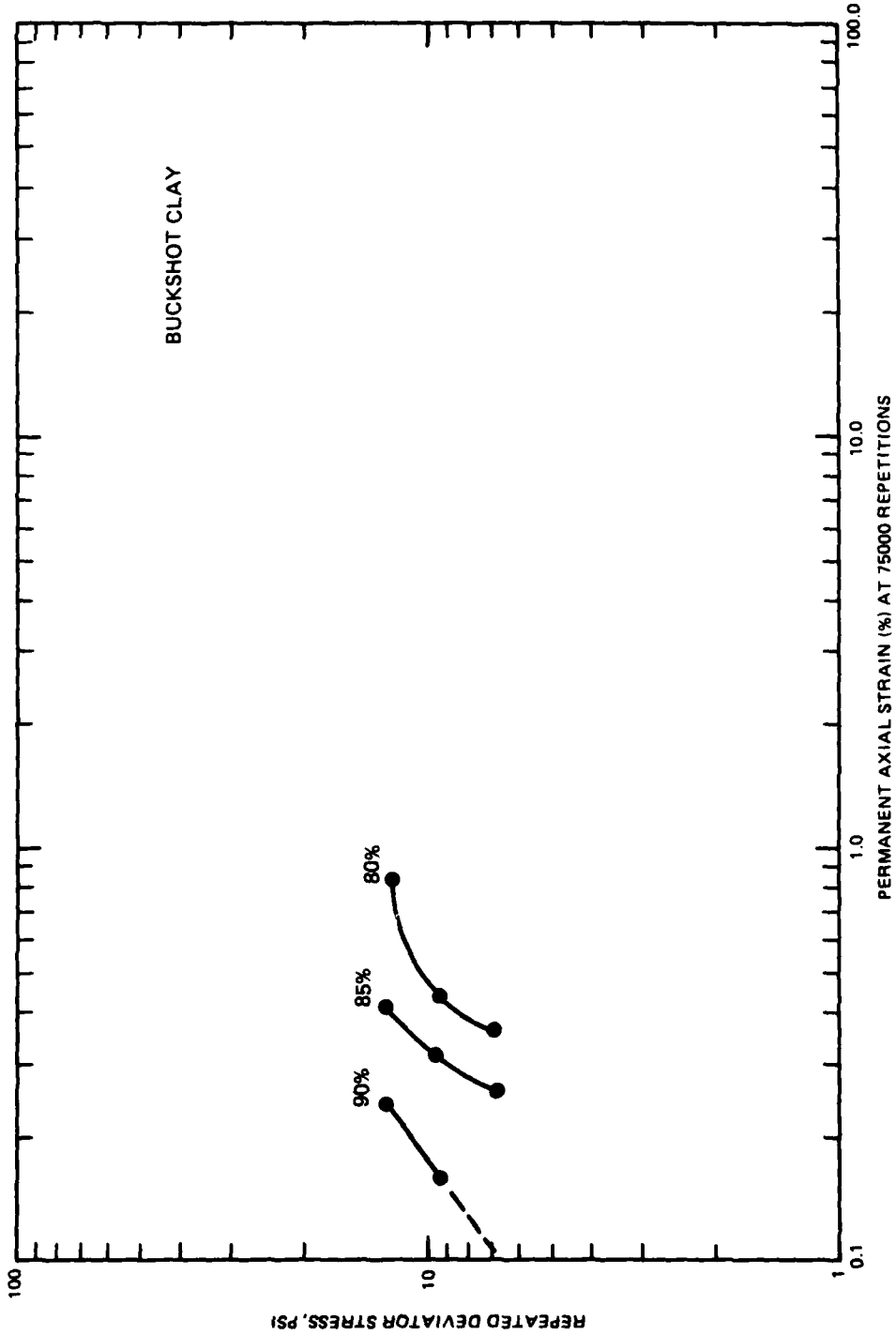


Figure 49. Repeated deviator stress versus permanent axial strain at 75,000 repetitions for buckshot clay (1 psi = 6.89 kPa)

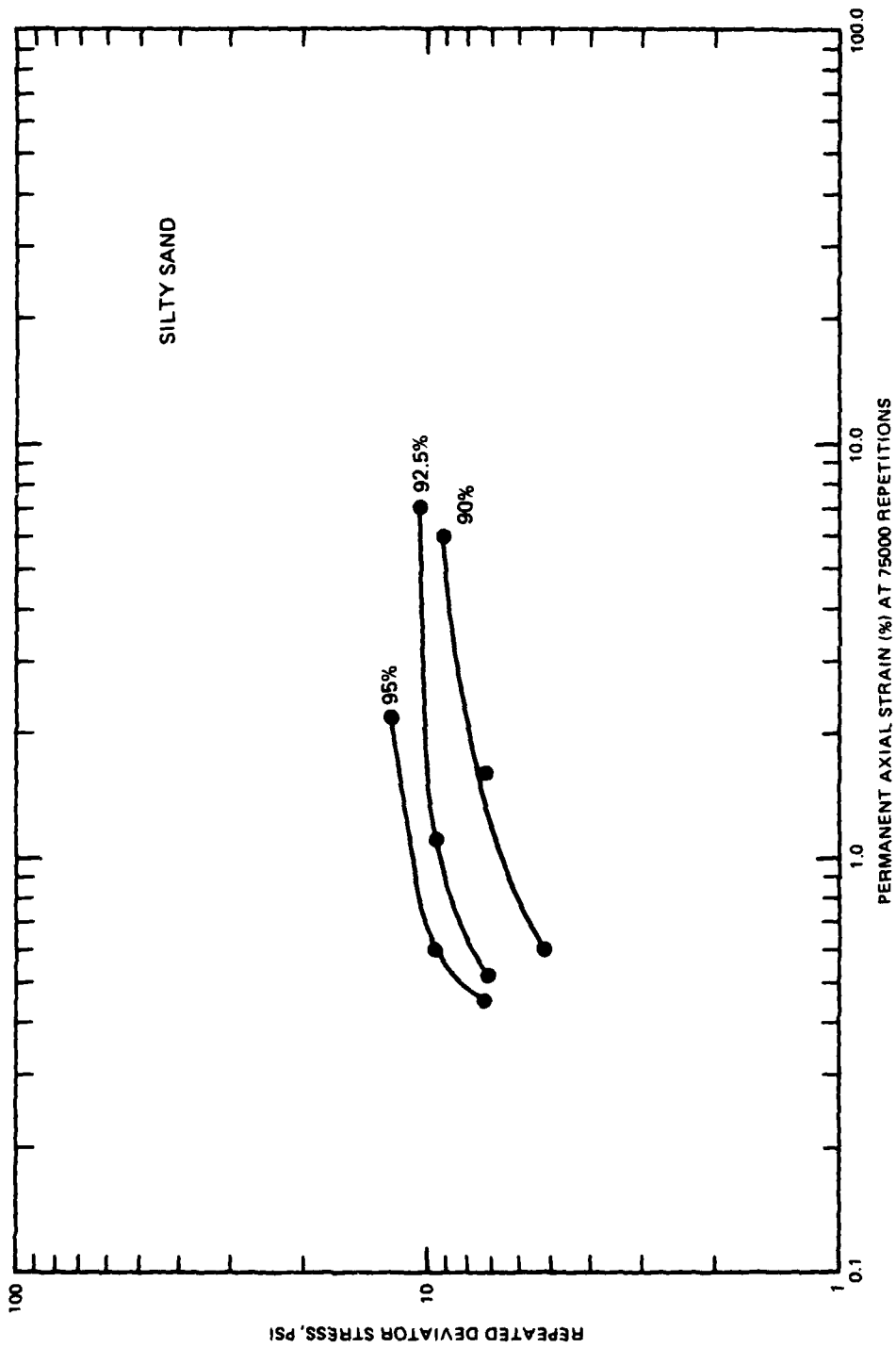


Figure 50. Repeated deviator stress versus permanent axial strain at 75,000 repetitions for silty sand (1 psi = 6.89 kPa)

is shown in Figure 51. This plot indicates a qualitative relationship between stress ratio and permanent axial strain. The plots for the buckshot clay are grouped to the left and have steeper slopes, indicating lower strain values and high stiffness. Interestingly, except for the plot for the silty clay at 83 percent density, the plots for this soil also indicate relatively steep slopes similar to those for the buckshot clay. The range in strain values over the testing sequence is much larger, however. The plots for the silty sand have flat slopes indicating high sensitivity to stress ratio as well as density.

#### STATIC LOAD TEST

The effect of a decrease in density value with the corresponding increase in soil moisture content on the failure deviator stress of the silty clay may be seen from data presented in Table 13. Lowering the density from 90.7 to 84.7 percent, a reduction of 6.6 percent in density, results in a decrease in failure deviator stress from 40.7 to 19.0 psi (280.61 to 131.0 kPa), or 53.3 percent. Realizing that for purely cohesive soils the shear strength is simply half of the deviator stress at failure, the effect on shear strength similarly applies. A further reduction in density to 83 percent, or 8.5 percent change, resulted in a decrease in 70.3 percent in soil strength.

Table 13. Effect of Changes in Density on Failure Deviator Stress - Silty Clay

Nominal	Density		Percent Change	Failure Deviator Stress, psi	Percent Change
	Percent ASTM D 1557	Actual (Average)			
90	90.7		0	40.7	0
85	84.7		-6.6	19.0	-53.3
83	83.0		-8.5	12.1	-70.3

Note: 1 psi = 6.89 kPa.

The effect of lowering density and increasing water content on the failure deviator stress of the buckshot clay is shown in Table 14. It should be noted first that the basic values of failure deviator stress for this soil were considerably higher than for the silty clay.

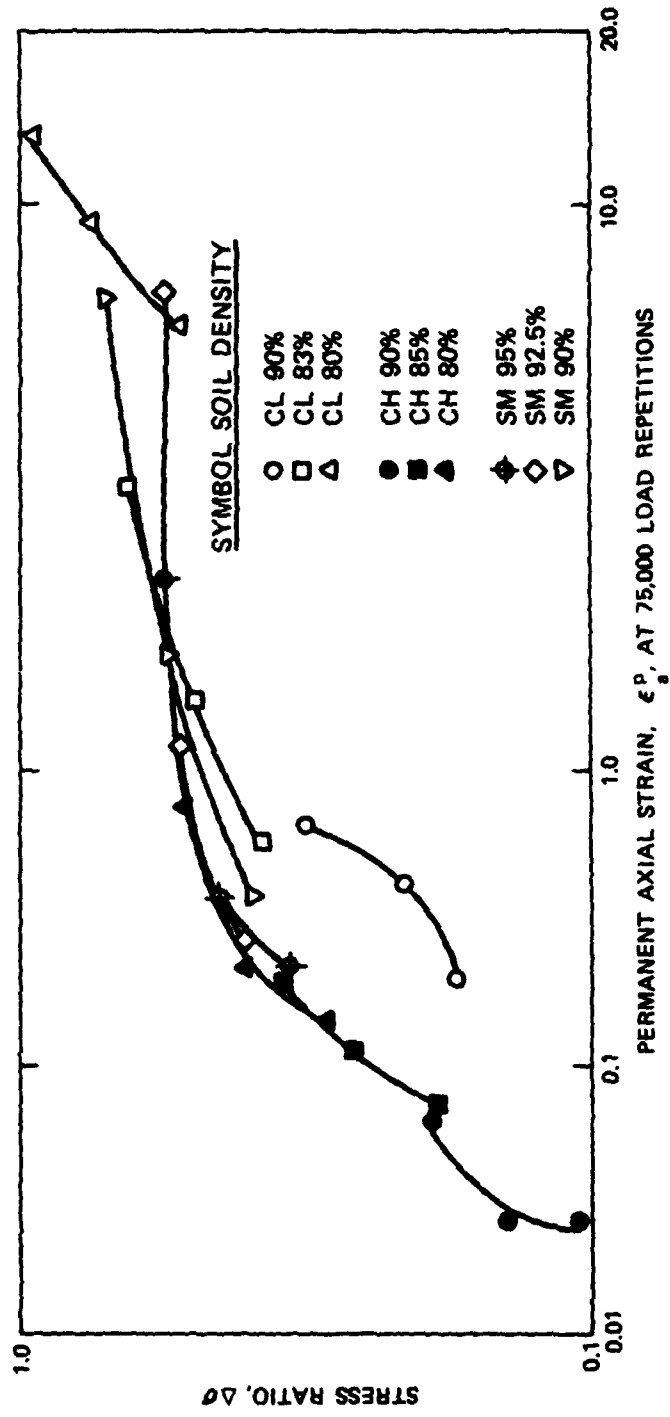


Figure 51. Stress ratio versus permanent axial strain at 75,000 load repetitions

Second, the failure deviator stress for the buckshot clay at 80.4 percent density, the lowest value, was almost twice that for the silty clay at 93 percent, also the lowest density for that sort of specimen. The effect of lowering density of the soil from 89.8 to 84.4 and 80.4 percent was to decrease the respective values of failure deviator stress from 67.0 to 36.5 and 23.5 psi (461.95 to 251.66 and 162.03 kPa). In terms of percentage, therefore, reductions in density by 6.0 and 10.5 percent resulted in strength decreases of 45.5 and 64.9 percent, respectively.

Table 14. Effect of Changes in Density on Failure Deviator Stress - Buckshot Clay

Nominal	Density		Percent Change	Failure Deviator Stress, psi	Percent Change
	Percent ASTM D 1557	Actual (Average)			
90		89.8	0	67.0	--
85		84.4	-6.0	36.5	-45.5
80		80.4	-10.5	23.5	-64.9

Note: 1 psi = 6.89 kPa.

The effect of reducing density and the accompanying increase in moisture content on the failure stress of the silty sand are presented in Table 15. Specimens of the silty sand material indicated the lowest strength values of all three soils. This table also shows the sensitivity of the soil to change in density. A reduction in density from 95.4 to 92.1 percent, a decrease of only 3.5 percent, resulted in a reduction in failure deviator stress of from 21.9 to 17.9 psi (150.99 to 123.42 kPa), or 18.3 percent. By lowering the density to 90.3 percent or a total reduction of only 5.4 percent, the failure deviator stress was decreased to 13.0 psi (89.63 kPa) for a total reduction of 40.6 percent.

Table 15. Effect of Changes in Density on Failure Deviator Stress - Silty Sand

Nominal	Density		Percent Change	Failure Deviator Stress, psi	Percent Change
	Percent ASTM D 1557	Actual (Average)			
95.0		95.4	0	21.9	--
92.5		92.1	-3.5	17.9	-18.3
90.0		90.3	-5.4	13.0	-40.6

Note: 1 psi = 6.89 kPa.

#### SUMMARY

The resilient strain values indicated that the relative stiffness of the three materials in order of increasing resilient stiffness were the silty clay, the buckshot clay, and the silty sand. The magnitudes of the strain values appeared to be relatively small, however, especially when compared with representative data by other researchers. In general, it was found that there was no evidence of the fatigue phenomenon in any of the soils tested within the range of stresses and repetition levels used.

Based on the permanent strain values, the buckshot clay demonstrated the largest resistance to deformation under repetitive load, the lowest deformation values, and the least sensitivity to reduction in density.

The silty clay at the 83 percent density actually demonstrated the highest permanent deformation, indicating extreme sensitivity to reduction in density by 7 percent, i.e. from 90 to 83 percent. Resistance to the deformation under repetitive loading was indicative of a soil of medium plasticity.

The silty sand was extremely sensitive to changes in density along with the accompanying increase in water content, as evidenced by the requirement to maintain density values within the 90 to 95 percent limit and simultaneously reduce repetitive stress levels.

In review, it appears that based on the small magnitudes of the resilient strain values, especially compared with representative data by other researchers, these data would not provide a suitable model

for the study as a vehicle for the translation of laboratory results to predicted field performance. Comparison of the resilient strain values with the permanent strain values also leads to the conclusion that since the permanent strain values are much larger than the resilient strain values, permanent deformation would be the predominant factor in pavement behavior. The result of the laboratory tests, then, provides the basis of the permanent strain model.

## STRAIN MODEL AND EFFECT ON PAVEMENT PERFORMANCE

### STRAIN MODEL

#### GENERAL

The objective of the statistical analysis was, ultimately, to develop a soil strain model that was based on the results of laboratory tests and that incorporated as regression parameters certain characteristics and properties of the individual soils. The first step in the process was to characterize each individual plot of permanent axial strain versus number of load repetitions in terms of a common mathematical relation having the functional form:

$$\epsilon_a^P = f(N) \quad (10)$$

where

$\epsilon_a^P$  = permanent axial strain

N = number of load repetitions

A simple, two-variable, curve-fitting program was used to analyze the form of the deformation plots. In the program, data fits are made against nine preselected mathematical forms. These forms included first, second, and third degree polynomials; exponential, power, and hyperbolic functions; and two common and one natural logarithmic function.

Once an acceptable mathematical form was adopted, the next step was to relate the appropriate regression coefficients to certain general properties of the soils, particular characteristics of the specimens, and stress states used in the tests that would seem pertinent to the results obtained. For this procedure, a stepwise regression program was used that relates a number of independent variables to a single dependent variable using a "step-up" mode. In the computational process, a sequence of multiple linear regression equations is calculated, beginning with the independent variable that best correlates with the dependent variable, and adding to the regression equation at each step the independent variable that next best correlates, etc., until the sequence is completed. At each step, the multiple R of the correlation equation

is increased. The general form of the final regression equation is

$$C_i = A_0 + A_1X_1 + A_2X_2 \dots A_nX_n \quad (11)$$

where

$C_i$  = coefficient based on specific form of the equation from the previous correlation (Equation 10)

$$\epsilon_a^P = f(N)$$

$A_i$  = correlation coefficient

$X_i$  = independent variables based on soil properties, specimen characteristics, and stress states

The specific parameters used in the correlations with the coefficients developed in the curve-fitting program involved properties of the compacted specimens, general characteristics of the soils, and stress states used in the repetitive and static load tests. The two primary characteristics of the test specimens were density (in terms of percent ASTM D 1557<sup>6</sup>) and moisture content. Since these two properties are interdependent because of the line of optimums relationship, only the soil density  $\gamma_d$  was used as a correlation parameter.

The engineering characteristics that may generally be used in the description of all soils are gradation, Atterberg limits, etc. Two selected for this analysis, as being pertinent to the behavior of the soil under repetitive loading, were the percent clay in each soil and the slope of a plot of the maximum dry density from each compaction curve of the moisture density relations versus the compaction energy used in developing each respective curve. The percent clay (% < 2 $\mu$ ) is defined as that portion of the soil smaller than 2 $\mu$  as determined from the gradation curves (Figure 8). The density-compaction energy plots were generated based on data from the three moisture density relations for each soil (Figures 9, 10, and 11). Maximum dry density for each curve, in pounds per cubic foot (pcf), was plotted along with the compaction energy in foot-pounds per cubic foot (ft-lb/ft<sup>3</sup>) to develop the plots shown in Figure 52. The slope of each plot, compaction energy

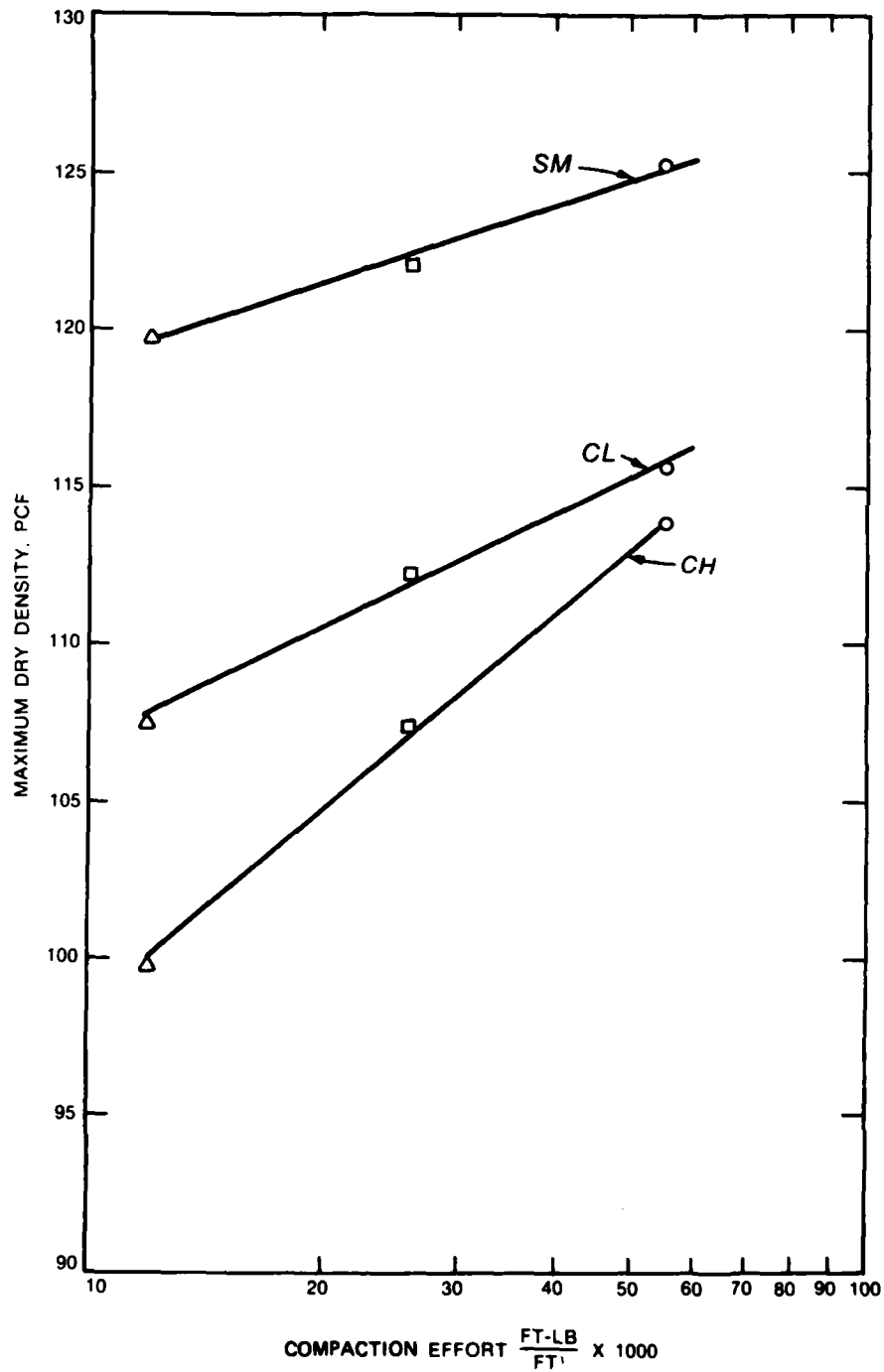


Figure 52. Maximum dry density versus compaction effort for silty clay (CL), buckshot clay (CH), and silty sand (SM)  
 (1 pcf = 16.02 kg/m<sup>3</sup>; 1 ft-lb/ft<sup>3</sup> = 0.048 kJm<sup>3</sup>)

slope (CES), was then used as a parameter in the regression analysis.

The final parameter involved in the analysis was the stress ratio  $\Delta\sigma$  previously described, which represents the ratio of the repetitive axial stress to the deviator stress at failure of the specimens tested under static axial loading.

#### DEVELOPMENT OF FUNCTIONS

Using the curve-fitting program, data from each individual repetitive load test, except tests 23 and 24 for which the data were averaged, were input to obtain a suitable mathematical function. Paired sets of data, permanent axial strain and associated repetition level, were input for each test with the strain value as the dependent variable and repetitions as the independent variable. Results of the analysis indicated that two general forms best suited the data based on highest values of nonlinear correlation and lowest values of standard error of estimate for the 27 data sets entered. The regression equations in order of preference were

$$\varepsilon_a = A_0 + A_1 N + A_2 \log N \quad (12)$$

and

$$\varepsilon_a = AN^B \quad (13)$$

The next step involved correlation of the regression coefficients with soil and test parameters using the stepwise regression analysis. Results of the stepwise analysis using Equation 12 indicated poor correlation with any of the three coefficients. Therefore, it was decided that Equation 13 would be the final form used to describe the strain-repetition relation, and thus correlations of the coefficient A and exponent B with the soils and test parameters would take the functional form

$$\left. \begin{array}{l} A \\ B \end{array} \right\} = f(\gamma_D, \%<2\mu, CES, \Delta\sigma) \quad (14)$$

To obtain a more accurate general model that would reasonably predict permanent strain, it was decided that in individual cases where the value of the intercept A, or slope B, was obviously not consonant

with the surrounding values, adjustments should be made to obtain a more rational arrangement. Plots were made of the regression equations originally generated in the curve-fitting program in log-log form (Figures 53-61), and adjustments were made to the slope and intercept of the straight-line plots in the instances indicated. In all cases, there was little significant change in the overall magnitude of the test results. After the plots had been adjusted, the revised values of slope and intercept were determined.

Regression equations relating the soil and test parameters to the slope and intercept constants were then generated using the stepwise regression program. A summary of all variables used in the regression is shown in Table 16. All variables were entered in logarithmic form. To ensure that all variables were of about the same magnitude, the density values were multiplied by 0.01 and the percent clay values by 0.1 before transformation to logarithmic form. Results of the regression analyses are shown below:

For the intercept A:

MULTIPLE R            0.9554  
 STD. ERROR OF EST.    0.2201

VARIABLE		COEFFICIENT	STD. ERROR
CONSTANT		-8.68976	
IVAR2	2	4.57115	4.38086
IVAR3	3	5.05241	0.75578
IVAR4	4	-11.26392	1.53771
IVAR5	5	2.08357	0.36200

For the slope B:

MULTIPLE R            0.7063  
 STD. ERROR OF EST.    0.1114

VARIABLE		COEFFICIENT	STD. ERROR
CONSTANT		2.05266	
IVAR2	2	-1.70143	1.38296
IVAR3	3	-1.68431	0.37271
IVAR4	4	3.65294	0.77042

where

- IVAR2 = density
- IVAR3 = percent clay
- IVAR4 = slope (CES)
- IVAR5 = stress ratio

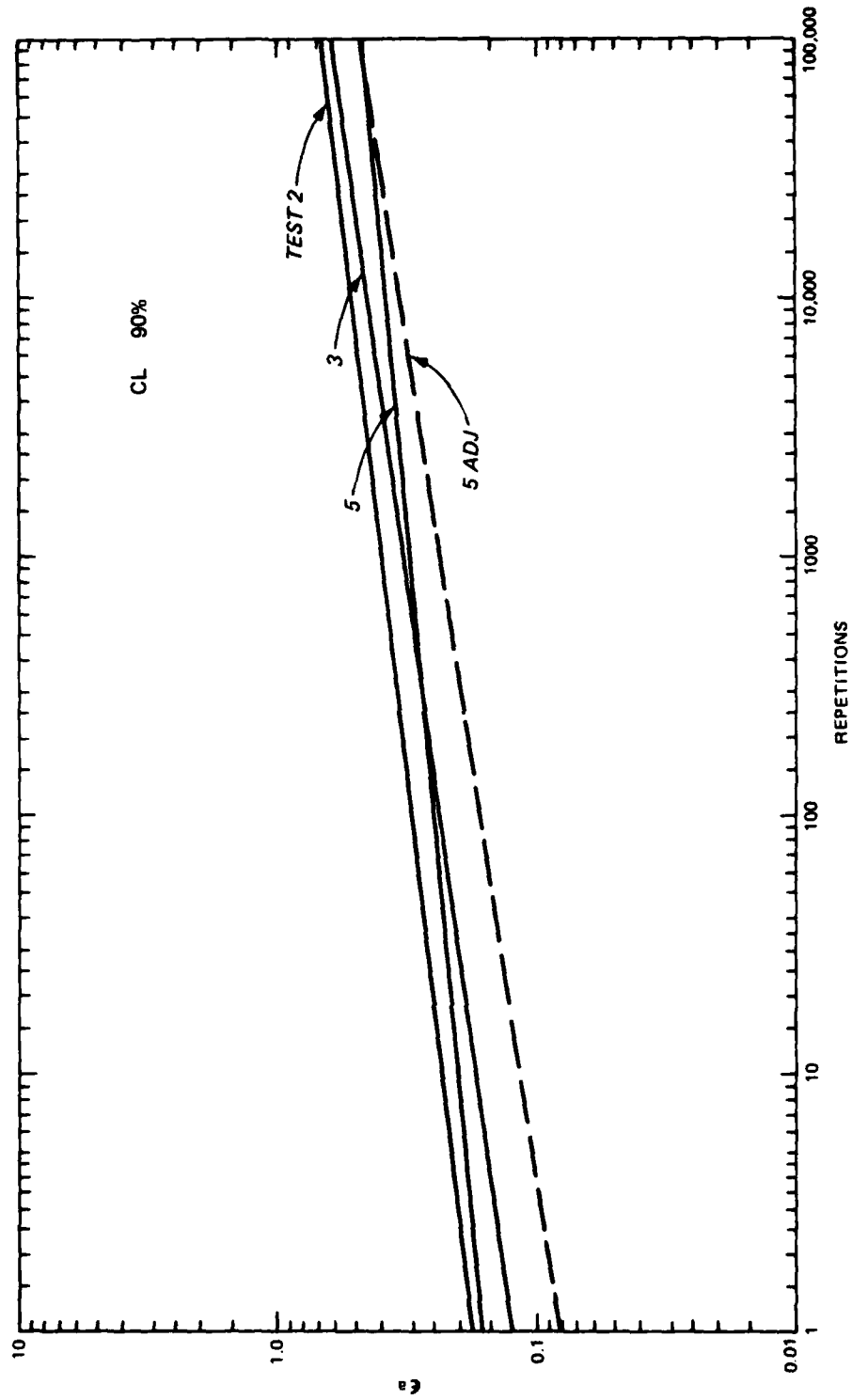


Figure 53. Log-log plot of strain versus repetitions, tests 2, 3, 5, and 5 adjusted

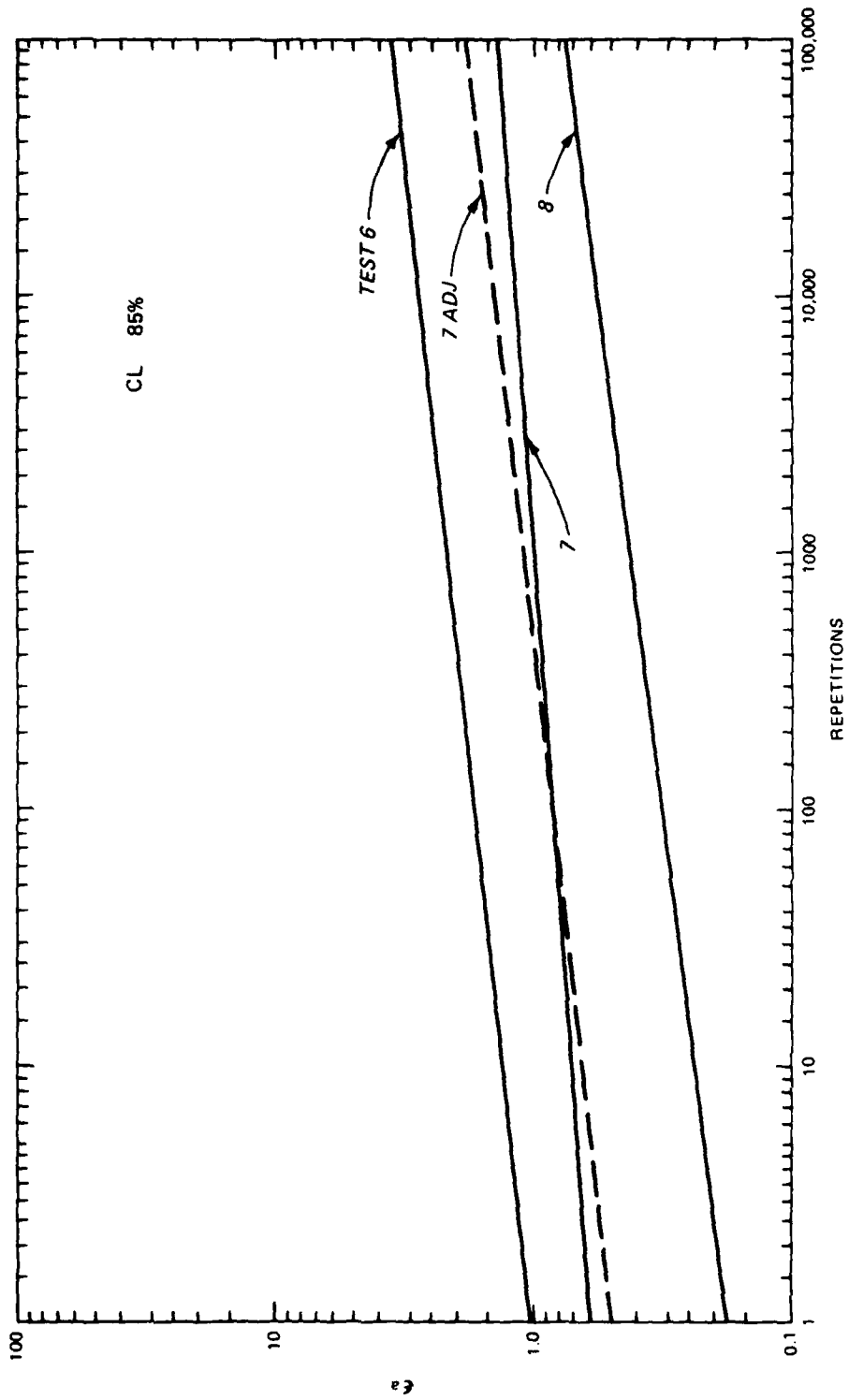


Figure 54. Log-log plot of strain versus repetitions, tests 6, 7, 7 adjusted, and 8

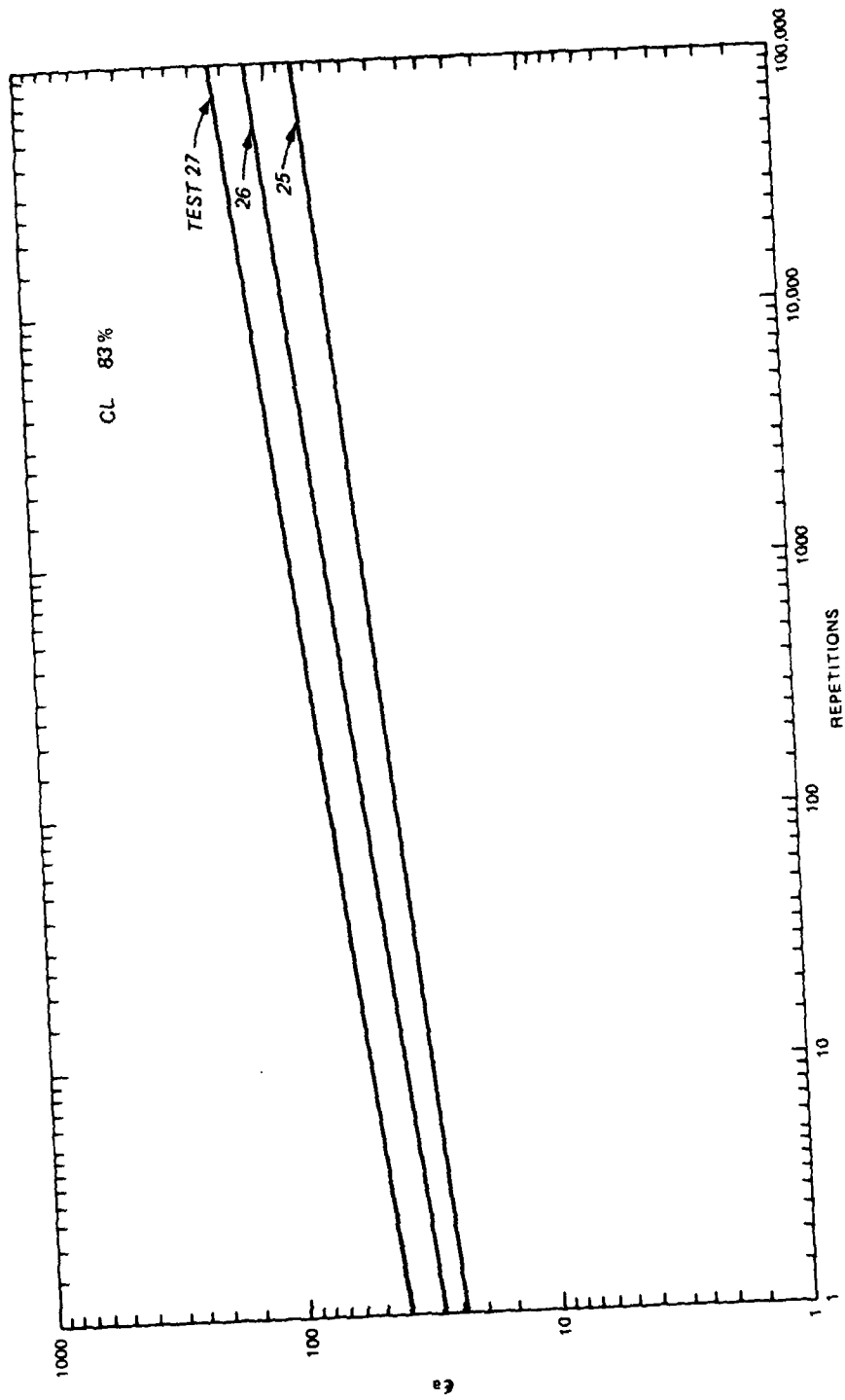


Figure 55. Log-log plot of strain versus repetitions, tests 25, 26, and 27

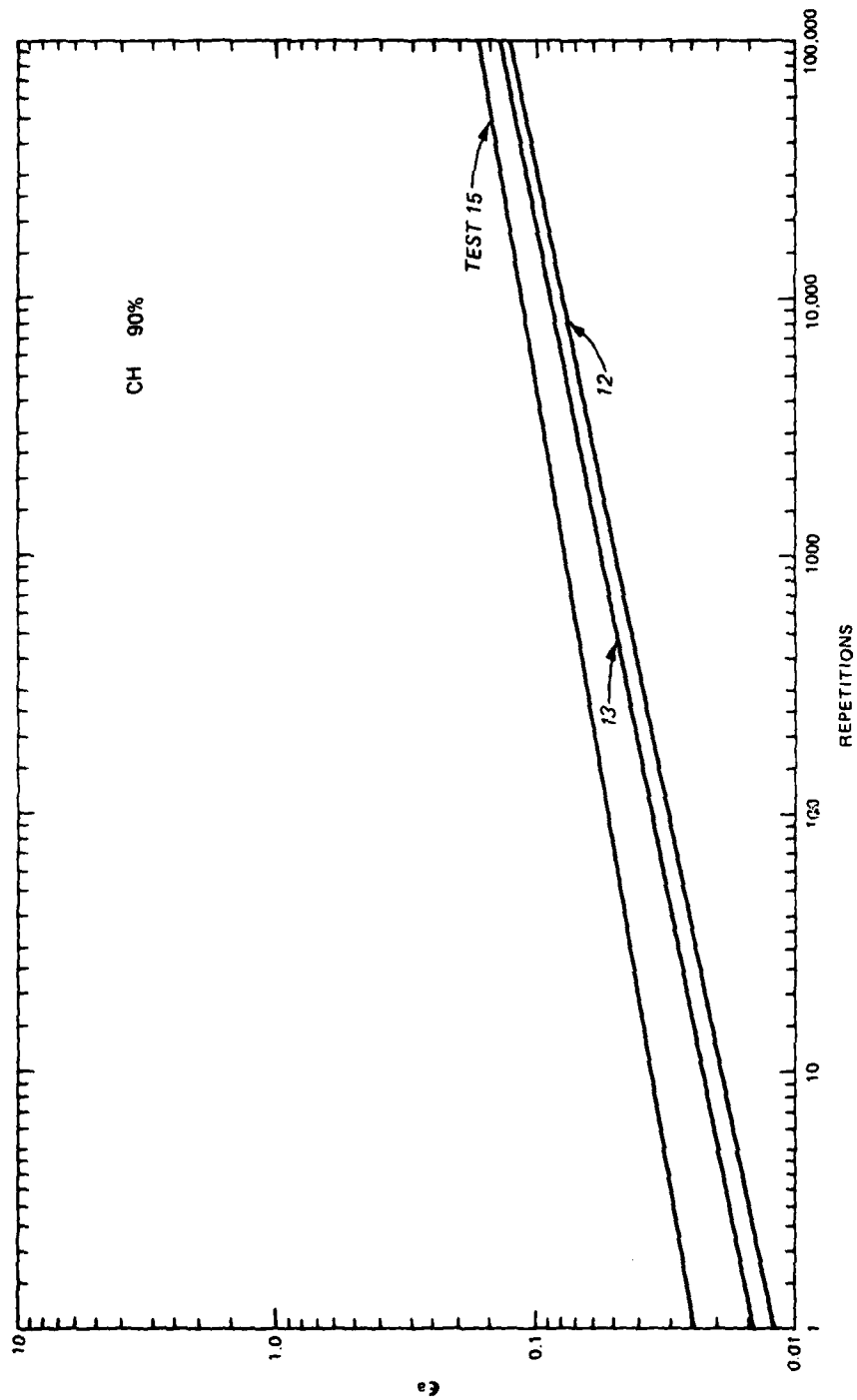


Figure 56. Log-log plot of strain versus repetitions, tests 12, 13, and 15

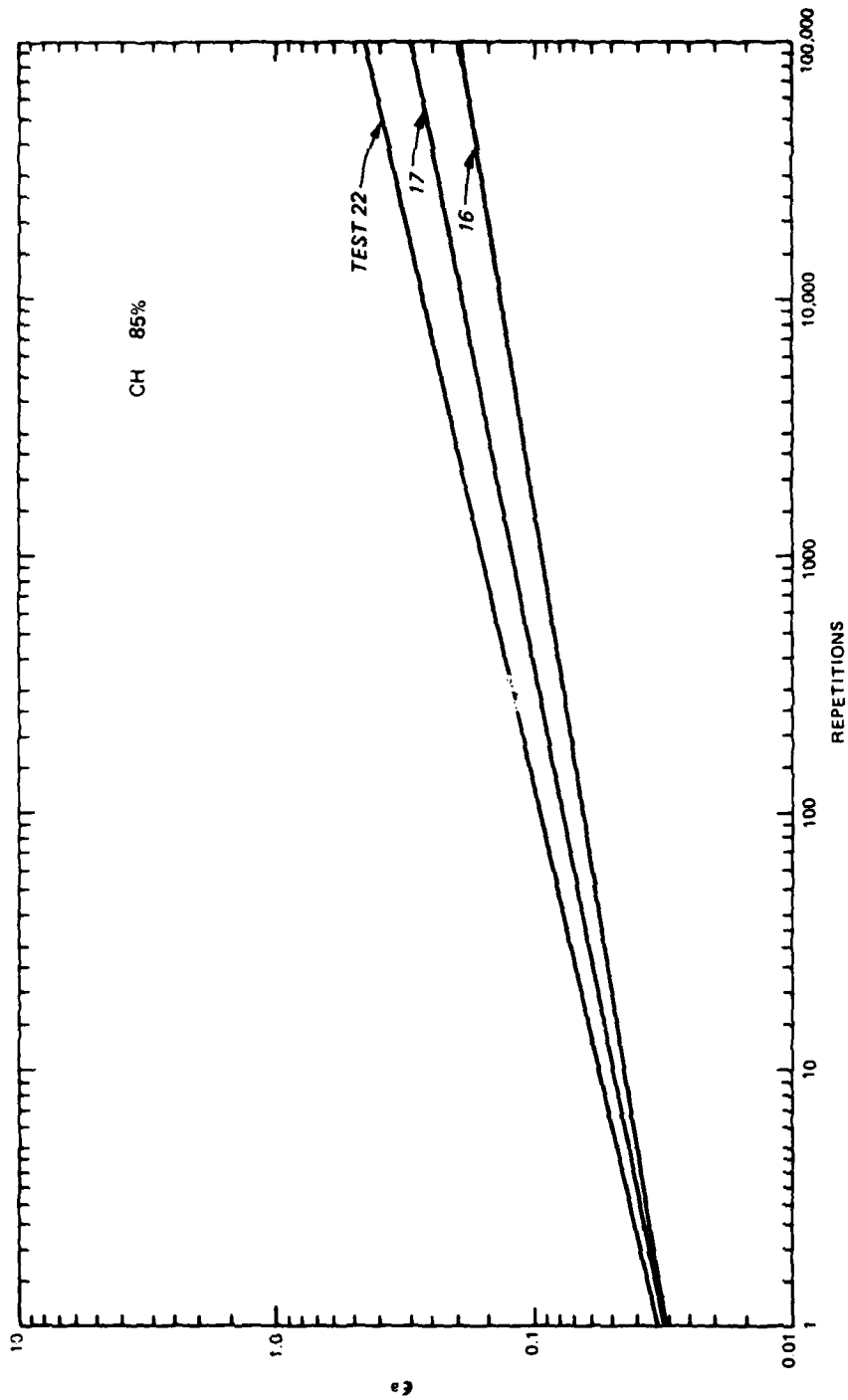


Figure 57. Log-log plot of strain versus repetitions, tests 16, 17, and 22

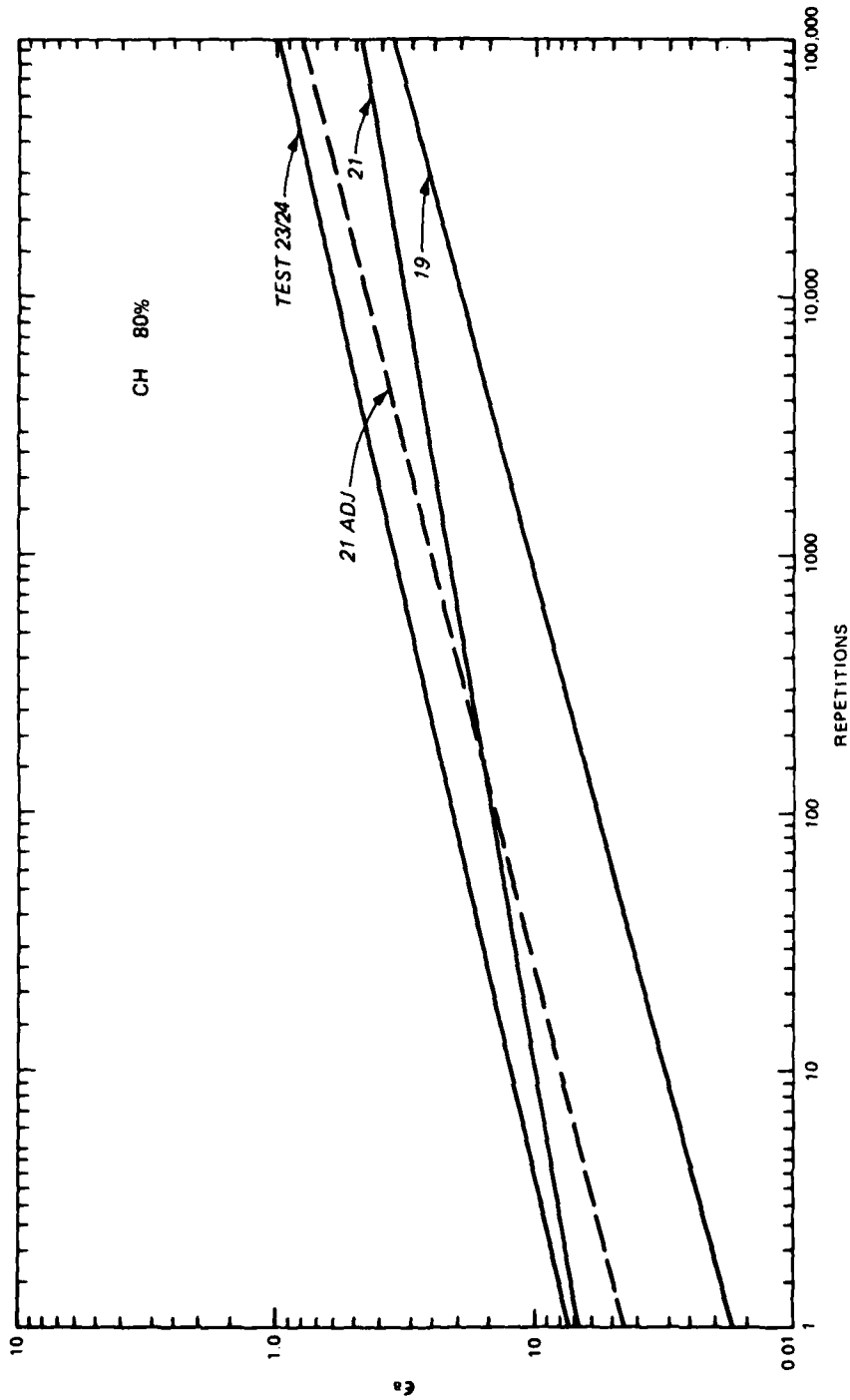


Figure 58. Log-log plot of strain versus repetitions, tests 19, 21, 21 adjusted, and average data from tests 23 and 24

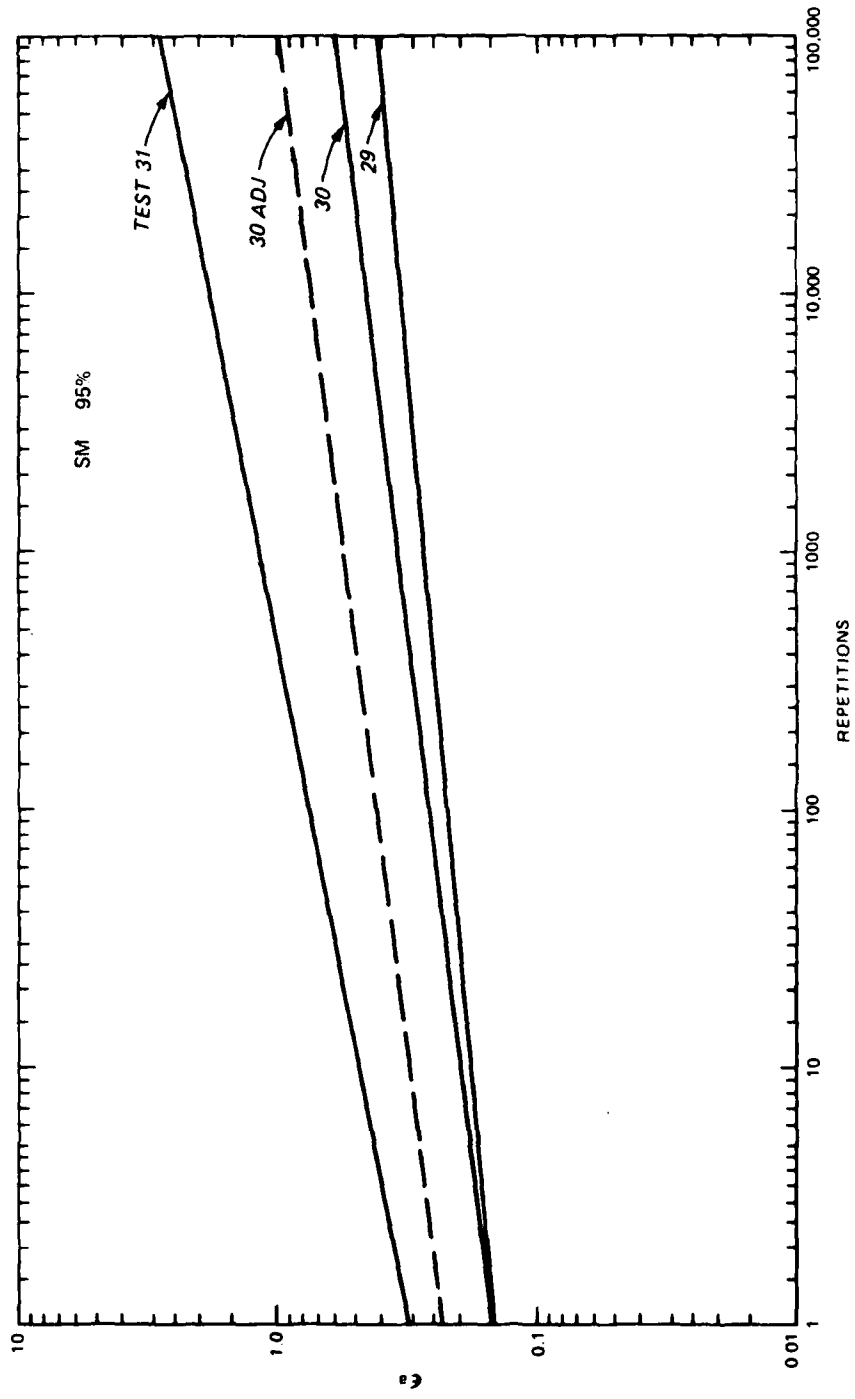


Figure 59. Log-log plot of strain versus repetitions, tests 29, 30, 30 adjusted, and 31

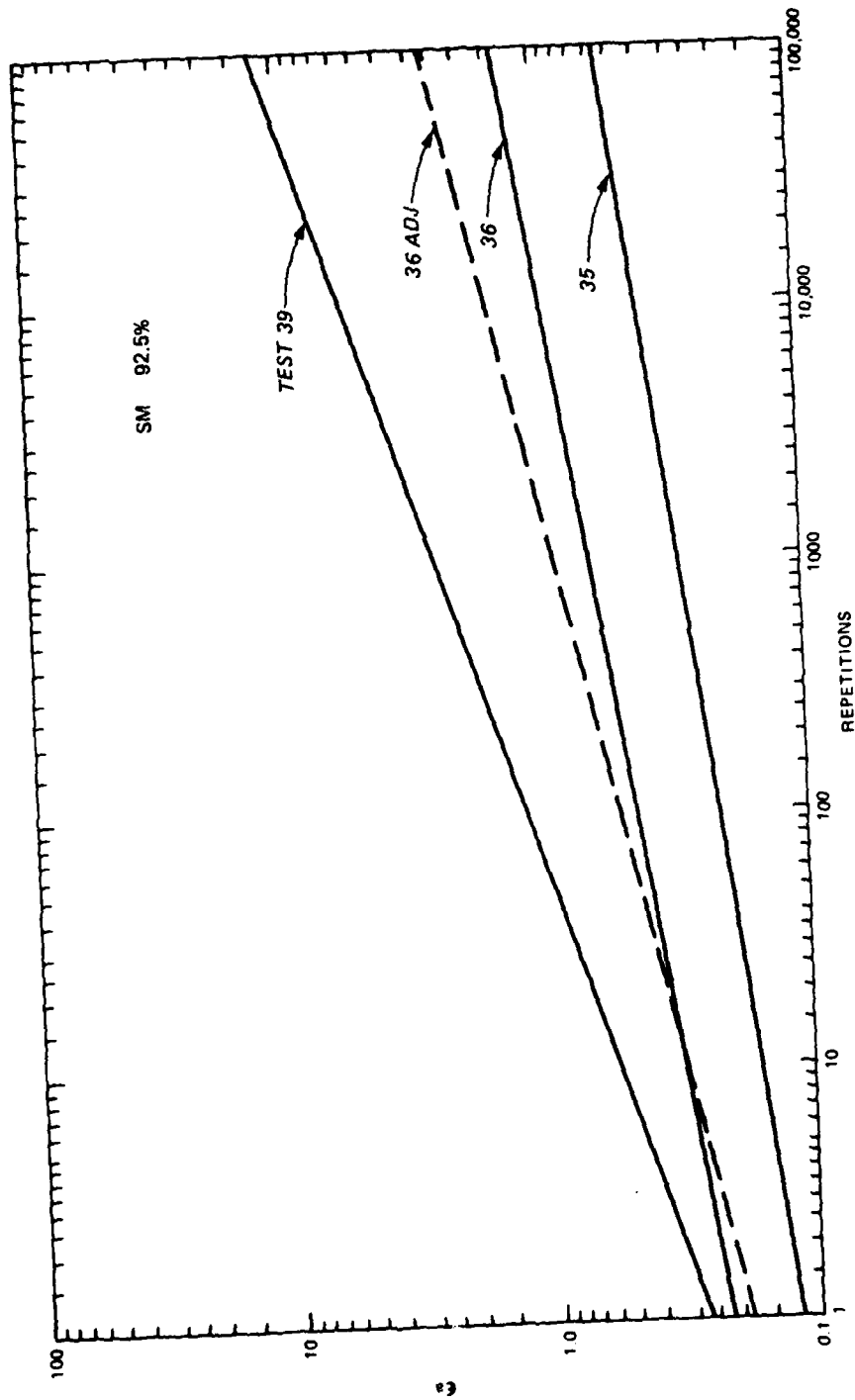


Figure 60. Log-log plot of strain versus repetitions, tests 35, 36, 36 adjusted, and 39

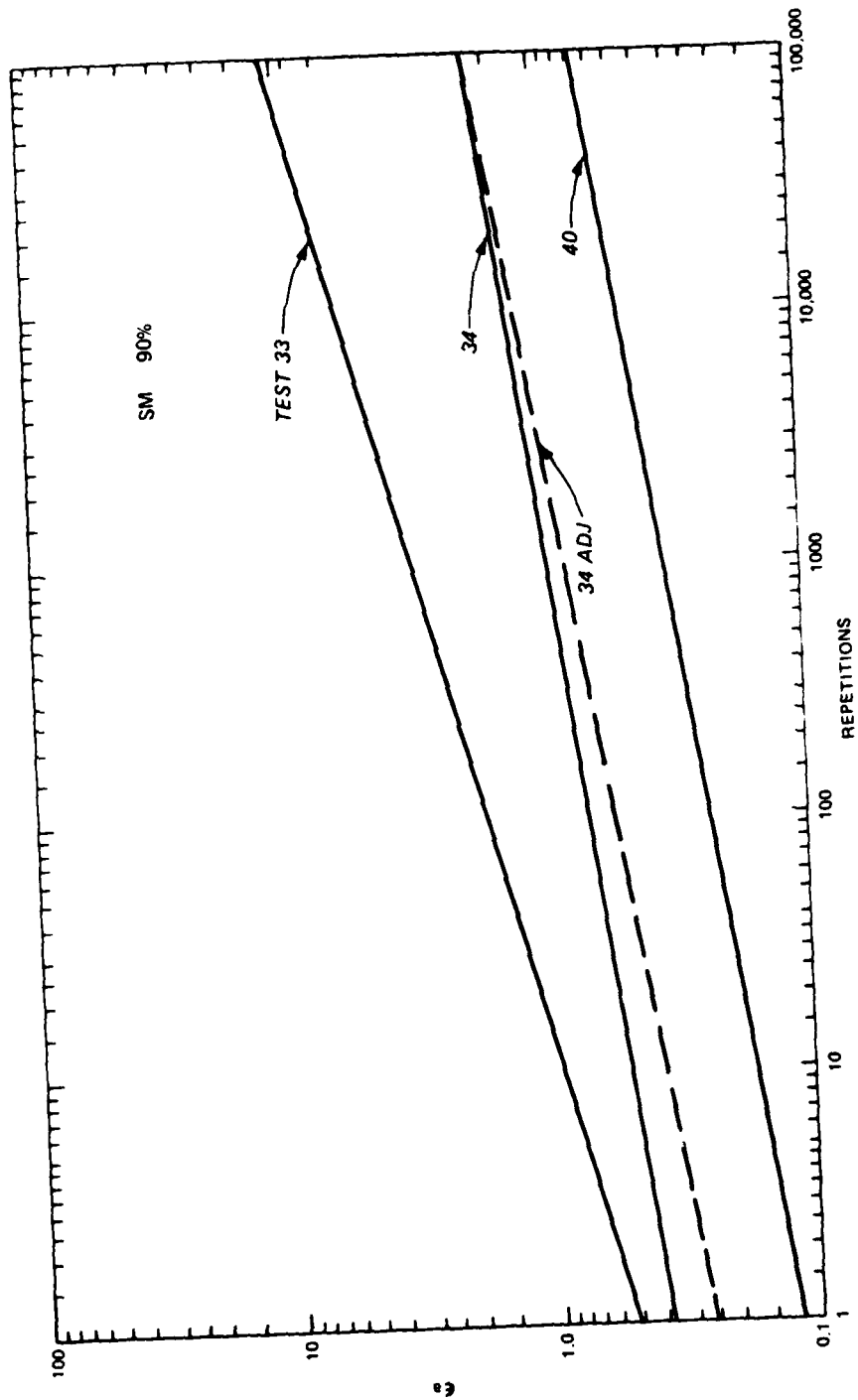


Figure 61. Log-log plot of strain versus repetitions, tests 33, 34, 34 adjusted, and 40

Table 16. Summary of Variables Used in Statistical Analysis

Soil Type	Test No.	Constants from Power Functions			Variables Used in Stepwise Regression			Stress Ratio $\Delta\sigma$	
		Intercept A	Slope B	Intercept (Adj) $A'$	Slope (Adj) $B'$	Density $\sigma$	Percent Clay $\% < 2\mu$		Compaction Energy Slope (CES)
Silty clay (CL)	2	0.1707	0.1194	0.1707	0.1194	89.7	18.0	0.188	0.317
	3	0.1256	0.1387	0.1256	0.1387	90.1	18.0	0.188	0.226
	5	0.1622	0.0944	0.0780	0.1580	90.2	18.0	0.188	0.175
	6	1.0050	0.1079	1.0050	0.1079	84.8	18.0	0.188	0.653
	7	0.5839	0.0735	0.5086	0.1091	85.6	18.0	0.188	0.490
	8	0.1793	0.1234	0.1793	0.1234	85.5	18.0	0.188	0.379
	27	4.0020	0.1227	4.0020	0.1227	83.3	18.0	0.188	0.975
	26	2.9397	0.1185	2.9340	0.1185	82.3	18.0	0.188	0.760
25	2.4170	0.0991	2.4170	0.0991	83.6	18.0	0.188	0.562	
Buckshot clay (CH)	15	0.0263	0.1667	0.0263	0.1667	90.5	44.0	0.326	0.190
	13	0.0136	0.1971	0.0136	0.1971	88.9	44.0	0.326	0.140
	12	0.0120	0.2030	0.0120	0.2030	89.4	44.0	0.326	0.105
	22	0.0336	0.2257	0.0336	0.2257	86.1	44.0	0.326	0.348
	17	0.0325	0.1909	0.0325	0.1901	84.1	44.0	0.326	0.263
	16	0.0323	0.1539	0.0323	0.1539	84.5	44.0	0.326	0.186
	23/24	0.0718	0.2309	0.0718	0.2309	79.9	44.0	0.326	0.528
	21	0.0656	0.1711	0.0445	0.2472	79.6	44.0	0.326	0.404
	19	0.0171	0.2635	0.0171	0.2635	80.1	44.0	0.326	0.294
	31	0.3189	0.1917	0.3189	0.1917	94.6	5.5	0.126	0.562
Silty sand (SM)	30	0.1473	0.1227	0.2315	0.1227	94.8	5.5	0.126	0.448
	29	0.1442	0.0931	0.1442	0.0931	96.4	5.5	0.126	0.338
	39	0.2757	0.3305	0.2757	0.3305	92.4	5.5	0.126	0.570
	36	0.2231	0.1601	0.1808	0.2319	92.7	5.5	0.126	0.531
	35	0.1185	0.1333	0.1185	0.1808	92.0	5.5	0.126	0.402
	33	0.5133	0.2701	0.5133	0.2701	90.2	5.5	0.126	0.708
	34	0.3746	0.1405	0.2468	0.1767	90.2	5.5	0.126	0.554
	40	0.1187	0.1535	0.1187	0.1535	90.0	5.5	0.126	0.392

In the statistical analysis, the stress ratio (IVAR5) was rejected in the computational process for the slope B as being not statistically significant compared with the other variables. Obviously, such a rejection does not reflect the true relationships that may be seen in Figure 51, but is only detected as such because of possible interrelationships between the independent variables or possibly because of low significance in computing the "B" parameter. Therefore, the final permanent strain model was developed in the form:

$$\epsilon_a^p = AN^B \quad (15)$$

where

$$\begin{aligned} \log A = & -8.68976 + 4.57115 \log X_1 + 5.05241 \log X_2 \\ & - 11.26392 \log X_3 + 2.08357 \log X_4 \end{aligned} \quad (15a)$$

and

$$\begin{aligned} \log B = & 2.05266 - 1.70143 \log X_1 - 1.68431 \log X_2 \\ & + 3.65294 \log X_3 \end{aligned} \quad (15b)$$

where

- $X_1$  = density  $\times$  0.01
- $X_2$  = percent clay  $\times$  0.01
- $X_3$  = slope of density-energy plot
- $X_4$  = stress ratio

Actual values of A and B used in the statistical analysis along with values of A and B calculated using Equations 15a and 15b are shown in Table 17. Also indicated are 75,000-repetition strain values as determined from actual test data along with those calculated using Equation 15.

#### EFFECT ON PAVEMENT PERFORMANCE

In order to consider the effect of reducing density on pavement performance, the strain model (Equation 15) was used to make calculations of estimated subgrade deformations for various density combinations of the three soils. Deformation calculations for flexible and rigid pavement subgrades were made using a layer concept. The subgrade

Table 17. Actual and Estimated Values of A and B Parameters, and Permanent Axial Strain at 75,000 Load Repetitions

Test No.	A Parameter		B Parameter		Strain at 75,000 Repetitions, percent	
	Actual	Estimated	Actual	Estimated	Actual	Estimated
2	0.1707	0.3314	0.1194	0.1126	0.80	1.17
3	0.1256	0.1671	0.1387	0.1118	0.63	0.59
5	0.0780	0.0986	0.1580	0.1116	0.43	0.34
6	1.0050	1.1559	0.1079	0.1239	3.20	4.65
7	0.5086	0.6631	0.1091	0.1219	1.34	2.61
8	0.1793	0.3863	0.1234	0.1222	0.75	1.52
27	4.0020	2.4558	0.1227	0.1277	13.10	10.30
26	2.9340	1.3829	0.1185	0.1304	9.30	5.98
25	2.4170	0.7922	0.0991	0.1269	6.10	3.29
15	0.0263	0.0221	0.1667	0.1839	0.24	0.17
13	0.0136	0.0110	0.1971	0.1877	0.16	0.09
12	0.0120	0.0059	0.2030	0.1895	0.16	0.05
22	0.0336	0.0619	0.2257	0.2001	0.42	0.59
17	0.0325	0.0310	0.1901	0.2083	0.32	0.32
16	0.0323	0.0154	0.1539	0.2066	0.26	0.16
23/24	0.0718	0.1049	0.2309	0.2273	0.86	1.35
21	0.0445	0.0591	0.2472	0.2287	0.44	0.77
19	0.0171	0.0313	0.2635	0.2263	0.36	0.40
31	0.3189	0.3164	0.1917	0.1757	2.20	2.27
30	0.2315	0.1992	0.1227	0.1750	0.60	1.42
29	0.1442	0.1195	0.0931	0.1701	0.45	0.81
39	0.2757	0.2926	0.3305	0.1829	7.00	2.29
36	0.1808	0.2562	0.2319	0.1818	1.10	1.97
35	0.1185	0.1386	0.1808	0.1842	0.50	1.10
33	0.5133	0.4117	0.2701	0.1905	6.80	3.49
34	0.2468	0.2470	0.1767	0.1905	1.60	2.10
40	0.1187	0.1189	0.1535	0.1912	0.60	1.02

under the hypothetical pavement structure was first divided into three layers of finite thickness, as shown in Figure 62. Appropriate mid-layer stress values were then selected based on previous calculations. Table 18 presents layer thicknesses along with the stress values used in the calculation of strain for each pavement. Then, using the properties of the soils as tested along with the calculated stress ratios for each depth as input parameters, the values of A and B were calculated from Equations 15a and 15b. The associated strain value was determined using the basic strain model (Equation 15). By multiplying the strain value by the layer thickness, the layer deformation was thus estimated and the total deformation was determined by summing the three individual layer deformation values.

Based on the three values of density at which each soil was tested and the associated soil properties, deformation calculations were made for eight combinations of the three-layer subgrade system (combinations A through H). Tables 19 and 20 show the density combinations and layer and total deformation calculations for the rigid and flexible pavement subgrades, respectively. It should be noted that these calculations represent general estimates that reflect at least qualitatively the difference in behavior of the three soil types based on the laboratory study. Since the stress values and layer thicknesses used in calculation of the layer deformations for the rigid and flexible pavement structures were similar and in some cases equal, then obviously the magnitude of total deformation values would be very close for the same combination of layer density values.

For purposes of comparing the deformation data, two assumptions are made: first, that the deformation calculations made for the condition in which the density of all three layers is the same and is the highest for which the soil was tested (combination A) provide baseline deformation data for that soil; and second, although the density of the upper subgrade layer is below criteria specifications, i.e., below 95 and 100 percent for cohesive and noncohesive soils, respectively, at least minimum acceptable performances would be obtained with these conditions. Thus, the deformation values may then be viewed in two

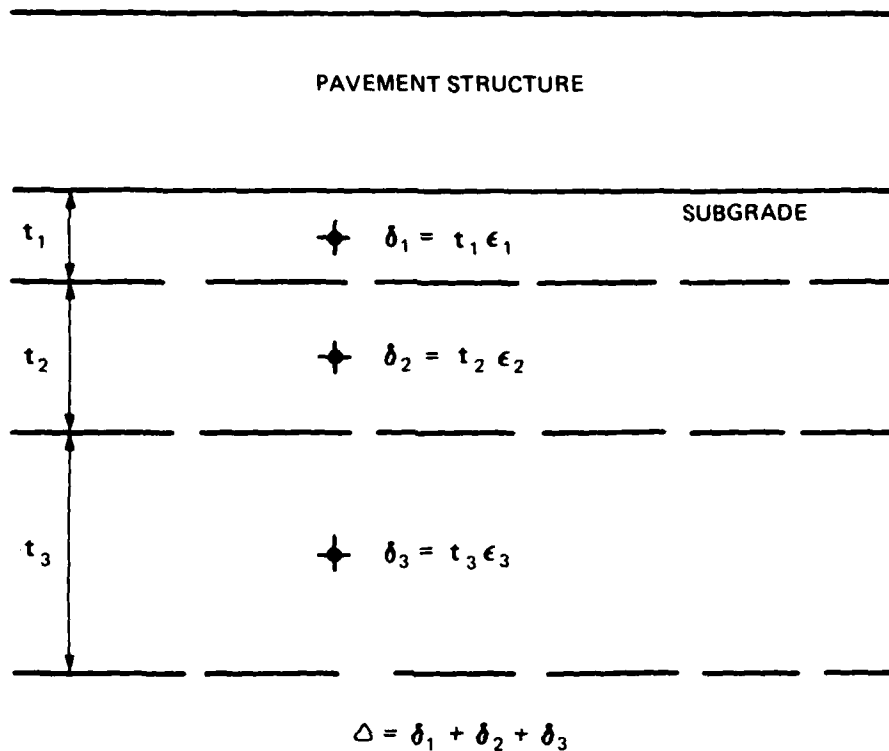


Figure 62. Subgrade layers for computation of permanent deformation

Table 18. Layer Thickness and Midlayer Stress Values Used in Stress Conditions

Pavement Type	Layer No.	Thickness in.	Midlayer Stress psi
Rigid	1	6	8.5
	2	18	7.5
	3	36	6.0
Flexible	1	9	9.0
	2	15	7.5
	3	36	6.0

Note: 1 in. = 2.54 cm; 1 psi = 6.89 kPa.

Table 13. Layer and Total Deformations - Rigid Pavement Subgrade

Soil Type	Depth in. (lb.)	Combination A		Combination B		Combination C		Combination D		Combination E		Combination F		Combination G		Combination H	
		Density Percent	Deformation in.														
Silty clay	3-6	90.0	0.05	90.0	0.05	85.0	0.19	85.0	0.19	85.0	0.19	83.0	0.19	83.0	0.16	83.0	0.05
	6-24	90.0	0.26	85.0	0.25	85.0	0.25	83.0	0.25	83.0	0.25	83.0	0.60	83.0	0.60	83.0	0.45
	24-60	90.0	0.22	95.0	0.31	85.0	0.31	83.0	0.31	83.0	0.31	83.0	0.20	83.0	0.20	83.0	0.20
TOTAL DEFORMATION			0.67		0.67		0.81		0.81		1.34		1.69		1.96		4.20
Backshot clay	3-6	90.0	0.01	90.0	0.01	95.0	0.02	95.0	0.02	95.0	0.02	85.0	0.02	80.0	0.06	80.0	0.02
	6-24	90.0	0.01	95.0	0.03	85.0	0.03	85.0	0.03	85.0	0.03	80.0	0.07	80.0	0.07	85.0	0.03
	24-60	90.0	0.01	95.0	0.04	85.0	0.04	90.0	0.04	90.0	0.04	80.0	0.11	80.0	0.11	80.0	0.11
TOTAL DEFORMATION			0.06		0.06		0.09		0.09		0.16		0.20		0.24		0.15
Silty sand	3-6	95.0	0.10	95.0	0.10	92.5	0.16	92.5	0.16	92.5	0.16	90.0	0.16	90.0	0.27	90.0	0.10
	6-24	95.0	0.12	92.5	0.18	92.5	0.18	92.5	0.18	92.5	0.18	90.0	0.34	90.0	0.34	92.5	0.16
	24-60	95.0	0.18	92.5	0.27	92.5	0.27	90.0	0.27	90.0	0.27	90.0	0.52	90.0	0.52	90.0	0.52
TOTAL DEFORMATION			0.40		0.55		0.61		0.61		0.96		1.02		1.13		0.80

Note: 1 in. = 2.54 cm.

Table 2. Layer and Total Deformations - Flexible Pavement Subgrade

Layer No.	Combination A		Combination B		Combination C		Combination D		Combination E		Combination F		Combination G		Combination H	
	Density Percent	Deformation in.														
1117	92.0	0.05	90.0	0.05	85.0	0.22	85.0	0.22	85.0	0.22	85.0	0.22	83.0	0.22	80.0	0.05
1118	92.0	0.06	90.0	0.06	85.0	0.26	85.0	0.26	85.0	0.26	85.0	0.26	83.0	0.26	80.0	0.05
1119	92.0	0.29	90.0	0.29	85.0	0.37	85.0	0.37	85.0	0.37	85.0	0.37	83.0	0.37	80.0	0.20
TOTAL DEFORMATION		0.69		0.67		0.74		0.74		0.74		0.74		0.72		0.20
1120	92.0	0.01	90.0	0.01	85.0	0.74	85.0	0.74	85.0	0.74	85.0	0.74	83.0	0.74	80.0	0.01
1121	92.0	0.01	90.0	0.01	85.0	0.74	85.0	0.74	85.0	0.74	85.0	0.74	83.0	0.74	80.0	0.01
1122	92.0	0.01	90.0	0.01	85.0	0.74	85.0	0.74	85.0	0.74	85.0	0.74	83.0	0.74	80.0	0.01
TOTAL DEFORMATION		0.03		0.06		0.10		0.10		0.10		0.10		0.10		0.15
1123	92.0	0.11	90.0	0.11	85.0	0.16	85.0	0.16	85.0	0.16	85.0	0.16	83.0	0.16	80.0	0.11
1124	92.0	0.12	90.0	0.12	85.0	0.15	85.0	0.15	85.0	0.15	85.0	0.15	83.0	0.15	80.0	0.11
1125	92.0	0.27	90.0	0.27	85.0	0.27	85.0	0.27	85.0	0.27	85.0	0.27	83.0	0.27	80.0	0.11
TOTAL DEFORMATION		0.51		0.51		0.61		0.61		0.61		0.61		0.61		0.81

Note: 1 in. = 2.54 cm.

perspectives: first, with respect to the effect of change in density condition for each individual soil type, and second, with respect to change in soil type for each density condition.

Based on the rigid pavement subgrade configuration, the soil for which the least deformation is indicated is the buckshot clay. The change in density from combination A, with all layers at 90 percent, through combination G, with all layers at 80 percent, indicates a continual increase in total deformation from 0.03 to 0.24 in. (0.76 to 6.10 mm), or a difference of 0.21 in. (5.33 mm). A combination of all three density values, 90, 85, and 80 percent, in combination H indicates a deformation of 0.15 in. (3.81 mm), or slightly higher than the mid-range of the end values of combinations A and G. The baseline deformation of the silty clay (also at 90 percent) at combination A is about 0.20 in. (5.08 mm) and increases proportionally as the layer densities are decreased incrementally to combination G, where all layers are at 83 percent, with a deformation of 1.96 in. (4.98 cm) is indicated, or an increase of 1.76 in. (4.47 cm). Combination H in which all three density values, 90, 85, and 83 percent, were involved indicates a deformation value of 1.20 in. (3.05 cm). The silty sand, which has a larger initial deformation value of 0.40 in. (10.16 mm) than the silty clay at combination A, indicated a smaller deformation value of 1.13 in. (2.87 cm) at combination G even though the density values of the silty sand were higher than those of the silty clay in both cases, i.e., 95 percent at combination A and 90 percent at combination G. Again, the deformation of 0.80 in. (80.32 mm) at combination H, which involved densities of 95, 92.5, and 90 percent, was slightly over the midrange values between combinations A and G.

Deformation calculations for the flexible pavement shown in Table 20 indicated that the buckshot, or plastic, clay showed the least deformation of the three soils. From combination A, with all three layers at 90 percent density, through combination G, with all three layers at 80 percent density, the increase in deformation was from 0.03 to 0.24 in. (0.76 to 6.10 mm). With successive reduction in layer densities, there was a proportional increase in layer deformation. With

all three densities, 90, 85, and 80 percent, involved in combination H, the deformation was 0.15 in. (3.81 mm). For the silty clay, the deformation increase from combination A, with all three layers at 90 percent, to combination G, with all three layers at 83 percent, was 1.82 in. (4.62 cm), or from 0.20 to 2.02 in. (0.51 to 5.13 cm). With all three densities, 90, 85, and 83 percent, at combination H involved, the deformation was 1.20 in. (3.05 cm). The silty sand at combination A, with all three layers at 95 percent density, indicated a deformation value of 0.41 in. (10.41 mm). With all three layers at 90 percent density at combination G, the computed deformation was 1.16 in. (2.95 cm), or an increase of 0.75 in. (19.05 mm). The deformation at combination H in which densities of 95, 92.5, and 90 percent were involved was 0.81 in. (20.57 mm). For all three soils, the deformation value at combination H was slightly above the midrange values between combinations A and G.

A review of the estimated deformation values for both flexible and rigid pavements indicates that the strain model is reasonably accurate within the range of parameters involved. It is important to note, however, that the response of the individual soils is significantly different. If it is assumed that the baseline deformation (combination A) of the buckshot clay is within acceptable values, then it would appear that decrease in density involving all of the layer combinations could well be acceptable for either flexible or rigid pavements. Also, by assuming baseline acceptability for the other two soils and considering only the increase in deformation, then possibly combinations A, B, and C would be acceptable for the silty clay and combinations A through E for the silty sand.

The effect of incorporating any of the density combinations in the subgrade of a flexible or rigid pavement structure must be reviewed on a somewhat qualitative basis at this time, however. The considerable variation in computed deformation values points out two significant behavior patterns. First, for some soils, such as the silty clay and silty sand, even a slight decrease in the soil density along the line of optimums can bring about large reductions in strength and possibly critical changes in deformation characteristics. Second, by contrast,

stiffer soils, such as the buckshot clay, are not nearly as sensitive to similar density changes. Since pavements are designed based on the strength of the subgrade and not the density, it becomes obvious that for soils such as the silty clay and silty sand one result of lowering density would be a requirement for increased thickness.

On the other hand, since most design processes generally satisfy performance requirements, the following question then arises: Does the present methodology require excessive thickness for stiffer soils such as the buckshot clay? It should be noted that the density and thickness criteria with which pavements are now designed were evolved empirically and conservatively on an all-inclusive basis.

To provide a finite comparison of the three soils based on total subgrade deformations, the density combinations which result in approximately the same deformation values should be investigated. For example, in Table 20, the total deformation for the silty clay at combination A, in which the density of all three layers is 90 percent, gives approximately the same deformation as the buckshot clay at combination F, in which the density of the top 9 in. (22.86 cm) of the subgrade is 85 percent and the density of the remainder of the subgrade is 80 percent. A similar comparison may be made between the silty clay at combination B, for which the density of the top 24 in. (60.96 cm) of subgrade is 90 percent and the remainder is 83 percent, and the silty sand at combination A, for which the density of all layers is 95 percent. No direct comparison can be made between the buckshot clay and the silty sand since for no combination of densities does the computed deformation for the buckshot clay exceed that of the silty sand.

Other very rough comparisons, as shown in Table 21, may be made on the basis of soil strength from the static load tests.

One means of comparing the soils in terms of pavement performance would be to hypothetically place the original rigid pavement structure on the layered subgrade combinations and observe the effect on slab deformation or tensile strain; then, based on the appropriate design factor, interpret some allowable repetitive level. However, based on observed and theoretical portland cement concrete slab deflections, it

Table 21. Comparison of Compressive Strength Values  
from Static Load Tests

Soil Type	Comparison 1		Comparison 2		Comparison 3	
	Density Percent	Strength	Density Percent	Strength	Density Percent	Strength
	ASTM D 1557	psi	ASTM D 1557	psi	ASTM D 1557	psi
Silty clay (CL)	90	40.7	85	19.0	83	12.1
Buckshot clay (CH)	85	36.5	80	23.5	--	--
Silty sand (SM)	--	--	95	21.9	90	13.0

Note: 1 psi = 6.89 kPa.

may be seen that practically all calculated deformations exceed reasonable deflection values. Thus, for these cases, fatigue life would be based on an unsupported slab, and no difference in performance could be determined in terms of differences in soil properties.

A hypothetical basis for the comparison of performance may also be found by placing the original flexible pavement designs on the layer combinations. On the basis of assuming that the cumulative subgrade deformation would be reflected at the surface as a rut or depression, then the total values indicated would be representative of estimated rut depth. By arbitrarily assuming a maximum allowable rut depth of 0.75 in. (19.05 mm), then the following combinations of layer density would be acceptable: all combinations of the buckshot clay soil, combinations A, B, and C of the silty clay, and combinations, A, B, C, and D of the silty sand. If the baseline validity is assumed and only the increase in deformation is considered, then the following combinations could be acceptable: all combinations of the buckshot clay, combinations A through D for the silty clay, and all combinations of the silty sand.

In summary, therefore, the results of the investigation have demonstrated the wide variability of soil response due to differences in

the engineering properties of the individual soil and due to the basis on which various soil responses are compared.

It has also been demonstrated that the differences in soil response can be defined in terms of specific soil characteristics and that permanent strain response may be predicted with reasonable accuracy. This investigation revealed that across-the-board generalities concerning response of soils based on density alone are impractical.

It must be concluded, therefore, that no general and sweeping changes should be made to FAA compaction criteria at this time. However, results of this study do provide the foundation for development in the future of a system of density requirements based on specific engineering properties of different soil types. Such a system could be developed following initially the laboratory procedures and methodology used in this study combined with a comprehensive field validation program.

## CONCLUSIONS AND RECOMMENDATIONS

### CONCLUSIONS

Based on the results of this study, the following conclusions are drawn:

- a. Within the conditions of repetitive stress, soil strength, and load repetition levels used in the laboratory study, there was no evidence of soil fatigue for the three soils involved.
- b. The resilient strain response of the three soils studied provided qualitative evidence of the relative stiffness of each material under the various conditions of moisture content and density, but the magnitude of the resilient strain values appeared to be somewhat low.
- c. The permanent strain response data provided much significant information on the behavior of each soil and demonstrated the relative susceptibility of each material to change in strength and stiffness as a result of decrease in density along the line of optimums.
- d. Of the three soils tested, the buckshot clay did not demonstrate large increase in permanent deformation with reduction in density. The silty clay and silty sand indicated significant increase in permanent deformation with reduction in density although to varying degrees.
- e. The permanent deformation response of soils under laboratory conditions can be modeled with reasonable accuracy based on use of the parameters cited herein.
- f. The significant difference in the change in response among the three soils tested as a result of density decrease demonstrates clearly the variability among the soils and illustrates the potential danger of making across-the-board changes in current density criteria now used by FAA without regard to soil type.
- g. An improved system of density criteria can be developed following the techniques and methodology used in this study coupled with a comprehensive field verification program and involving a broad spectrum of soil types.

### RECOMMENDATIONS

As a result of this study, the following recommendations are presented:

- a. No changes should be made in current FAA compaction criteria for subgrade soils in flexible and rigid airport pavements.

- b. Following the basic techniques and methodology used in this investigation coupled with substantial field validation, a comprehensive test program should be planned and pursued to develop an improved system of soil density requirements for airport subgrades based on the engineering characteristics of different soil types.

## REFERENCES

1. American Society for Testing and Materials, "Compaction of Soils," Special Technical Publication No. 377, Philadelphia, Pa., 1964.
2. Highway Research Board, "Soil Compaction and Proof-Rolling of Subgrades," Highway Research Bulletin 254, Washington, D. C., 1960.
3. Highway Research Board, "Symposium on Compaction of Earthwork and Granular Bases," Highway Research Record 177, Washington, D. C., 1967.
4. Department of Transportation, Federal Aviation Administration, "Airport Pavement Design and Evaluation," Advisory Circular AC 150/5320-6C, Washington, D. C., 1978.
5. Ahlvin, R. G., Brown, D. N., and Ladd, D. M., "Compaction Requirements for Soil Components of Flexible Airfield Pavements," Technical Report No. 3-529, U. S. Army Engineer Waterways Experiment Station, CE, Vicksburg, Miss., Nov 1959.
6. American Society for Testing and Materials, "Moisture-Density Relations of Soils Using 10-lb (4.5-kg) Rammer and 18-in. (457-mm) Drop," Designation: D 1557, 1978 Annual Book of ASTM Standards, Part 19, Philadelphia, Pa., 1978.
7. Department of Defense, "Determination of Moisture-Density Relations," Test Method for Pavement Subgrade, Subbase, and Base-Course Materials, MIL-STD-621A, Method 100, Washington, D. C., 1964.
8. Livneh, M., Ishai, I., and Uzan, J., "Compaction Requirements for Flexible Pavement Structures," Proceedings, Sixth Asian Regional Conference on Soil Mechanics and Foundation Engineering, Vol 1, Singapore, 1979.
9. Papazian, H. S., "The Response of Linear Viscoelastic Materials in the Frequency Domain with Emphasis on Asphaltic Concrete," Proceedings, First International Conference on the Structural Design of Asphalt Pavements, Ann Arbor, Mich., 1962.
10. Barksdale, R. D., "Compressive Stress Pulse in Flexible Pavements for Use in Dynamic Testing," Highway Research Record 345, Highway Research Board, Washington, D. C., 1971.
11. Barker, W. R., and Brabston, W. N., "Development of a Structural Design Procedure for Flexible Airfield Pavements," Technical Report S-75-17, U. S. Army Engineer Waterways Experiment Station, CE, Vicksburg, Miss., Sep 1975.

12. Seed, H. B., Chan, C. K., and Monismith, C. L., "Effects of Repeated Loading on the Strength and Deformation of Compacted Clay," Proceedings, Vol 34, Highway Research Board, Washington, D. C., 1955.
13. Seed, H. B., and Chan, C. K., "Effect of Stress History and Frequency of Stress Applications on Deformation of Clay Subgrade Under Repeated Loading," Proceedings, Vol 37, Highway Research Board, Washington, D. C., 1958.
14. Seed, H. B., McNeill, R. L., and Guenin, S. de, "Increased Resistance of Deformation of Clay Caused by Repeated Loading," Journal of the Soil Mechanics and Foundations Division, Paper 1645, Vol 84, No. SM2, American Society of Civil Engineers, New York, May 1958.
15. Seed, H. B. and McNeill, R. L., "Soil Deformation in Normal Compression and Repeated Loading Tests," Highway Research Bulletin 141, Highway Research Board, Washington, D. C., 1956.
16. Seed, H. B., and Chan, C. K., "Thixotropic Characteristics of Compacted Clay," Journal of the Soil Mechanics and Foundations Division, Paper 1427, Vol 83, No. SM4, American Society of Civil Engineers, New York, Nov 1957.
17. Kashmeeri, N. A., "Thixotropic Behavior of Compacted Clays," Ph.D. Dissertation, University of Michigan, Ann Arbor, Mich., 1970.
18. Larew, H. G., "Strength and Deformation Characteristics of Compacted Clay Soils Under the Action of Repeated Axial Loads," Ph.D. Dissertation, Purdue University, Lafayette, Ind., Jan 1960.
19. Larew, H. G., and Leonards, G. A., "A Strength Criterion for Repeated Loads," Proceedings, Vol 41, Highway Research Board, Washington, D. C., 1962.
20. Brown, S. F., LaShine, A. K. F., and Hyde, A. F. L., "Repeated Load Triaxial Testing of a Silty Clay," Geotechnique, Vol XXV, No. 1., London, Mar 1975.
21. Townsend, F. C., and Chisolm, E. E., "Plastic and Resilient Properties of Vicksburg Buckshot Clay Under Repetitive Loading," Technical Report S-76-16, U. S. Army Engineer Waterways Experiment Station, CE, Vicksburg, Miss., Nov 1976.
22. Monismith, C. L., Ogawa, N., and Freeme, C. R., "Permanent Deformation Characteristics of Subgrade Soils Due to Repeated Loading," Transportation Research Record 527, National Research Council, Transportation Research Board, Washington, D. C., 1975.

23. Kondner, R. L., "Hyperbolic Stress-Strain Response: Cohesive Soils," Journal of the Soil Mechanics and Foundations Division, Vol 89, No. SMI, American Society of Civil Engineers, New York, Feb 1963.
24. Barksdale, R. D., "Laboratory Evaluation of Rutting in Base Course Materials," Proceedings, Third International Conference on the Structural Design of Asphalt Pavements, Ann Arbor, Mich., Sep 1972.
25. Brown, S. F., and Bell, C. A., "The Prediction of Permanent Deformation in Asphalt Pavements," Proceedings, Vol 48, Association of Asphalt Paving Technologists, Denver, Colo., Feb 1979.
26. American Society for Testing and Materials, "Classification of Soils for Engineering Purposes," Designation: D 2487, 1978 Annual Book of ASTM Standards, Part 19, Philadelphia, Pa., 1978.
27. Snowden, J. O., Jr., and Priddy, R. R., "Geology of Mississippi Loess, Loess Investigations in Mississippi," Bulletin 111, Mississippi Geological, Economic, and Topographical Survey, Jackson, Miss., 1968.
28. Durham, C. O., Jr., Moore, C. H., Jr., and Parsons, B., "An Agnostic View of the Terraces: Natchez to New Orleans," Field Trip Guidebook, Mississippi Alluvial Valley and Terraces, Geological Society of America, Annual Meeting, New Orleans, La., 1967.
29. Tippetts-Abbott-McCarthy-Stratton, "Airfield Pavement Design, Dallas/Fort Worth Regional Airport," Dallas, Sep 1971.
30. Asphalt Institute, "Full-Depth Asphalt Pavements for Air Carrier Airports," Manual Series No. 11 (MS-11), College Park, Md., Jan 1973.
31. Koninklijke/Shell Laboratorium, "BISAR Users Manual; Layered Systems Under Normal and Tangential Loads," Amsterdam, Holland, Jul 1972.
32. Crawford, J. E., "An Analytical Model for Airfield Pavement Analysis (AFPAV)," Technical Report 71-70, Air Force Weapons Laboratory, Kirtland Air Force Base, N. Mex., 1971.
33. Herrmann, C. R., "User's Manual for DSI (Three-Dimensional Elasticity Analysis of Periodically Loaded Prismatic Solids)," University of California, Davis, Calif., Nov 1968.
34. Pichumani, R., "Finite Element Analysis of Pavement Structures Using AFPAV Code (Linear Elastic Analysis)," Technical Report 72-186, Air Force Weapons Laboratory, Kirtland Air Force Base, N. Mex., May 1973.

35. Ahlvin, R. G. et al., "Multiple-Wheel Heavy Gear Load Pavement Tests, Volume I," Technical Report S-71-17, U. S. Army Engineer Waterways Experiment Station, CE, Vicksburg, Miss., Nov 1971.
36. Heukelom, W., and Klomp, A. J. G., "Road Design and Dynamic Loadings," Proceedings, Vol 33, Association of Asphalt Paving Technologists, Denver, Colo., 1964.
37. Thompson, M. R., and Robnett, Q. L., "Final Report, Resilient Properties of Subgrade Soils," Transportation Engineering Series No. 14, Illinois Department of Transportation, Springfield, Ill.

APPENDIX A  
OUTPUT DATA FROM REPETITIVE LOAD TESTS

REPEATED LOAD TRIAXIAL COMPRESSION TEST .D

MATERIAL TYPE: CL CP=2.0 PULSE STRESS=12.5PSI

SAMPLE NUMBER: TEST NO 2 DATA FILE: BRAB1

CYCLE	AXIAL STRES PSI	CHAMB PRESS PSI	RESIL E1*10**6	RESIL E3*10**6	RESIL MODULUS PSI	POIS RATIO	PERM E1 STN	PERM E3 STN	VOLUME E1-2E3 =STN,
1	12.19	2.0	1222.99	313.70	9966.7	0.257	0.18	0.03	0.12
2	12.37	2.0	1223.19	313.69	10116.1	0.256	0.20	0.03	0.14
5	12.37	2.0	1223.60	348.53	10112.0	0.285	0.23	0.04	0.15
10	12.37	2.0	1223.81	313.67	10109.6	0.256	0.25	0.04	0.17
20	12.57	2.0	1224.03	313.65	10271.3	0.256	0.27	0.05	0.17
50	12.57	2.0	1224.09	313.64	10270.1	0.256	0.27	0.05	0.17
100	12.57	2.0	1224.22	313.64	10269.0	0.256	0.28	0.05	0.18
200	12.88	2.0	1224.42	313.64	10519.9	0.256	0.30	0.05	0.20
500	12.88	2.0	1224.69	348.49	10517.6	0.285	0.32	0.05	0.22
1000	12.88	2.0	1560.27	348.49	8255.5	0.223	0.33	0.05	0.23
2000	12.88	2.0	1225.20	348.49	10513.2	0.284	0.36	0.05	0.26
3000	12.88	2.0	1393.37	383.34	9244.4	0.275	0.39	0.05	0.29
4334	12.88	2.0	1393.53	453.02	9242.6	0.325	0.40	0.05	0.30
5659	12.88	2.0	1561.74	452.99	8246.0	0.290	0.42	0.06	0.30
7000	12.75	2.0	1729.99	487.82	7372.0	0.282	0.44	0.06	0.32
8000	12.95	2.0	1729.99	487.82	7488.2	0.282	0.44	0.06	0.32
9600	12.95	2.0	1730.42	522.56	7483.2	0.302	0.46	0.08	0.30
16200	12.94	2.0	2068.03	557.28	6258.9	0.269	0.54	0.10	0.34
27050	12.87	2.0	1901.43	592.11	6766.7	0.311	0.62	0.10	0.42
28416	12.82	2.0	1565.50	592.11	8189.1	0.378	0.66	0.10	0.46
36750	12.95	2.0	1566.13	522.48	8265.9	0.334	0.70	0.10	0.50
40000	12.94	2.0	1566.13	522.43	8264.2	0.334	0.70	0.11	0.48
55645	12.94	2.0	1567.03	487.62	8260.0	0.311	0.76	0.10	0.56
72050	12.87	2.0	1567.58	452.82	8209.0	0.289	0.79	0.10	0.59

REPEATED LOAD TRIAXIAL COMPRESSION TEST .D

MATERIAL TYPE: CP=2.5PSI PULSE STRESS=9.5 PSI

SAMPLE NUMBER: TEST NO 3 DATA FILE: BRAB2

CYCLE	AXIAL STRES PSI	CHAMB PRESS PSI	RESIL E1*10**6	RESIL E3*10**6	RESIL MODULUS PSI	POIS RATIO	PERM E1 STN	PERM E3 STN	VOLUME E1-2E3 =STN,
1	8.81	2.5	2147.43	519.10	4104.3	0.242	0.12	0.02	0.08
2	8.84	2.5	1208.30	207.63	7319.1	0.172	0.15	0.02	0.11
5	8.84	2.5	1074.40	207.62	8230.1	0.193	0.19	0.03	0.13
10	8.92	2.5	1041.00	207.62	8567.4	0.199	0.20	0.03	0.14
20	8.99	2.5	940.42	207.61	9564.1	0.221	0.22	0.03	0.16
50	8.99	2.5	1041.42	207.61	8635.9	0.199	0.24	0.04	0.16
100	8.99	2.5	940.73	173.00	9560.2	0.184	0.25	0.04	0.17
235	8.92	2.5	840.28	207.61	10613.2	0.247	0.29	0.03	0.23
550	8.92	2.5	773.27	173.01	11533.0	0.224	0.32	0.03	0.26
1082	9.07	2.5	907.90	207.63	9992.0	0.229	0.34	0.03	0.28
2000	9.07	2.5	807.27	207.63	11237.6	0.257	0.37	0.03	0.31
5000	9.15	2.5	874.91	207.62	10455.2	0.237	0.41	0.03	0.35
10400	9.28	2.5	942.57	242.21	9849.6	0.257	0.45	0.03	0.39
16100	9.32	2.5	942.86	242.23	9880.3	0.257	0.48	0.03	0.42
29160	9.24	2.5	875.95	276.80	10545.0	0.316	0.53	0.04	0.45
39100	9.10	2.5	909.90	346.04	10003.5	0.380	0.56	0.03	0.50
58670	9.25	2.5	876.53	2283.66	10556.2	2.605	0.59	0.04	0.51
83380	9.40	2.5	775.66	242.20	12124.5	0.312	0.63	0.04	0.55
85360	8.92	2.5	843.20	242.21	10576.4	0.287	0.64	0.03	0.58

REPEATED LOAD TRIAXIAL COMPRESSION TEST .D

MATERIAL TYPE: CL CP = 3.0 PULSE STRESS = 7.0 PSI

SAMPLE NUMBER: TEST NO 5 DATA FILE: BRAB4

CYCLE	AXIAL STRESS PSI	CHAMB PRESS PSI	RESIL E1*10**6	RESIL E3*10**6	RESIL MODULUS PSI	POIS RATIO	PERM E1 STN	PERM E3 STN	VOLUME =STN,
1	6.77	3.0	1978.80	243.36	3421.9	0.123	0.15	0.01	0.13
2	6.77	3.0	687.64	104.29	9846.2	0.152	0.16	0.02	0.12
5	6.77	3.0	587.21	139.06	11530.3	0.237	0.19	0.02	0.15
10	6.77	3.0	620.85	104.29	10904.1	0.168	0.21	0.02	0.17
20	6.77	3.0	520.33	104.29	13010.6	0.200	0.24	0.02	0.20
50	6.77	3.0	486.84	104.29	13905.6	0.214	0.25	0.02	0.21
100	7.08	3.0	486.88	104.29	14536.4	0.214	0.26	0.02	0.22
200	7.08	3.0	486.97	104.28	14532.7	0.214	0.28	0.03	0.22
500	7.12	3.0	453.43	104.28	15709.4	0.230	0.29	0.03	0.23
1000	7.14	3.0	453.48	104.28	15741.8	0.230	0.30	0.03	0.24
2000	6.98	3.0	453.56	104.28	15399.7	0.230	0.32	0.03	0.26
5034	7.02	3.0	487.26	104.29	14399.6	0.214	0.34	0.02	0.30
10000	7.20	3.0	453.77	139.05	15869.3	0.306	0.37	0.02	0.33
25520	7.03	3.0	454.02	104.30	15490.1	0.230	0.42	0.01	0.40
53880	7.08	3.0	487.84	104.31	14513.9	0.214	0.46	0.	0.46
83030	7.02	3.0	454.32	104.31	15449.0	0.230	0.49	0.	0.49

REPEATED LOAD TRIAXIAL COMPRESSION TEST .D

MATERIAL TYPE: CL CP=2.0 PULSE STRESS=12.5 PSI

SAMPLE NUMBER: TEST NO 6 DATA FILE: BRAB7

CYCLE	AXIAL STRESS PSI	CHAMB PRESS PSI	RESIL E1*10**6	RESIL E3*10**6	RESIL MODULUS PSI	POIS RATIO	PERM E1 STN	PERM E3 STN	VOLUME E1-2E3 =STN,
5	11.89	2.0	3183.96	973.24	3734.6	0.306	0.90	0.31	0.28
10	11.96	2.0	2852.99	868.81	4193.3	0.305	1.11	0.33	0.45
20	11.95	2.0	2148.97	764.05	5559.7	0.356	1.34	0.40	0.54
50	11.93	2.0	2088.39	659.33	5711.9	0.316	1.67	0.48	0.71
100	11.96	2.0	1956.95	589.60	6112.3	0.301	1.89	0.53	0.83
200	12.30	2.0	1892.97	589.23	6496.8	0.311	2.11	0.60	0.91
500	12.29	2.0	1897.08	588.93	6476.0	0.310	2.32	0.65	1.02
1000	12.30	2.0	1864.84	588.85	6594.3	0.316	2.42	0.66	1.10
2000	12.37	2.0	2003.32	623.51	6177.0	0.311	2.50	0.66	1.18
5000	12.36	2.0	2023.15	658.05	6107.3	0.325	2.63	0.67	1.29
10000	12.55	2.0	2110.97	657.96	5945.6	0.312	2.73	0.69	1.35
21660	12.34	2.0	1942.42	692.59	6351.5	0.357	2.88	0.69	1.50
35000	12.62	2.0	2116.78	692.52	5964.1	0.327	2.99	0.70	1.59
52125	12.47	2.0	2118.83	727.20	5887.1	0.343	3.09	0.69	1.71
62000	12.23	2.0	2292.00	727.15	5335.0	0.317	3.13	0.70	1.73
78360	12.32	2.0	2379.76	727.17	5177.1	0.306	3.19	0.69	1.81
90000	12.32	2.0	2466.92	761.80	4994.2	0.309	3.23	0.69	1.85
107840	12.31	2.0	2467.99	761.83	4986.2	0.309	3.27	0.69	1.89

REPEATED LOAD TRIAXIAL COMPRESSION TEST .D

MATERIAL TYPE: CL CP=2.5 PULSE STRESS=9.5 PSI

SAMPLE NUMBER: TEST NO 7 DATA FILE: BRAB9

CYCLE	AXIAL STRES PSI	CHAMB PRESS PSI	RESIL E1*10**6	RESIL E3*10**6	RESIL MODULUS PSI	POIS RATIO	PERM E1 STN	PERM E3 STN	VOLUME E1-2E3 =STN,
10	8.95	2.5	1281.45	382.94	6984.2	0.299	0.69	0.12	0.45
20	8.95	2.5	1619.49	348.06	5524.1	0.215	0.74	0.14	0.46
50	8.94	2.5	1282.44	347.98	6973.0	0.271	0.77	0.16	0.45
100	9.25	2.5	1198.80	313.16	7715.6	0.261	0.83	0.17	0.49
200	9.25	2.5	1199.26	313.15	7712.1	0.261	0.87	0.17	0.53
500	9.17	2.5	1284.35	347.94	7140.7	0.271	0.91	0.18	0.55
1000	9.25	2.5	1285.02	347.92	7196.4	0.271	0.97	0.18	0.61
2400	9.33	2.5	1285.74	347.94	7252.8	0.271	1.02	0.18	0.66
5000	9.40	2.5	1286.39	347.92	7308.6	0.270	1.07	0.18	0.71
9000	9.40	2.5	1287.02	347.92	7305.0	0.270	1.12	0.18	0.76
19921	9.25	2.5	1457.75	382.76	6345.0	0.263	1.21	0.17	0.87
30000	8.94	2.5	1458.52	452.36	6130.7	0.310	1.27	0.17	0.93
50000	9.25	2.5	1459.16	452.36	6339.4	0.310	1.31	0.17	0.97
75000	9.25	2.5	1459.66	452.36	6337.2	0.310	1.34	0.17	1.00

REPEATED LOAD TRIAXIAL COMPRESSION TEST .D

MATERIAL TYPE: CL CP=3.0 PULSE STRESS=7.0 PSI

SAMPLE NUMBER: TEST NO 8 DATA FILE: BRAB11

CYCLE	AXIAL STRESS PSI	CHAMB PRESS PSI	RESIL E1*10**6	RESIL E3*10**6	RESIL MODULUS PSI	POIS RATIO	PERM E1 STN	PERM E3 STN	VOLUME E1-2E3 =STN,
1	5.41	3.0	384.92	139.42	14065.3	0.362	0.11	0.03	0.05
2	6.77	3.0	720.23	174.26	9405.0	0.242	0.20	0.05	0.10
5	6.77	3.0	888.17	174.26	7626.7	0.196	0.25	0.05	0.15
10	6.96	3.0	888.32	174.25	7833.2	0.196	0.26	0.05	0.16
20	6.96	3.0	888.77	174.24	7828.7	0.196	0.31	0.06	0.19
50	6.96	3.0	721.28	174.23	9645.2	0.242	0.34	0.06	0.22
100	6.96	3.0	721.43	174.23	9643.3	0.242	0.36	0.06	0.24
200	6.96	3.0	721.50	174.23	9642.3	0.241	0.37	0.06	0.25
500	7.03	3.0	721.66	174.22	9746.7	0.241	0.39	0.07	0.25
1000	7.11	3.0	721.76	174.22	9852.4	0.241	0.41	0.07	0.27
2000	7.11	3.0	721.92	174.22	9850.1	0.241	0.43	0.07	0.29
5000	7.03	3.0	890.22	174.21	7900.1	0.196	0.47	0.07	0.33
10000	7.03	3.0	890.59	174.20	7896.2	0.196	0.52	0.08	0.36
28745	7.03	3.0	723.20	174.19	9722.5	0.241	0.61	0.08	0.45
40500	7.11	3.0	723.48	174.18	9824.2	0.241	0.64	0.09	0.46
58385	7.26	3.0	723.80	209.04	10036.1	0.289	0.69	0.08	0.53
69000	7.26	3.0	892.23	174.20	8141.0	0.195	0.70	0.08	0.54
85840	7.12	3.0	892.78	174.28	7970.6	0.195	0.76	0.03	0.70

REPEATED LOAD TRIAXIAL COMPRESSION TEST .D

MATERIAL TYPE: CL CP=2.0 PULSE STRESS= 12.5 PSI

SAMPLE NUMBER: TEST NO.27 DATA FILE: BRAB30

CYCLE	AXIAL STRES PSI	CHAMB PRESS PSI	RESIL E1*10**6	RESIL E3*10**6	RESIL MODULUS PSI	POIS RATIO	PERM E1 STN	PERM E3 STN	VOLUME E1-2E3 =STN,
1	10.82	2.0	3424.01	1314.56	3159.6	0.384	2.57	0.76	1.05
2	11.24	2.0	3449.90	1312.38	3257.5	0.380	3.30	0.92	1.46
5	7.40	2.0	3491.45	1308.49	2118.7	0.375	4.45	1.22	2.01
10	12.32	2.0	3528.66	1305.44	3491.9	0.370	5.46	1.46	2.54
20	12.26	2.0	3562.24	1301.90	3440.3	0.365	6.35	1.74	2.87
50	12.16	2.0	3161.20	853.04	3845.3	0.270	7.79	2.15	3.49
100	11.93	2.0	2274.79	850.31	5244.8	0.374	8.89	2.48	3.93
200	11.87	2.0	2299.07	847.98	5160.9	0.369	9.86	2.76	4.34
500	11.79	2.0	2325.85	845.39	5070.5	0.363	10.89	3.07	4.75
1000	11.75	2.0	2341.83	843.88	5017.9	0.360	11.50	3.26	4.98
2000	11.72	2.0	2351.41	842.94	4986.3	0.358	11.86	3.37	5.12
2250	11.72	2.0	2352.81	842.77	4981.4	0.358	11.92	3.39	5.14
5000	11.84	2.0	2360.30	942.86	5015.7	0.399	12.20	3.51	5.18
8542	11.67	2.0	2365.38	941.97	4934.6	0.398	12.38	3.61	5.16
21562	11.67	2.0	2852.13	1009.05	4090.8	0.354	12.57	3.63	5.31
32362	11.80	2.1	2858.25	1109.39	4128.3	0.388	12.75	3.68	5.39
50312	11.79	2.0	2379.62	1008.17	4954.9	0.424	12.91	3.72	5.47
61262	11.79	2.0	2381.83	1008.00	4948.7	0.423	12.99	3.74	5.51
80462	11.92	2.0	2383.49	1007.73	5002.8	0.423	13.05	3.76	5.53
85462	12.46	2.0	2384.28	1133.05	5225.2	0.475	13.08	1.52	10.04

REPEATED LOAD TRIAXIAL COMPRESSION TEST .D

MATERIAL TYPE: CL CP=2.5 PULSE STRESS=9.5 PSI

SAMPLE NUMBER: TEST NO. 26 DATA FILE: BRAB29

CYCLE	AXIAL STRES PSI	CHAMB PRESS PSI	RESIL E1*10**6	RESIL E3*10**6	RESIL MODULUS PSI	POIS RATIO	PERM E1 STN	PERM E3 STN	VOLUME =STN,
1	7.33	2.5	1725.32	870.20	4247.1	0.504	1.89	0.56	0.77
2	8.00	2.5	2163.35	868.99	3697.7	0.402	2.39	0.70	0.99
5	8.73	2.5	2182.54	866.91	3998.5	0.397	3.25	0.94	1.37
10	9.60	2.5	2198.65	865.05	4368.2	0.393	3.96	1.16	1.64
20	10.02	2.5	1778.04	863.32	5636.0	0.486	4.80	1.36	2.08
50	9.97	2.5	1796.03	861.24	5552.7	0.480	5.76	1.60	2.56
100	9.18	2.5	1811.79	859.64	5068.5	0.474	6.58	1.79	3.00
200	9.16	2.5	1823.47	858.37	5021.2	0.471	7.17	1.94	3.29
500	9.06	2.5	1836.63	857.57	4935.2	0.467	7.84	2.04	3.76
1030	9.13	2.5	1570.32	857.16	5814.3	0.546	8.22	2.09	4.04
2000	9.05	2.5	1573.71	514.21	5752.3	0.327	8.42	2.10	4.22
5000	9.12	2.5	1577.52	514.07	5782.6	0.326	8.64	2.13	4.38
10000	9.27	2.5	1580.59	513.95	5863.2	0.325	8.82	2.16	4.50
26300	9.26	2.5	1584.09	616.48	5845.4	0.389	9.02	2.20	4.62
38500	9.26	2.4	1585.84	616.33	5836.2	0.389	9.12	2.22	4.68
65000	9.25	2.5	1588.68	616.27	5824.5	0.388	9.28	2.23	4.82
84700	9.25	2.8	1589.62	616.27	5821.1	0.388	9.33	2.23	4.87
88500	9.10	2.4	1589.97	616.25	5725.5	0.388	9.35	2.24	4.87

REPEATED LOAD TRIAXIAL COMPRESSION TEST .D

MATERIAL TYPE: CL CP=3.0 PULSE STRESS= 7.0 PSI

SAMPLE NUMBER: TEST NO 25 DATA FILE: BRAB28

CYCLE	AXIAL STRES PSI	CHAMB PRESS PSI	RESIL EI*10**6	RESIL E3*10**6	RESIL MODULUS PSI	PCIS RATIO	PERM EI STN	PERM E3 STN	VOLUME =STN,
1	5.58	3.0	1440.82	860.32	3872.0	0.597	1.73	0.48	0.77
2	5.87	3.0	1446.93	859.40	4055.5	0.594	2.14	0.59	0.96
5	6.45	3.0	1454.92	858.19	4434.3	0.590	2.68	0.73	1.22
10	6.44	3.0	1461.14	857.28	4406.1	0.587	3.10	0.84	1.42
20	6.42	3.0	1467.26	445.31	4378.4	0.303	3.50	0.94	1.62
50	6.85	3.0	1477.00	444.57	4637.4	0.301	4.14	1.11	1.92
100	6.84	3.0	1482.96	444.11	4609.3	0.299	4.52	1.22	2.08
200	6.66	3.0	1493.18	443.28	4461.4	0.297	5.18	1.41	2.36
500	6.80	3.0	1046.65	442.96	6497.0	0.423	5.47	1.48	2.51
1000	6.80	3.0	1048.12	442.82	6483.8	0.422	5.60	1.51	2.58
2000	6.79	3.0	1049.20	442.75	6474.9	0.422	5.70	1.53	2.64
5000	6.79	3.0	1050.46	442.61	6463.3	0.421	5.81	1.56	2.69
10000	6.79	3.0	1051.62	442.60	6455.7	0.421	5.91	1.56	2.79
25260	6.79	3.0	1052.77	442.55	6447.3	0.420	6.02	1.57	2.88
35500	6.79	3.0	1053.55	442.61	6444.3	0.420	6.09	1.56	2.97
55230	6.79	3.0	1054.05	442.58	6440.4	0.420	6.13	1.57	2.99
83150	6.79	3.0	600.00	442.58	11314.1	0.738	6.18	1.57	3.04

REPEATED LOAD TRIAXIAL COMPRESSION TEST .D

MATERIAL TYPE: CH CP=2.0 PULSE STRESS=12.5 PSI

SAMPLE NUMBER: TEST NO 15 DATA FILE: BRAB20X

CYCLE	AXIAL STRES PSI	CHAMB PRESS PSI	RESIL E1*10**6	RESIL E3*10**6	RESIL MODULUS PSI	POIS RATIO	PERM E1 STN	PERM E3 STN	VOLUME E1-2E3 =STN,
1	12.47	1.7	819.41	104.31	15215.4	0.127	0.04	0.	0.04
2	12.47	2.0	819.44	104.31	15216.0	0.127	0.04	0.	0.04
5	12.31	2.0	819.44	104.31	15028.1	0.127	0.04	0.	0.04
10	12.47	2.0	819.45	104.31	15215.7	0.127	0.04	0.	0.04
20	12.47	2.0	819.47	104.31	15214.4	0.127	0.04	0.	0.04
50	12.47	2.0	819.49	104.31	15213.9	0.127	0.05	0.	0.05
100	12.62	2.0	819.54	104.31	15401.0	0.127	0.05	0.	0.05
200	12.47	2.0	819.54	104.31	15213.2	0.127	0.05	0.	0.05
500	12.31	2.0	819.55	104.31	15025.1	0.127	0.05	0.	0.05
1000	12.47	2.0	819.58	104.30	15211.3	0.127	0.06	0.01	0.04
2000	12.62	2.0	819.63	104.30	15398.1	0.127	0.06	0.01	0.04
5000	12.62	2.0	819.77	104.30	15394.4	0.127	0.08	0.01	0.06
10000	12.69	1.9	819.85	104.28	15481.4	0.127	0.09	0.03	0.03
24565	12.84	1.7	820.07	104.27	15661.6	0.127	0.12	0.04	0.04
36500	12.77	2.1	401.84	69.52	31777.0	0.173	0.16	0.03	0.10
53925	12.92	2.0	401.96	69.52	32152.4	0.173	0.19	0.02	0.15
60000	12.77	2.0	820.83	69.52	15557.8	0.085	0.21	0.02	0.17
64400	12.77	2.0	820.88	69.52	15556.7	0.085	0.21	0.02	0.17
82500	12.77	2.4	821.28	69.53	15553.5	0.085	0.26	0.01	0.24
90049	12.62	2.0	821.35	69.54	15365.9	0.085	0.27	0.01	0.25

REPEATED LOAD TRIAXIAL COMPRESSION TEST .D

MATERIAL TYPE: CH CP=2.5 PULSE STRESS=9.5 PSI

SAMPLE NUMBER: TEST NO 13 DATA FILE: BRAB170

CYCLE	AXIAL STRESS PSI	CHAMB PRESS PSI	RESIL E1*10**6	RESIL E3*10**6	RESIL MODULUS PSI	POIS RATIO	PERM E1 STN	PERM E3 STN	VOLUME E1-2E3 =STN,
1	9.26	2.8	617.29	34.82	15002.7	0.056	0.02	0.	0.02
2	9.26	3.0	617.30	34.82	15002.5	0.056	0.02	0.	0.02
5	9.26	3.0	617.30	34.82	15002.5	0.056	0.02	0.	0.02
10	9.26	3.0	617.30	34.82	15002.5	0.056	0.02	0.	0.02
20	9.26	3.0	617.30	34.82	15002.5	0.056	0.02	0.	0.02
50	9.26	3.0	617.34	34.82	15001.7	0.056	0.03	0.	0.03
100	9.26	3.0	617.37	34.82	15001.0	0.056	0.03	0.	0.03
200	9.26	3.0	617.39	34.82	15000.5	0.056	0.03	0.	0.03
500	9.26	3.0	617.41	34.82	15000.0	0.056	0.04	0.	0.04
1000	9.26	3.0	617.42	34.82	14999.7	0.056	0.04	0.	0.04
2000	9.26	3.0	617.48	34.82	14999.2	0.056	0.05	0.	0.05
5000	9.26	3.0	617.53	34.82	14995.9	0.056	0.06	0.01	0.04
10000	9.26	3.0	617.64	34.82	14993.2	0.056	0.08	0.01	0.06
22290	9.26	2.9	617.73	34.82	14993.2	0.056	0.09	0.	0.09
50975	9.26	3.0	617.91	34.82	14987.7	0.056	0.12	0.	0.12
80385	9.26	3.0	618.25	34.82	14978.4	0.056	0.17	0.01	0.15
107225	9.26	3.0	618.49	34.81	14970.5	0.056	0.21	0.01	0.19

REPEATED LOAD TRIAXIAL COMPRESSION TEST .D

MATERIAL TYPE: CH CP=3.0 PULSE STRESS= 7.0 PSI

SAMPLE NUMBER: TEST NO 12 DATA FILE: BRABI60

CYCLE	AXIAL STRES PSI	CHAMB PRESS PSI	RESIL E1*10**6	RESIL E3*10**6	RESIL MODULUS PSI	POIS RATIO	PERM E1 STN	PERM E3 STN	VOLUME E1-2E3 =STN,
1	7.01	2.5	284.18	69.98	24683.7	0.246	0.01	0.	0.01
2	7.01	2.5	284.19	69.98	24682.8	0.246	0.02	0.	0.02
5	7.01	2.5	284.19	69.98	24682.4	0.246	0.02	0.	0.02
10	7.01	2.5	284.20	69.98	24680.3	0.246	0.02	0.	0.02
20	7.01	2.5	284.20	69.98	24679.9	0.246	0.02	0.	0.02
50	7.01	2.5	284.21	69.98	24678.6	0.246	0.03	0.	0.03
100	7.01	2.5	284.23	69.98	24677.4	0.246	0.03	0.	0.03
200	7.01	2.5	284.23	69.98	24677.4	0.246	0.03	0.	0.03
500	7.01	2.5	284.24	69.98	24676.2	0.246	0.04	0.	0.04
1000	7.01	2.5	284.25	69.98	24675.3	0.246	0.04	0.	0.04
2000	7.01	2.5	284.26	69.97	24672.8	0.246	0.04	0.01	0.02
5465	7.01	2.5	284.30	34.99	24672.5	0.123	0.06	0.	0.06
10000	7.01	2.5	284.32	34.99	24667.8	0.123	0.06	0.01	0.04
34250	7.01	2.5	284.42	69.97	24658.8	0.246	0.10	0.01	0.08
40400	7.01	2.5	284.44	69.97	24657.1	0.246	0.11	0.01	0.09
63408	7.01	2.5	284.56	69.98	24648.9	0.246	0.15	0.	0.15
83455	7.01	2.5	284.62	69.97	24639.7	0.246	0.17	0.01	0.15

REPEATED LOAD TRIAXIAL COMPRESSION TEST .D

MATERIAL TYPE: CH CP=2.0 PULSE STRESS= 12.5 PSI

SAMPLE NUMBER: TEST NO 22 DATA FILE: BRAB25X

CYCLE	AXIAL STRES PSI	CHAMB PRESS PSI	RESIL E1*10**6	RESIL E3*10**6	RESIL MODULUS PSI	POIS RATIO	PERM E1 STN	PERM E3 STN	VOLUME E1-2E3 =STN,
1	12.37	2.0	1156.17	209.05	10695.1	0.181	0.03	0.	0.03
2	12.37	2.0	1156.22	209.05	10694.6	0.181	0.04	0.	0.04
5	12.52	2.0	1156.34	278.74	10827.2	0.241	0.05	0.	0.05
10	12.52	2.0	1156.44	278.74	10826.3	0.241	0.06	0.	0.06
20	12.52	2.0	1156.55	278.73	10824.4	0.241	0.07	0.01	0.05
50	12.52	2.0	1240.57	278.72	10090.6	0.225	0.08	0.01	0.06
100	12.52	2.0	1240.69	278.72	10089.6	0.225	0.09	0.01	0.07
200	12.52	2.0	1324.75	278.71	9448.8	0.210	0.11	0.01	0.09
500	12.52	2.0	1325.08	278.71	9446.4	0.210	0.14	0.01	0.12
1000	12.52	2.0	1325.35	278.70	9443.9	0.210	0.16	0.02	0.12
2000	12.52	2.0	1325.77	278.69	9440.2	0.210	0.19	0.02	0.15
5000	12.59	2.0	1242.40	278.67	10134.4	0.224	0.23	0.03	0.17
10000	12.67	2.0	1075.03	278.67	11784.1	0.259	0.28	0.03	0.22
23355	12.67	2.0	991.55	209.00	12776.3	0.211	0.33	0.03	0.27
31775	12.67	2.0	991.80	174.16	12772.2	0.176	0.36	0.03	0.30
51350	12.82	2.0	907.88	174.16	14122.8	0.192	0.37	0.03	0.31
60000	12.82	2.0	907.94	174.15	14119.9	0.192	0.38	0.04	0.30

REPEATED LOAD TRIAXIAL COMPRESSION TEST .D

MATERIAL TYPE: CH CP=2.5 PULSE STRESS= 9.5 PSI

SAMPLE NUMBER: TEST NO 17 DATA FILE: BRAB22X

CYCLE	AXIAL STRESS PSI	CHAMB PRESS PSI	RESIL E1*10**6	RESIL E3*10**6	RESIL MODULUS PSI	POIS RATIO	PERM E1 STN	PERM E3 STN	VOLUME E1-2E3 =STN,
1	9.24	2.1	870.28	139.08	10611.9	0.160	0.03	0.	0.03
2	9.54	2.5	870.34	139.07	10964.2	0.160	0.04	0.01	0.02
5	9.54	2.5	786.70	139.07	12129.8	0.177	0.05	0.01	0.03
10	9.54	2.5	870.45	139.07	10962.7	0.160	0.05	0.01	0.03
20	9.54	2.6	954.25	173.84	10000.1	0.182	0.06	0.01	0.04
50	9.54	2.6	954.34	173.84	9999.1	0.182	0.07	0.01	0.05
100	9.54	2.5	870.69	139.07	10959.8	0.160	0.08	0.01	0.06
200	9.54	2.5	870.76	139.07	10958.9	0.160	0.09	0.01	0.07
500	9.54	2.5	870.88	139.07	10956.6	0.160	0.10	0.01	0.08
1000	9.39	2.5	870.95	139.07	10779.0	0.160	0.11	0.01	0.09
2327	9.39	2.5	871.11	139.07	10777.8	0.160	0.13	0.01	0.11
5000	9.70	2.5	787.61	104.30	12311.2	0.132	0.16	0.01	0.14
10000	9.08	2.5	787.67	104.29	11526.3	0.132	0.17	0.02	0.13
22140	9.15	2.5	703.97	104.29	13004.3	0.148	0.18	0.02	0.14
33700	9.70	2.5	620.52	104.31	15627.3	0.168	0.24	0.	0.24
51200	10.00	2.5	620.65	104.30	16119.0	0.168	0.26	0.01	0.24
62300	9.85	2.5	537.05	104.29	18337.8	0.194	0.31	0.02	0.27
85000	9.77	2.6	537.33	104.28	18180.0	0.194	0.36	0.03	0.30

REPEATED LOAD TRIAXIAL COMPRESSION TEST .D

MATERIAL TYPE: CH CP=3.0 PULSE STRESS= 7.0 PSI

SAMPLE NUMBER: TEST NO 16 DATA FILE: BRAB21X

CYCLE	AXIAL STRES PSI	CHAMB PRESS PSI	RESIL E1*10**6	RESIL E3*10**6	RESIL MODULUS PSI	POIS RATIO	PERM E1 STN	PERM E3 STN	VOLUME E1-2E3 =STN,
1	6.78	2.5	451.90	69.59	15007.8	0.154	0.04	0.	0.04
2	6.78	2.5	451.92	104.38	15007.1	0.231	0.04	0.	0.04
5	6.78	2.5	451.94	104.38	15006.3	0.231	0.05	0.	0.05
10	6.78	2.5	451.95	104.38	15006.1	0.231	0.05	0.	0.05
20	6.78	2.5	451.97	104.38	15005.6	0.231	0.05	0.	0.05
50	6.78	2.5	451.98	104.38	15005.1	0.231	0.06	0.	0.06
100	6.78	2.5	452.00	104.38	15003.5	0.231	0.06	0.01	0.04
200	6.78	2.5	452.00	104.38	15003.3	0.231	0.06	0.01	0.04
500	6.78	2.5	452.03	104.38	15002.5	0.231	0.07	0.01	0.05
1000	6.78	2.5	452.06	104.38	15001.5	0.231	0.07	0.01	0.05
2000	6.78	2.5	452.09	104.38	15000.3	0.231	0.08	0.01	0.06
5000	6.78	2.5	368.41	69.58	18405.0	0.189	0.09	0.01	0.07
11000	6.78	2.5	368.45	69.57	18395.5	0.189	0.10	0.03	0.04
25000	6.78	2.5	368.64	69.57	18391.0	0.189	0.15	0.02	0.11
33705	6.78	2.5	368.73	34.79	18390.3	0.094	0.18	0.01	0.16
53545	6.78	2.7	368.84	34.79	18379.9	0.094	0.21	0.02	0.17
63185	6.78	2.5	368.97	69.59	18382.4	0.189	0.24	0.	0.24
84290	6.78	2.5	369.12	69.59	18375.0	0.189	0.28	0.	0.28

REPEATED LOAD TRIAXIAL COMPRESSION TEST .D

MATERIAL TYPE: CH CP=2.0 PULSE STRESS= 12.5 PSI

SAMPLE NUMBER: TEST NO 23 DATA FILE: BRAB26X

CYCLE	AXIAL STRES PSI	CHAMB PRESS PSI	RESIL E1*10**6	RESIL E3*10**6	RESIL MODULUS PSI	POIS RATIO	PERM E1 STN	PERM E3 STN	VOLUME E1-2E3 =STN,
1	12.51	2.0	1256.54	208.97	9956.2	0.166	0.05	0.01	0.03
2	12.51	2.0	1256.62	208.97	9955.5	0.166	0.05	0.01	0.03
5	12.51	2.5	1426.58	278.63	8769.4	0.195	0.06	0.01	0.04
10	12.51	2.0	1426.73	278.63	8768.5	0.195	0.07	0.01	0.05
20	12.51	2.0	1426.95	278.62	8766.6	0.195	0.09	0.01	0.07
50	12.51	2.0	1597.04	278.61	7832.4	0.174	0.10	0.01	0.08
100	12.51	2.0	1597.20	278.61	7831.6	0.174	0.11	0.01	0.09
200	12.51	2.0	1597.42	278.60	7829.9	0.174	0.13	0.02	0.09
500	12.51	2.0	1597.82	278.59	7827.4	0.174	0.15	0.02	0.11
1000	12.51	2.0	1598.12	313.39	7824.9	0.196	0.17	0.03	0.11
2000	12.50	2.0	1598.67	348.19	7821.1	0.218	0.21	0.03	0.15
5000	12.50	2.0	1769.85	348.17	7063.6	0.197	0.27	0.04	0.19
10000	12.50	2.0	1770.94	348.14	7058.3	0.197	0.33	0.05	0.23
26320	12.49	2.0	1771.96	348.07	7051.3	0.196	0.39	0.07	0.25
36000	12.57	2.0	1772.29	348.03	7092.0	0.196	0.41	0.08	0.25
56290	12.49	2.0	1431.83	313.22	8723.9	0.219	0.43	0.08	0.27
60000	12.49	2.0	1431.83	313.20	8722.7	0.219	0.43	0.09	0.25
81543	12.33	2.0	1432.52	313.15	8608.5	0.219	0.48	0.10	0.28

REPEATED LOAD TRIAXIAL COMPRESSION TEST .D

MATERIAL TYPE: CH CP=2.0 PULSE STRESS=12.5 PSI

SAMPLE NUMBER: TEST NO 24 DATA FILE: BRAB27X

CYCLE	AXIAL STRES PSI	CHAMB PRESS PSI	RESIL E1*10**6	RESIL E3*10**6	RESIL MODULUS PSI	POIS RATIO	PERM E1 STN	PERM E3 STN	VOLUME E1-2E3 =STN,
2	12.32	2.0	2242.90	380.19	5492.8	0.170	0.09	0.01	0.07
5	12.32	2.0	2578.61	483.86	4777.4	0.188	0.13	0.01	0.11
10	12.32	2.0	2746.56	483.84	4485.0	0.176	0.15	0.02	0.11
20	12.39	2.0	2915.45	518.37	4250.6	0.178	0.20	0.02	0.16
50	12.31	2.0	3085.28	552.87	3991.2	0.179	0.27	0.03	0.21
100	12.31	2.0	3422.47	621.93	3597.5	0.182	0.32	0.04	0.24
200	12.16	2.0	3424.49	656.44	3550.5	0.192	0.38	0.05	0.28
500	12.31	2.0	3596.76	690.87	3421.5	0.192	0.51	0.07	0.37
1012	12.00	2.0	3599.85	690.80	3333.5	0.192	0.59	0.08	0.43
2000	12.30	2.0	3604.82	690.66	3411.7	0.192	0.73	0.10	0.53
5000	12.44	2.0	3610.90	690.46	3446.1	0.191	0.89	0.12	0.65
10000	12.44	2.0	3276.25	655.78	3796.3	0.200	0.98	0.15	0.68
25000	12.43	2.0	2772.10	517.58	4484.2	0.187	1.07	0.18	0.71
36100	12.43	2.0	2603.68	483.03	4773.3	0.186	1.09	0.19	0.71
59420	12.42	1.8	2268.42	448.37	5475.0	0.198	1.22	0.22	0.78

REPEATED LOAD TRIAXIAL COMPRESSION TEST .D

MATERIAL TYPE: CH CP=2.5 PULSE STRESS= 9.5 PSI

SAMPLE NUMBER: TEST NO 21 DATA FILE: BRAB24X

CYCLE	AXIAL STRES PSI	CHAMB PRESS PSI	RESIL E1*10**6	RESIL E3*10**6	RESIL MODULUS PSI	POIS RATIO	PERM E1 STN	PERM E3 STN	VOLUME E1-2E3 =STN,
1	9.45	2.5	1302.13	281.38	7258.1	0.216	0.06	0.	0.06
2	9.45	2.5	1302.28	281.37	7256.7	0.216	0.07	0.01	0.05
5	9.45	2.5	1387.01	281.37	6813.4	0.203	0.08	0.01	0.06
10	9.45	2.5	1387.22	281.37	6812.4	0.203	0.10	0.01	0.08
20	9.45	2.5	1387.43	281.36	6810.9	0.203	0.11	0.01	0.09
50	9.45	2.5	1387.78	281.35	6808.7	0.203	0.14	0.01	0.12
100	9.45	2.5	1557.26	281.35	6067.7	0.181	0.16	0.01	0.14
200	9.45	2.5	1557.53	281.35	6066.7	0.181	0.17	0.01	0.15
500	9.45	2.5	1473.28	281.33	6412.7	0.191	0.20	0.02	0.16
1000	9.29	2.5	1558.32	281.33	5961.7	0.181	0.22	0.02	0.18
2000	9.45	2.5	1474.08	281.32	6408.7	0.191	0.25	0.02	0.21
5000	9.45	2.5	1389.90	210.98	6795.9	0.152	0.29	0.03	0.23
10000	9.68	2.5	1305.46	210.96	7414.8	0.162	0.32	0.04	0.24
22211	9.76	2.4	1220.84	210.92	7990.4	0.173	0.33	0.06	0.21
33700	9.52	2.4	1136.67	175.74	8372.1	0.155	0.38	0.07	0.24
52285	9.44	2.6	1052.06	175.72	8968.2	0.167	0.40	0.09	0.22
58000	9.28	2.6	1052.20	175.71	8816.9	0.167	0.42	0.09	0.24
80080	9.43	2.5	967.69	140.55	9747.3	0.145	0.45	0.10	0.25

REPEATED LOAD TRIAXIAL COMPRESSION TEST .D

MATERIAL TYPE: CH CP=3.0 PULSE STRESS = 7.0

SAMPLE NUMBER: TEST NO 19 DATA FILE: BRAB23X

CYCLE	AXIAL STRES PSI	CHAMB PRESS PSI	RESIL E1*10**6	RESIL E3*10**6	RESIL MODULUS PSI	POIS RATIO	PERM E1 STN	PERM E3 STN	PERM VOLUME =STN,
1	6.91	2.6	874.07	138.94	7908.5	0.159	0.01	0.	0.01
2	6.91	3.1	874.14	138.94	7907.8	0.159	0.02	0.	0.02
5	6.91	3.0	790.15	138.94	8748.4	0.176	0.03	0.	0.03
10	6.91	3.0	790.21	138.94	8747.8	0.176	0.04	0.	0.04
20	6.91	3.0	790.27	138.94	8747.0	0.176	0.05	0.	0.05
50	6.91	3.0	790.35	138.94	8746.2	0.176	0.06	0.	0.06
100	6.91	3.0	790.41	138.94	8745.6	0.176	0.06	0.	0.06
200	6.91	3.0	790.49	138.94	8744.7	0.176	0.07	0.	0.07
500	6.91	3.0	790.61	138.94	8743.4	0.176	0.09	0.	0.09
1000	6.91	3.0	790.71	138.94	8742.2	0.176	0.10	0.	0.10
2500	6.91	3.0	790.89	138.94	8740.3	0.176	0.12	0.	0.12
5000	6.91	3.0	706.90	138.93	9778.0	0.197	0.14	0.	0.14
8000	6.91	3.0	706.98	138.94	9777.6	0.197	0.15	0.	0.15
18815	6.91	2.6	622.96	138.94	11096.3	0.223	0.18	0.	0.18
33900	6.91	3.5	623.49	138.90	11080.7	0.223	0.26	0.03	0.20
48892	6.91	2.7	623.58	138.91	11081.5	0.223	0.28	0.02	0.24
60050	6.91	3.3	539.64	104.16	12798.1	0.193	0.34	0.05	0.24
77750	6.91	3.0	539.77	104.16	12795.9	0.193	0.36	0.04	0.28
85975	6.90	3.2	540.08	104.13	12782.2	0.193	0.42	0.07	0.28

REPEATED LOAD TRIAXIAL COMPRESSION TEST .D

MATERIAL TYPE: SM CP=2.0 PSI PULSE STRESS=12.5 PSI

SAMPLE NUMBER: TEST NO 31 DATA FILE: BRAB33

CYCLE	AXIAL STRES PSI	CHAMB PRESS PSI	RESIL EI*10**6	RESIL E3*10**6	RESIL MODULUS PSI	POIS RATIO	PERM EI STN	PERM E3 STN	VOLUME EI-2E3 =STN,
1	12.18	2.0	3345.89	1418.84	3638.8	0.424	0.24	0.04	0.16
2	12.17	2.0	1497.18	780.22	8129.1	0.521	0.29	0.06	0.17
5	12.16	2.0	1212.37	496.28	10029.6	0.409	0.39	0.11	0.17
10	12.42	2.0	1028.15	425.14	12077.5	0.414	0.49	0.16	0.17
20	12.45	2.0	961.90	354.06	12942.7	0.368	0.61	0.23	0.15
50	12.42	2.0	896.04	318.31	13864.4	0.355	0.79	0.33	0.13
100	12.40	2.0	846.74	247.38	14647.8	0.292	0.96	0.42	0.12
200	12.38	2.1	865.07	211.86	14313.2	0.245	1.12	0.50	0.12
500	12.36	2.1	782.13	211.63	15797.6	0.271	1.35	0.61	0.13
1000	12.33	2.0	800.78	211.45	15403.6	0.264	1.55	0.69	0.17
2000	12.32	2.0	802.27	211.30	15353.3	0.263	1.74	0.76	0.22
5000	12.30	2.0	718.16	140.79	17132.1	0.196	1.91	0.82	0.27
10000	12.30	2.0	701.55	140.75	17527.8	0.201	1.98	0.85	0.28
23320	12.29	2.0	633.56	105.54	19399.2	0.167	2.05	0.87	0.31
31850	12.29	2.0	599.59	105.54	20501.1	0.176	2.09	0.87	0.35
52560	12.29	1.0	617.01	105.53	19915.4	0.171	2.14	0.88	0.38
63000	12.29	2.0	548.66	105.53	22399.6	0.192	2.17	0.88	0.41
83100	12.28	2.0	548.70	105.51	22387.0	0.192	2.18	0.90	0.38

REPEATED LOAD TRIAXIAL COMPRESSION TEST .D

MATERIAL TYPE: SM CP=2.5 PSI PULSE STRESS=9.5 PSI

SAMPLE NUMBER: TEST NO 30 DATA FILE: BRAB32

CYCLE	AXIAL STRES PSI	CHAMB PRESS PSI	RESIL E1*10**6	RESIL E3*10**6	RESIL MODULUS PSI	POIS RATIO	PERM E1 STN	PERM E3 STN	VOLUME E1-2E3 =STN,
1	9.56	2.5	1963.35	568.34	4868.7	0.289	0.13	0.01	0.11
2	9.56	2.5	755.30	177.61	12655.8	0.235	0.15	0.01	0.13
5	9.56	2.5	654.76	106.56	14598.1	0.163	0.18	0.01	0.16
10	9.56	2.5	570.94	106.55	16738.9	0.187	0.20	0.02	0.16
20	9.56	2.5	587.87	106.55	16255.6	0.181	0.22	0.02	0.18
50	9.55	2.5	571.26	106.54	16726.0	0.187	0.25	0.03	0.19
100	9.55	2.5	520.99	106.54	18338.4	0.204	0.28	0.03	0.22
200	9.55	2.5	571.54	71.02	16715.2	0.124	0.31	0.04	0.23
500	9.56	2.5	521.26	71.03	18331.5	0.136	0.33	0.02	0.29
1000	9.56	2.5	521.36	71.05	18335.9	0.136	0.35	0.	0.35
2000	9.55	2.5	538.30	71.03	17748.6	0.132	0.38	0.03	0.32
5000	9.55	2.5	521.67	71.00	18301.7	0.136	0.41	0.07	0.27
10300	10.03	2.4	521.89	71.00	19217.7	0.136	0.45	0.06	0.33
25000	9.88	2.5	437.89	71.03	22553.7	0.162	0.49	0.03	0.43
32000	9.72	2.5	488.50	71.03	19889.9	0.145	0.51	0.02	0.47
52500	10.04	2.4	488.59	71.04	20550.9	0.145	0.53	0.01	0.51
82250	9.88	2.5	472.02	71.04	20931.9	0.151	0.59	0.01	0.57

REPEATED LOAD TRIAXIAL COMPRESSION TEST .D

MATERIAL TYPE: SM CP=3.0 PSI PULSE STRESS=7.0 PSI

SAMPLE NUMBER: TEST NO 29 DATA FILE: BRAB31

CYCLE	AXIAL STRES PSI	CHAMB PRESS PSI	RESIL E1*10**6	RESIL E3*10**6	RESIL MODULUS PSI	POIS RATIO	PERM E1 STN	PERM E3 STN	VOLUME E1-2E3 =STN,
1	7.05	2.8	454.22	212.81	15516.0	0.469	0.13	0.01	0.11
2	7.21	3.0	454.32	106.41	15865.4	0.234	0.15	0.01	0.13
5	7.29	3.0	454.40	106.41	16038.7	0.234	0.17	0.01	0.15
10	7.29	3.0	454.47	106.40	16035.1	0.234	0.18	0.02	0.14
20	7.29	3.0	454.54	106.40	16032.7	0.234	0.20	0.02	0.16
50	7.21	3.0	454.62	106.39	15851.3	0.234	0.22	0.02	0.18
100	7.21	3.0	454.74	106.40	15848.5	0.234	0.24	0.02	0.20
200	7.21	3.0	454.74	106.40	15848.5	0.234	0.24	0.02	0.20
500	7.05	3.0	370.58	106.40	19015.3	0.287	0.26	0.02	0.22
1000	7.05	3.0	370.63	106.42	19019.8	0.287	0.27	0.	0.27
2000	7.21	3.0	370.68	106.41	19446.3	0.287	0.29	0.01	0.27
5000	7.37	3.0	370.74	106.40	19872.6	0.287	0.30	0.02	0.26
10000	7.37	3.0	370.87	106.40	19865.6	0.287	0.34	0.02	0.30
23270	7.37	3.1	370.96	106.41	19863.4	0.287	0.36	0.01	0.34
32770	7.37	3.0	371.04	106.40	19854.8	0.287	0.38	0.02	0.34
34765	7.37	3.0	371.04	106.39	19853.4	0.287	0.38	0.02	0.34
54000	7.36	3.0	371.06	106.36	19838.3	0.287	0.39	0.06	0.27
61400	7.36	3.0	371.13	106.36	19834.7	0.287	0.41	0.06	0.29

REPEATED LOAD TRIAXIAL COMPRESSION TEST .D

MATERIAL TYPE: SM CP=2.0 PSI PULSE STRESS=10.5 PSI

SAMPLE NUMBER: TEST NO 39 DATA FILE: BRAB38

CYCLE	AXIAL STRES PSI	CHAMB PRESS PSI	RESIL E1*10**6	RESIL E3*10**6	RESIL MODULUS PSI	POIS RATIO	PERM E1 STN	PERM E3 STN	VOLUME E1-2E3 =STN,
1	10.30	1.6	4020.86	1599.49	2560.4	0.398	0.30	0.12	0.06
2	10.29	2.0	1666.86	710.68	6172.8	0.426	0.38	0.15	0.08
5	10.44	2.0	1247.60	532.67	8365.3	0.427	0.51	0.21	0.09
10	10.42	2.0	996.13	532.29	10462.2	0.534	0.66	0.28	0.10
20	10.56	2.0	998.07	389.99	10583.0	0.391	0.85	0.38	0.09
50	10.37	2.0	1001.26	353.99	10357.9	0.354	1.16	0.53	0.10
100	10.34	2.0	902.42	318.09	11455.8	0.352	1.49	0.69	0.11
200	10.30	2.0	854.88	282.20	12046.0	0.330	1.90	0.89	0.12
500	10.22	2.0	844.29	246.02	12108.1	0.291	2.66	1.26	0.14
1000	10.30	2.0	851.27	245.03	12095.6	0.288	3.45	1.67	0.11
2000	10.18	2.0	843.27	243.68	12076.3	0.289	4.53	2.23	0.07
2210	10.17	2.0	809.60	243.47	12556.7	0.301	4.70	2.32	0.06
5000	10.22	2.0	729.99	173.03	13995.6	0.237	5.80	2.83	0.14
11720	10.16	2.0	645.21	138.07	15752.8	0.214	6.41	3.10	0.21
24800	10.14	2.0	664.98	137.91	15249.7	0.207	6.67	3.22	0.23

REPEATED LOAD TRIAXIAL COMPRESSION TEST .D

MATERIAL TYPE: SM CP=2.5 PSI PULSE STRESS=9.5 PSI

SAMPLE NUMBER: TEST NO 36 DATA FILE: BRAB37

CYCLE	AXIAL STRES PSI	CHAMB PRESS PSI	RESIL EI*10**6	RESIL E3*10**6	RESIL MODULUS PSI	POIS RATIO	PERM E1 STN	PERM E3 STN	VOLUME E1-2E3 =STN,
1	9.50	2.0	2641.63	746.85	3596.8	0.283	0.20	0.06	0.08
2	9.66	2.5	959.37	462.30	10070.3	0.482	0.23	0.07	0.09
5	9.66	2.5	707.21	568.91	13657.0	0.804	0.27	0.09	0.09
10	9.49	2.5	623.25	142.21	15234.2	0.228	0.31	0.10	0.11
20	9.49	2.5	657.25	142.19	14442.0	0.216	0.36	0.11	0.14
50	9.49	2.5	623.98	142.15	15204.6	0.228	0.42	0.14	0.14
100	9.48	2.6	624.39	106.59	15187.1	0.171	0.49	0.16	0.17
200	9.48	2.5	591.17	142.07	16029.1	0.240	0.58	0.20	0.18
500	9.47	2.5	625.82	106.50	15126.4	0.170	0.72	0.25	0.22
1000	9.46	2.4	592.57	106.46	15965.1	0.180	0.81	0.28	0.25
3450	9.46	2.5	525.42	106.47	18006.6	0.203	0.92	0.28	0.36
5000	9.46	2.5	525.58	106.47	18001.1	0.203	0.95	0.28	0.39
10000	9.62	2.5	559.69	70.98	17191.8	0.127	0.99	0.27	0.45
25000	9.62	2.5	424.25	177.42	22674.1	0.418	1.04	0.29	0.46
35420	9.30	2.5	492.39	70.98	18890.2	0.144	1.10	0.27	0.56
55650	9.30	2.5	424.58	70.97	21901.2	0.167	1.12	0.29	0.54
63400	9.94	2.5	526.58	70.97	18876.8	0.135	1.14	0.29	0.56

REPEATED LOAD TRIAXIAL COMPRESSION TEST .D

MATERIAL TYPE: SM CP=3.0 PSI PULSE STRESS= 7.0 PSI

SAMPLE NUMBER: TEST NO 35 DATA FILE: BRAB36

CYCLE	AXIAL STRES PSI	CHAMB PRESS PSI	RESIL E1*10**6	RESIL E3*10**6	RESIL MODULUS PSI	POIS RATIO	PERM E1 STN	PERM E3 STN	VOLUME E1-2E3 =STN,
1	7.07	2.6	622.01	213.17	11369.3	0.343	0.11	0.02	0.07
2	7.23	3.0	588.49	71.06	12290.8	0.121	0.13	0.02	0.09
5	7.23	3.0	420.42	35.53	17202.9	0.085	0.14	0.02	0.10
10	7.23	3.0	420.49	35.53	17198.8	0.084	0.16	0.02	0.12
20	7.39	3.0	386.92	35.53	19106.6	0.092	0.18	0.02	0.14
50	7.39	3.0	420.68	35.53	17572.1	0.084	0.20	0.03	0.14
100	7.23	3.0	387.10	35.53	18679.8	0.092	0.23	0.03	0.17
200	7.23	3.1	420.85	35.53	17181.6	0.084	0.25	0.03	0.19
500	7.39	3.0	387.36	35.52	19080.7	0.092	0.29	0.04	0.21
1000	7.39	3.0	353.80	35.52	20890.8	0.100	0.33	0.04	0.25
2000	7.07	3.0	387.52	35.53	18245.0	0.092	0.33	0.03	0.27
5250	7.23	3.0	387.68	35.53	18654.8	0.092	0.37	0.02	0.33
9300	7.07	3.0	421.46	35.53	16776.7	0.084	0.39	0.03	0.33
25275	7.23	3.0	387.88	35.52	18632.8	0.092	0.43	0.06	0.31
53000	7.22	3.0	320.62	35.51	22532.6	0.111	0.49	0.08	0.33
60000	7.22	3.0	354.42	35.51	20384.6	0.100	0.50	0.07	0.36

REPEATED LOAD TRIAXIAL COMPRESSION TEST .D

MATERIAL TYPE: SM CP=2.5 PSI PULSE STRESS=9.5 PSI

SAMPLE NUMBER: TEST NO 33 DATA FILE: BRAB34

CYCLE	AXIAL STRES PSI	CHAMB PRESS PSI	RESIL E1*10**6	RESIL E3*10**6	RESIL MODULUS PSI	POIS RATIO	PERM E1 STN	PERM E3 STN	VOLUME E1-2E3 =STN,
1	8.96	2.1	5174.27	2587.83	1731.7	0.500	0.43	0.21	0.01
2	8.95	2.5	2142.92	1098.51	4178.1	0.513	0.55	0.25	0.05
5	9.09	2.5	1471.48	813.99	6177.4	0.553	0.78	0.38	0.02
10	9.07	2.5	1135.52	565.69	7989.3	0.498	0.98	0.48	0.02
20	9.05	2.5	1053.29	565.09	8594.7	0.536	1.22	0.58	0.06
50	9.34	2.5	887.01	458.31	10526.1	0.517	1.62	0.76	0.10
100	9.31	2.5	924.52	316.83	10070.0	0.343	1.98	0.91	0.16
200	9.28	2.5	876.83	316.32	10583.3	0.361	2.39	1.07	0.25
500	9.23	2.5	900.81	280.39	10243.9	0.311	3.13	1.36	0.41
1000	9.04	2.5	784.37	209.91	11523.2	0.268	3.72	1.54	0.64
2050	9.17	2.5	877.22	244.52	10448.9	0.279	4.35	1.70	0.95
5000	9.13	2.5	760.42	209.15	12003.6	0.275	5.10	1.91	1.28
7295	9.26	2.5	727.34	174.10	12734.6	0.239	5.40	2.02	1.36
9300	9.24	2.5	657.58	173.93	14057.2	0.264	5.58	2.12	1.34
13210	9.23	2.5	569.78	173.80	16199.6	0.305	5.75	2.20	1.35
19210	9.52	2.5	571.05	173.68	16679.1	0.304	5.96	2.27	1.42
27113	8.99	2.5	589.36	168.69	15246.2	0.286	8.88	5.29	-1.70

REPEATED LOAD TRIAXIAL COMPRESSION TEST .D

MATERIAL TYPE: SM CP=3.0 PSI PULSE STRESS=7.0 PSI

SAMPLE NUMBER: TEST NO 34 DATA FILE: BRAB35

CYCLE	AXIAL STRES PSI	CHAMB PRESS PSI	RESIL E1*10**6	RESIL E3*10**6	RESIL MODULUS PSI	POIS RATIO	PERM E1 STN	PERM E3 STN	VOLUME =STN,
1	7.06	2.5	2976.49	922.97	2371.8	0.310	0.26	0.07	0.12
2	7.05	3.0	2646.48	993.15	2663.2	0.375	0.50	0.15	0.20
5	7.05	3.0	455.10	35.47	15488.1	0.078	0.49	0.15	0.19
10	7.05	3.0	455.26	106.41	15481.8	0.234	0.52	0.15	0.22
20	7.05	3.0	539.77	106.39	13054.2	0.197	0.56	0.17	0.22
50	7.04	3.0	489.54	106.38	14390.4	0.217	0.64	0.18	0.28
100	7.04	3.0	506.85	106.36	13893.1	0.210	0.72	0.20	0.32
200	7.04	3.0	490.47	141.78	14350.0	0.289	0.83	0.22	0.39
500	7.11	3.0	491.21	141.73	14482.0	0.289	0.98	0.26	0.46
1000	7.19	3.0	474.83	70.86	15146.8	0.149	1.09	0.27	0.55
2000	7.19	3.0	458.36	70.86	15692.1	0.155	1.20	0.26	0.68
5000	7.20	3.0	459.04	70.88	15676.4	0.154	1.35	0.24	0.87
10130	7.36	3.0	425.43	70.89	17295.8	0.167	1.44	0.22	1.00
28500	7.36	3.0	408.98	70.86	17985.2	0.173	1.57	0.24	1.09
32500	7.20	3.0	460.22	35.44	15635.1	0.077	1.60	0.24	1.12
48920	7.19	3.0	392.06	35.42	18336.4	0.090	1.60	0.29	1.02
59200	7.19	3.0	358.16	70.85	20074.9	0.198	1.66	0.28	1.10
80925	7.19	3.0	409.44	70.83	17550.5	0.173	1.68	0.31	1.06
107430	7.19	3.0	409.65	35.41	17540.6	0.086	1.73	0.31	1.11

REPEATED LOAD TRIAXIAL COMPRESSION TEST .D

MATERIAL TYPE: SM CP=3.5 PSI PULSE STRESS=5.0 PSI

SAMPLE NUMBER: TEST NO 40 DATA FILE: BRAB39

CYCLE	AXIAL STRES PSI	CHAMB PRESS PSI	RESIL E1*10**6	RESIL E3*10**6	RESIL MODULUS PSI	POIS RATIO	PERM E1 STN	PERM E3 STN	VOLUME E1-2E3 =STN,
1	5.00	3.2	1288.49	320.31	3880.1	0.249	0.10	0.03	0.04
2	5.00	3.4	535.61	142.36	9334.1	0.266	0.13	0.03	0.07
5	5.00	3.5	351.58	71.17	14218.0	0.202	0.15	0.04	0.07
10	5.00	3.5	318.16	71.17	15710.4	0.224	0.17	0.04	0.09
20	5.32	3.5	301.48	71.17	17648.0	0.236	0.19	0.04	0.11
50	5.00	3.5	335.10	71.16	14912.9	0.212	0.23	0.05	0.13
100	5.00	3.5	318.44	71.16	15690.9	0.223	0.26	0.06	0.14
200	5.00	3.5	318.54	71.16	15684.7	0.223	0.29	0.06	0.17
500	5.00	3.5	318.75	71.15	15672.3	0.223	0.35	0.07	0.21
1000	5.00	3.5	318.75	35.58	15672.3	0.112	0.35	0.07	0.21
2040	5.00	3.5	318.88	71.15	15664.8	0.223	0.39	0.07	0.25
5010	5.00	3.5	319.03	71.15	15658.3	0.223	0.44	0.07	0.30
10000	5.00	3.5	285.56	35.58	17495.3	0.125	0.48	0.06	0.36
26255	5.16	3.5	302.48	71.15	17047.9	0.235	0.52	0.07	0.38
51920	5.32	3.5	269.04	35.57	19762.8	0.132	0.59	0.07	0.45
61580	5.00	3.5	269.13	71.15	18560.5	0.264	0.62	0.07	0.48